Hypoxia-Inducible Factor-1α and the Control of Hypoxic Ventilatory and Metabolic Responses in Mice and African Naked Mole Rats

By

Lisa Borecky

B.Sc. Honours, University of British Columbia 2014

A Thesis Submitted to the Faculty of Graduate Studies and Research in Partial Fulfillment

of the Requirements for the Degree of

Master of Science

Department of Biology

University of Ottawa

Ottawa, Ontario, Canada

The undersigned hereby recommend to the Faculty of Graduate Studies and Research acceptance of this thesis

Hypoxia-Inducible Factor-1α and the Control of Hypoxic Ventilatory and Metabolic Responses in Mice and African Naked Mole Rats

By

Lisa Borecky, B.Sc. (HONS)

in partial fulfillment of the requirements for the degree of Master of Science

_____

Chair, Department of Biology

_____

Thesis Supervisor

University of Ottawa

ABSTRACT

Hypoxia-inducible factors (HIFs) are a highly conserved group of transcriptional regulators responsible for cellular and systemic O_2 homeostasis in animals. However, how HIFs are involved in basic adaptive ventilatory and metabolic responses to acute and chronic hypoxia remains incompletely characterized. Naked mole rats are among the most hypoxia tolerant mammals identified. As opposed to the typical hyperventilatory response of most adult mammals, naked mole rats exhibit a unique decline in ventilation, matching their substantial decrease in metabolic rate. Naked mole rats therefore provide an excellent model in which to investigate adaptations to hypoxic ventilatory and metabolic responses (HVR and HMR, respectively). Interestingly, naked mole rats possess a mutation within the von Hippel-Lindau (VHL) binding domain—a protein necessary for proteasomal degradation of HIFα subunits in normal O_2 concentrations—suggesting they retain elevated baseline expression of HIFα and thus an upregulation of downstream gene targets. In designing our experiment, we focused on sustained hypoxia and HIF1α, which is typically the first responder subunit upon exposure to low O_2 stress. We sought to determine how increased HIF1α expression might contribute to the distinct HVR and HMR of naked mole rats, first by confirming the observed VHL mutation translates into increased HIF1α protein expression via immunoblotting. HIF1α protein expression was found to be 3-fold higher in naked mole rat brain than mouse brain and 4-fold higher than in mouse liver tissue ($p < 0.05$). We then investigated how elevated HIF1α levels might contribute to the HVR and HMR by treating naked mole rats with two different HIF1α inhibitors (either echinomycin; 0.5 and 1.0 mg kg^{-1}, or PX-478; 80.0 mg kg^{-1}) and subsequently examined changes in ventilatory and metabolic parameters in awake animals exposed to sustained hypoxia (7% O_2; 1 hour).

In control naked mole rats, minute ventilation ($\dot{V}_E$) reversibly decreased by 32% in hypoxia (1298.3 ± 188.5 to 882.6 ± 117.0 mL min^{-1} kg^{-1}) because of changes in both breathing frequency (f_R) and tidal volume (V_T). Conversely, the HVR was not significantly affected in any of our three treatment groups however, normoxic ventilation increased in naked mole rats treated with low dose echinomycin (0.5 mg kg^{-1}) by 72% (from 1298.3 ± 188.5 to 2239.5 ± 221.1 mL min^{-1} kg^{-1}). Consistent with previous findings, metabolic rate in control naked mole rats decreased

70% (from 40.1 ± 5.0 to 11.9 ± 0.9 mL O_2 min^{-1} kg^{-1}). Again, treatment with our pharmacological agents did not significantly alter this response but did result in a 43% decrease in basal metabolic rate ($\dot{V}O_2$ and $\dot{V}CO_2$) in both high-dose echinomycin and PX-478 treated naked mole rats (40.1 ± 5.0 to 22.5 ± 3.6 and 23.0 ± 1.88 mL O_2 min^{-1} kg^{-1} respectively, $p < 0.05$), dulling the magnitude of the HMR. As a result of unmatched changes in $\dot{V}_E$ and $\dot{V}O_2$, HIF1α deficient naked mole rats treated with both low-dose echinomycin and PX-478 experienced an atypical increase in their air convection requirement (ACR; $\dot{V}_E$:$\dot{V}O_2^{-1}$) in hypoxia (from 77.4 ± 11.3 to 159.2 ± 34.63 and 123.5 ± 35.5 respectively, $p < 0.05$), resembling a hyperventilation response closer to that of hypoxia-intolerant mammals.

To further determine how increased HIF1α availability affects the HMR and HVR, we administered hypoxia-intolerant mice with a pharmacological HIF1α agonist (3,4- EDHB; 180 mg kg^{-1}) and used identical experimental design to measure downstream ventilatory and metabolic responses. Mice exhibit similar reductions in metabolic rate during hypoxic exposure (from 60.3 ± 2.4 to 21.8 ± 1.8 mL O_2 min^{-1} kg-1, $p < 0.05$) but experience a 30% increase in f_R (from 157.5 ± 9.5 to 200.4 ± 10.8 breaths min^{-1}, $p < 0.05$). In contrast, mice treated with EDHB and to exposed 7% O_2 exhibited a 20% increase in f_R (200.4 ± 10.8 to 236.5 ± 14.1 breaths min^{-1}, $p < 0.05$) and a 30% reduction in the magnitude of their HMR (from 38.5 ± 2.8 to 27.8 ± 3.6 $\Delta\dot{V}O_2$). No other significant trends were observed in any of the other parameters measured. We conclude metabolic and ventilatory control in naked mole rats and mice may partially depend on increased HIF1α expression.

ACKNOWLEDGEMENTS

You know what they say—it takes a village. I would like to thank mine:

Alexia Kirby

Thomas Goldsmith

Paige Sonmor

Cat Munro and Madison Lloyd

Chau Nguyen and Courtney Deck

Josh Lavigne and the rest of the ACVS team

Dr. Bill Willmore, Anaad, Shana, and Rowida

Dr. Michael Jonz

Dean Steve Perry

Dr. Katie Gilmour

Dr. Vance Trudeau

Dr. Victor LeBlanc

My generous father

My adequate brother *I guess*

My amazingly beautiful and selfless mother

TABLE OF CONTENTS

LIST OF FIGURES

LIST OF TABLES

ABBREVIATIONS

AHD	asparaginyl hydroxylase
ACR	air convection requirement
AMPK	5MPKMP-activated protein kinase
ATP	adenosine triphosphate
ARNT	aryl hydrocarbon receptor nuclear translocator
bHLH	basic helix-loop-helix
Ca^{2+}	calcium
CO_2	carbon dioxide
CP	chuvash polycythemia
CRB	CREB binding protein
DMSO	dimethyl sulfoxide
EDHB	ethyl-3,4 dihydroxybenzoate
EPO	erythropoietin
ET-1	endothelin-1
ET_A	endothelin-1 receptor
FIH	factor-inhibiting HIF
f_R	breathing frequency
GLUT-1	glucose transporter 1
HIF-1	hypoxia inducible factor 1
HVR	hypoxic ventilatory response
HMR	hypoxic metabolic response
HO	haem- oxygenase

HRE hypoxia response element

LDHA lactate dehydrogenase

MCT-4 monocarboxylate transporter 4

mTORC1 mammalian target of rapamycin complex 1

N_2 nitrogen

Na^+ sodium

NOS nitric oxide synthase

iNOS inducible nitric oxide synthase

nNOS neuronal nitric oxide synthase

ODD oxygen-dependent degradation (domain)

PAS PER-ARNT-SIM

PDK1 pyruvate dehydrogenase kinase 1

PDH pyruvate dehydrogenase

PHD prolyl hydroxylase

O_2 oxygen

DDIT4 DNA-damage-inducible transcript 4 (REDD1**)**

RER respiratory exchange ratio

TCA tricarboxylic acid

pVHL von Hippel-Lindau protein

VAH ventilatory acclimatization to hypoxia

$\dot{V}_E$ minute ventilation

VEGF vascular endothelin growth factor

$\dot{V}O_2$ rate of oxygen consumption

$\dot{V}CO_2$ rate of carbon dioxide production

V_T tidal volume

Chapter 1
INTRODUCTION

1.1 Physiological **Adaptations to Hypoxia**

Hypoxia is commonly defined in one of two ways: first, as a level of environmental O_2 below ambient atmospheric O_2 at sea level, and secondly as a level of systemic O_2 that is insufficient to meet the metabolic demand of the cell, tissue, or organism of interest. Systemic hypoxia is an important signal in human development and disease. For instance, it is a key component of the transient ischemic events leading up to stroke and myocardial infarction—two of the most common causes of mortality in Western society (Dirnagl et al., 1999; Michiels, 2004). Similarly, vascular adjustments to local ischemia are compromised in aging and diabetic populations, contributing to the pathogenesis of coronary and peripheral arterial disease (Benderro and Lamanna, 2011; Bosch-Marce et al., 2007). On the other hand, cerebral ischemia leads to an increase in reactive oxygen species (ROS) and beta-site amyloid precursor protein cleaving enzyme 1 (BACE1) production (Guzy et al., 2005; Sun et al., 2006). These events lead to the production of beta-amyloid peptides, which form the lesions and extracellular plaques hallmark to Alzheimer's disease (Peers et al., 2007; Sun et al., 2006; Zhang et al., 2007a). Moreover, hypoxia initiates a cascade of angiogenic and erythropoietic events within the microenvironment of malignant tumors. The formation of new blood vessels and erythrocytes induced by tumor-hypoxia maintains O_2 supply to cancer cells and leads to increased growth and aggressiveness, higher incidences of metastasis, and reduced responsiveness to standard therapies (Dhani et al., 2015; Hockel et al., 1996; Vaupel and Mayer, 2007).

Conversely, hypoxic environments are common on earth (*e.g* high-altitudes, poorly ventilated burrows, and hypoxic waters) and possess a myriad of species which successfully inhabit them. Understanding the mechanisms through which these animals survive low O_2 environments

therefore presents an opportunity to translate their unique physiological adaptations into new therapeutic approaches to human health.

The production of biological energy, or adenosine triphosphate (ATP), in aerobes requires O_2 act as the terminal electron acceptor during oxidative phosphorylation (Chance and Williams, 1956). To reach the mitochondrial respiratory chain in various tissues, inspired O_2 must be transported from the respiratory interface, along the O_2 transport cascade, and across the cellular membrane. The O_2 transport cascade bridges several organs and systems, and is divided into a series of convective and diffusive steps (Figure 1.1): (*i) ventilation* – convection of air across a respiratory interface; (*ii*) pulmonary convective–diffusion; (*iii*) circulation (perfusion); and (*iv*) convective—diffusion cellular level (Weibel, 1984).

In a typical hypoxia-intolerant vertebrate cell, hypoxia-ischemia sets into motion a cascade of physiological events which culminate in tissue damage and/or cell death. At the onset of O_2 deprivation, aerobic metabolism and oxidative phosphorylation are disrupted and available high energy phosphates (ATP) are rapidly depleted. ATP is required for virtually all synthetic and degradative processes within the cell, including the activity of energy-dependent ion pumps (*e.g.* the Na^+/K^+-ATPase) within the plasma membrane. Thus, reduced ATP leads to a loss of ionic integrity as these active transport systems fail to redistribute both intracellular and extracellular ions across the cell membrane. Consequently, Na^+ enters and accumulates inside the cell (Chidekel et al., 1997; Friedman and Haddad, 1994; Jiang and Haddad, 1991) while K^+ diffuses out (Colom et al., 1998; Dallaporta et al., 1998; Yu et al., 1997) causing cell swelling, and membrane depolarization (Golstein and Kroemer, 2007; Shimizu et al., 1996). Altered ion homeostasis and membrane depolarization also lead to a voltage-dependent influx of cytosolic Ca^{2+} ions initially due to a release of intracellular stores, and later as a result of increased influx

across the plasma membrane and failure of the Ca^{2+} pump. Perturbation of Ca^{2+} homeostasis activates several deleterious processes, such as activation of Ca^{2+} phospholipases that target subcellular structures including the plasma membrane, cytoskeleton, mitochondria, and nucleus. Ultimately, prolonged ischemic events lead to irreversible damage to mitochondrial and lysosomal membranes, triggering cell death by either apoptosis or necrosis (Golstein and Kroemer, 2007; Shimizu et al., 1996)

Although hypoxic ATP production can be temporarily maintained through the activation of anaerobic metabolism (i.e. anaerobic glycolysis), finite stores of fermentable substrates impose a limit on glycolysis as a long term solution to O_2 deprivation in hypoxia-intolerant species (Hochachka, 1986). Conversely, hypoxia-tolerant species adopt various physiological and behavioural mechanisms which moderate the O_2 transport cascade to protect cells against hypoxic injury. Indeed, the developing picture of hypoxia tolerance comprises a common set of physiological adaptations which maximize O_2 delivery to respiring cells, decrease O_2 demand, or sustain the use of alternative, anaerobic metabolic pathways. Such hypoxic adaptations may manifest as increased sensitivity of O_2 sensing systems (Vizek et al., 1987), structural modifications to O_2-carrying haem proteins (Storz and Moriyama, 2008), alterations of perfusion (e.g. heart rate and stroke volume) (Giussani et al., 1993) or ventilation (Powell et al., 1998), reduced basal metabolic rates (Guppy et al., 1994; Jackson, 1968), lowered body temperatures (T_b) (Gordon and Fogelson, 1991), or large glycogen stores (Bickler and Buck, 2007; Jackson et al., 2000). Perhaps the most common initial responses to hypoxic stimuli are reflex changes to metabolic and respiratory activity—referred to as the hypoxic metabolic response (HMR), and the hypoxic ventilatory response (HVR), respectively. While all animals exhibit distinct HVRs

and HMRs, they represent two areas in which hypoxia-tolerant animals may adapt to survive in their hypoxic environments.

1.2 The Hypoxic Metabolic Response

A unifying feature of hypoxia tolerance is a global reduction in metabolic energy expenditure otherwise known as metabolic rate depression (Grieshaber et al., 1994; Hochachka, 1986; Hochachka and Lutz, 2001). During metabolic rate depression, metabolic rate is reduced anywhere from 20 to 99% depending on the species, stage of maturation, and intensity of stimulus (Buck and Hochachka, 1993; Buck et al., 1993; Guppy and Withers, 1999; Jackson, 1968; Pamenter et al., 2014). Metabolic rate depression is achieved through the suppression of major behavioural, physiological, or biochemical energy sinks and is a response to hypoxia which is conserved across virtually all major animal phyla (Guppy and Withers, 1999; Hochachka, 1986; Hochachka et al., 1996).

For example, the hypoxia-intolerant laboratory mouse and the Liukiu Island flying fox—adapted for the high metabolic requirement of flight—experience a 29% and 91% reduction in metabolic rate in response to the same level of hypoxia (10% O_2), respectively (Frappell et al., 1992). In comparison, many anoxia-tolerant insects support overwintering by suppressing their metabolism to <10% of aerobic values (Hoback and Stanley, 2001). When exposed to 6% O_2, the Dover sole exhibits a 48% reduction in metabolic rate, but only a 27% reduction in 12% O_2 (Van Thillart et al., 1994). Although it appears the direct effects of age on metabolic depression has not been assessed, two studies on metabolic depression in cats reveals newborn animals may possess greater tolerance to hypoxia. For instance, newborn kittens respond to hypoxia (15 and 10% O_2) with a 27% and 39% reduction in metabolic rate respectively (Frappell et al., 1991),

while adult cats exposed to 12% O_2 only experience a 20% reduction in metabolic rate (Gautier et al., 1989).

To achieve metabolic rate depression, the onset of hypoxia and metabolic suppression is commonly accompanied by an overall decrease in skeletal muscle movement and an increase in behavioral strategies that reduce thermoregulatory set points and facilitate heat loss. Reductions in T_b facilitate metabolic rate depression both by reducing temperature-dependent O_2 utilization, and through the high Q_{10} effect associated with aerobic metabolism (Krogh, 1914). In most vertebrates, whole-body metabolic expenditure is halved for every 10ºC fall in T_b due to Q_{10} effects. In other words, for each 1ºC reduction there is an associated energetic saving of 11% (Skovgaard et al., 2010; Wood, 1991). To exploit these temperature effects on metabolism and minimize energy expenditure, freshwater fish (Bryan et al., 1984; Schurmann et al., 1991), reptiles (Hicks and Wood, 1985), rats (Gordon and Fogelson, 1991; Wood, 1991), and other animals will actively select an lower ambient temperature (T_a) to facilitate a reduction in T_b. In the absence of cold-selection, some animals—like the golden-mantled ground squirrel—reduce T_b by suppressing cold-induced shivering during hypoxic episodes (Barros et al., 2001). In contrast, neonatal mammals possess limited shivering thermogenesis capacity and so reduce conspecific interactions (huddling)—instead adopting postures which increase evaporative heat loss in response to hypoxia (Mortola and Feher, 1998).

Given sufficient hypoxic stimulus, metabolic rate can be depressed beyond standard or basal metabolic rate through reductions in major ATP-consuming pathways. For example, mitochondrial proton leak and non-mitochondrial respiration are responsible for approximately 20% of resting metabolic rate (Rolfe and Brown, 1997). The remaining 80% that is coupled to ATP consumption includes protein synthesis (25-40%), Na^+/K^+-ATPase (19-28%), Ca^{2+}-ATPase

(4-8%), gluconeogenesis (7-10%), actinomyosin-ATPase (2-8%), and ureagenesis (3%) (Rolfe and Brown, 1997; Storey and Storey, 2004; Storey and Storey, 2007). In effect, these ATP-consuming cellular activities possess different energetic requirements and are thus arranged in a hierarchy of O_2-sensitivity (Buttgereit and Brand, 1995). For instance, studies have demonstrated that macromolecular biosynthesis pathways are more sensitive to ATP availability during hypoxia than transmembrane ion pumping (Buc-Calderon et al., 1993; Buttgereit and Brand, 1995). Therefore, one of the first consequences of hypoxic metabolic reprogramming is an inhibition of new protein and RNA synthesis—translational arrest and transcriptional arrest, respectively—to favour osmotic and ionic homeostasis (Rolfe and Brown, 1997). Indeed, a 65-90% reduction in the rate of protein turnover has been observed in marine invertebrates like brine shrimp and intertidal snails (Larade and Storey, 2002a; Larade and Storey, 2002b), as well as anoxic turtles (Fraser et al., 2001), and hibernating mammals (Bocharova et al., 1992; Osborne et al., 2004; Van Breukelen and Martin, 2002) in response to hypoxia.

Severe and sustained hypoxia imposes a boundary to long-term transcriptional and translational arrest and thus reductions in the activity of ion-motive ATPases may further support hypoxic survival. During periods of reduced ATP production, cells are unable to maintain ATP-dependent ion pumping and thus reducing passive diffusion of ions through ion channels would both reduce the energetic burden of Na^+ and Ca^{2+} pump activity and maintain ionic integrity during O_2 limitation (Hochachka, 1986). O_2 lack therefore initiates an adaptive decrease of ion-channel densities and/or channel leak activities, which reduces cell membrane permeability, a phenomenon commonly known as channel arrest. Channel arrest is one of the first concepts proposed underlying hypoxic metabolic rate depression, and has been characterized in some species of anoxia-tolerant fish and turtles (Buck and Bickler, 1995; Pamenter et al., 2008; Pék

and Lutz, 1997; Wilkie et al., 2008). Additionally, some animals—such as anoxia-tolerant turtles—also experience a downregulation of firing rates or synaptic transmission involving localized channel suppression ('spike arrest') which suppresses cellular metabolism of the brain by 50-80% (Doll et al., 1991; Pamenter et al., 2011; Sick et al., 1993).

At the onset of metabolic rate depression, hypoxia may also shunt resources away from oxidative phosphorylation toward anaerobic glycolytic pathways, a shift known as the Pasteur effect (Hochachka, 1986). In the presence of sufficient glycogen, specific hypoxia-adapted organisms (e.g. Crucian carp) are able to circumvent the detriments of anaerobic metabolism and support sustained glycolysis through improved substrate recycling and an increased capacity to sequester or tolerate acidic end products (Bickler and Buck, 2007; Jackson et al., 2000). For example, goldfish and Crucian carp deal with the byproducts of anaerobic metabolism by converting lactic acid into ethanol which is then excreted across their gills (Johnston and Bernard, 1983; Shoubridge and Hochachka, 1980).

Hypoxia-tolerant animals may also turn to alternative combustible fuels to optimize mitochondrial respiration in hypoxic conditions (e.g. lipid *vs* carbohydrate metabolism) (Ainscow and Brand, 1999; Schippers et al., 2012). Relative to the oxidation of lipids, the oxidation of carbohydrates produces a lower overall yield of ATP per unit of fuel, but also consumes less O_2 in the process. This has led to the suggestion that hypoxic exposure promotes an increased dependence on carbohydrates similar to exercise-induced metabolic fuel switches (Brooks et al., 1991; Hochachka et al., 1991; Schippers et al., 2012). However, prolonged cold exposure experienced by many hypoxia-adapted mammals may impose a boundary on long term carbohydrate use in hypoxia due to the requirement of producing body heat by shivering thermogenesis (Vaillancourt et al., 2009; Weber and Haman, 2005). Instead endothermic

homeotherms likely still use lipids during chronic hypoxia which make up more than 80% of the total energy reserves in mammals. This has been demonstrated in high-altitude deer mice, in which prolonged thermogenesis during hypoxic exposure elicits a shift in metabolic fuel use to favour lipids over carbohydrates (Cheviron et al., 2012).

1.3 Hypoxic Ventilatory Response

The control of respiration during hypoxic events is fundamental to the preservation of cellular energy homeostasis. Reflex changes in ventilation in response to a decline in O_2 availability are known as the HVR. The HVR of vertebrates is diverse comprises a series of complex, time-dependent modulations which are often difficult to compare within and between species (Powell et al., 1998). Even studies replicated with the same methodology yield discrepancies between the same species. Despite these difficulties, well-documented ventilatory patterns have been described. These are typically divided into responses to transient acute hypoxic episodes, and responses to repetitive intermittent or sustained hypoxia.

The acute HVR involves an immediate augmentation of minute ventilation ($\dot{V}_E$) at the onset of hypoxia (within one breath) as a result of reflex changes in breathing frequency (f_R) and/or tidal volume (V_T) (Pamenter and Powell, 2016). Following the termination of the hypoxic stimulus, these ventilatory parameters rapidly return to baseline. To date, almost all adult mammals studied increase ventilation in response to decreased arterial O_2 saturation (P_aO_2) (reviewed in Powell 1998); however, the underlying changes in f_R versus V_T and the physiological mechanisms behind them are highly variable between species, strain, and hypoxic stimulus (Bouverot and Hildwein, 1978; Mitchell et al., 2001; Pamenter and Powell, 2016; Pamenter et al., 2015). Alternatively, in most neonatal mammals, acute hypoxia produces a

biphasic respiratory response—i.e. a temporary increase in ventilation followed by a rapid cessation of breathing movements (Mortola et al., 1989).

1.4 Hypoxia Inducible Factor-1

Survival in sustained hypoxia depends on the activation of O_2-sensitive genes that support energy homeostasis through increased O_2 tissue delivery, reduced ATP demand, and/or improved glycolytic ATP production (Semenza, 1999). Hypoxic gene regulation requires several transcription factors which are first regulated by O_2 themselves, and which possess recognition site specificity within gene-target binding domains. HIFs are one such, highly conserved, family of transcriptional activators initially identified in a pioneer study led by Semenza and Wang in 1992. In meeting the aforementioned prerequisites for transcription, HIF activity is inducible in an O_2-dependent, post-translational manner and subsequently binds to DNA to initiates transcription.

The transcriptionally active form of HIF is a heterodimeric protein complex consisting of one of three O_2-labile α-subunits (HIF1α, HIF2α, or HIF3α) and a β subunit called aryl hydrocarbon receptor nuclear translocator (ARNT) (Figure 1.2). Both HIFα and HIFβ belong to the basic helix-loop-helix (bHLH)/Per-ARNT-Sim (PAS) family of transcription factors. The PAS domain contains approximately 300 amino acids and operates in conjunction with the primary HLH interface to mediate protein-protein interactions and α/β dimerization (Jiang et al., 1996; Wang et al., 1995). Under well-oxygenated conditions, HIFα is rapidly hydroxylated on at least one of two conserved proline residue within the O_2-dependent degradation domain (Pro-402 and/or Pro-564) by members of the EGL-9/prolyl hydroxylase (PHD) superfamily of Fe(II)- and 2-oxoglutarate-dependent dioxygenases (Epstein et al., 2001). These hydroxyproline

substitutions within the O_2-dependent degradation domain label HIFα subunits for proteasomal degradation under normoxic conditions.

Three novel HIF prolyl hydroxylase enzymes (PHDs 1,2,3) have been identified, of which PHD2 appears to be the most important in regulating α-subunits (Epstein et al., 2001). PHDs require Fe^{2+}, O_2, and 2-oxoglutarate to yield the proline hydroxyl groups. During hydroxylation, one oxygen atom is used in the oxidative decarboxylation of 2-oxoglutarate yielding succinate and CO_2, and the other is incorporated directly into the hydroxyl group bound to HIF1α (Hewitson et al., 2002; McNeill et al., 2002). Once hydroxylated, HIFα is captured by the β-domain of the von Hippel-Lindau tumor suppressor protein (pVHL), the substrate recognition component of the Elongin BC/Cul2/pVHL (E3) ubiquitin-ligase complex (Ivan et al., 2001; Kornitzer and Ciechanover, 2000; Maxwell et al., 1999). As a result, given sufficient O_2 availability, HIFα is polyubiquitylated on hydroxyproline substitutions and subjected to degradation by the 26S proteasome.

VHL disease is an inherited multisystem cancer syndrome first discovered in 1894 which is characterized by a mutation in the VHL binding domain. The clinical hallmarks of VHL disease include a high degree of vascularization in the brain and spinal cord leading to hemangioblastomas (blood vessel tumors). The potential connection between dysfunctional pVHL and the constitutive expression of a large number of hypoxia inducible genes such as vascular endothelin growth factor (VEGF) led to the discovery that VHL was indeed necessary for proteasomal degradation of HIF1α (Kaelin and Maher, 1998). Studies have since supported its participation in the negative regulation of HIFα by demonstrating biallelic or genetic inactivation ($VHL^{-/-}$) as well as pharmacological antagonism of VHL stabilizes HIFα in normoxia (Kaelin and Maher, 1998; Maxwell et al., 1999).

Under O_2-deprived conditions, PHD catalytic activity is interrupted, allowing HIFα to escape recognition by the pVHL ubiquitin-ligase complex (Ivan et al., 2001). When stabilized, HIFα is translocated to the nucleus, where it associates with nuclear ARNT. The HIF dimer then recruits the general transcriptional activator CREB binding protein (CBP)/p300 which interacts with the carboxy-terminal transactivation domain, and the completed complex binds to hypoxia response elements (HREs) represented by a core consensus sequence (5'-RCGTG-3') present in the promoter region of hypoxia-inducible genes (Figure 1.2)(Jiang et al., 1996; Semenza et al., 1996). The discovery that transcription factors binding to this sequence could be induced by hypoxia led to an avalanche of new insights into O_2-regulated gene expression (Wang and Semenza, 1995; Wang et al., 1995). Since its discovery, hundreds of hypoxic survival genes have been demonstrated to be inducible by HIF.

Interestingly, asparaginyl hydroxylase—otherwise known as factor-inhibiting HIF (FIH)—further contributes to O_2-dependent regulation of HIF (Ivan et al., 2001; Webb et al., 2009). At sufficient O_2 tensions, an asparagine residue (ASP-803 in humans) is hydroxylated, preventing the interaction of HIF with CBP/p300 and thereby reducing HRE binding activity (Kaelin, 2005). FIH remains active at lower O_2 concentrations than PHDs suggesting these two enzymes may fine-tune HIF functional activity within distinct tissue-types or target genes at different O_2-dependence profiles (Kaelin, 2005). Additionally, the different affinities of PHDs and FIH for O_2 may explain differences in gene function and adaptive responses in different species groups. Together, the depth of hypoxia required to stimulate a given HIF-responsive gene depends on isoform activity and/or cross-talk with other signaling pathways.

HIF and the HMR

The downstream mechanisms by which HIF1α contributes to metabolic rate depression are only partially understood. However, some research teams have explored a link between HIF1α and mammalian target of rapamycin complex 1 (mTORC1), a serine/threonine kinase that coordinates a variety of cellular functions such as growth, metabolism, and autophagy (Fingar and Blenis, 2004; Sarbassov et al., 2005). Of interest, mTORC1 plays a key role in protein synthesis by phosphorylating a myriad of translational regulators (Reviewed in: Ma & Blenis, 2009). HIF1α has been shown to affect mTORC1 activity during hypoxic episodes by inducing the expression of DNA-damage-inducible transcript 4 (DDIT4, also known as REDD1) (Cam et al., 2010). Overexpression of REDD1 has been shown to significantly inhibit mTORC1 activity, while genetic loss of REDD1 results in a failure to downregulate mTORC1 activity in response to hypoxia (Brugarolas et al., 2004; Corradetti et al., 2005; Sofer et al., 2005). Thus, HIF1α may regulate metabolic rate depression by promoting REDD1 transcription, consequently inhibiting mTORC1-dependent protein synthesis.

It has also been suggested that HIF1α may mediate metabolic depression through a complex relationship between itself and cellular-myelocytomatosis viral oncogene (c-MYC), a central transcription factor involved in cell proliferation and differentiation, growth, apoptosis, and stem cell self-renewal (Dominguez-Sola et al., 2007; Iritani and Eisenman, 1999; Poortinga et al., 2004; Schmidt, 1999). In O_2 depleted conditions, the corresponding increase in HIF1α expression leads to a decrease in the expression of c-MYC (Koshiji et al., 2004; Zhang et al., 2007b). Inhibition of c-MYC has also been associated with a reduction in mitochondrial DNA content (Hervouet et al., 2005), reflecting a reduction in mitochondrial mass and a decrease in O_2 consumption (Li et al., 2005; Zhang et al., 2007b). This pathway is observed in models with

VHL loss of function mutations leading to elevated HIF1α levels (Zhang et al., 2007b). HIF1α may therefore facilitate metabolic rate depression by counteracting c-MYC mediated mitochondrial biogenesis, protein translation, and transcription (reviewed by Gordan *et al.*, 2007; Dang *et al.*, 2008).

Stabilization of HIF1α supports metabolic rate depression by coordinating a shift to anaerobic forms of ATP production through transactivation of genes encoding glucose transporters and nearly all known glycolytic enzymes. Previous studies have demonstrated that the HIF1α complex reprograms glucose metabolism through upregulation of pyruvate dehydrogenase kinase 1 (PDK1), lactate dehydrogenase (LDHA) and monocarboxylate transporter 4 (Firth et al., 1995; Kim et al., 2006; Papandreou et al., 2006; Robey et al., 2005; Seagroves et al., 2001; Semenza et al., 1996; Sowter et al., 2001). PDK1 phosphorylates and inhibits mitochondrial pyruvate dehydrogenase which converts pyruvate to mitochondrial NADH and acetyl-CoA. Together, PDK1, LDHA, and monocarboxylate transporter 4 increase the conversion of pyruvate to lactate, and funnel pyruvate toward the glycolytic pathway and away from the tricarboxylic acid cycle thereby reducing mitochondrial O_2 consumption (Papandreou et al., 2006).

HIF and the HVR

Prolonged or repeated hypoxic challenge elicits progressive increases in ventilation which further improve oxygenation of tissues (Bisgard, 2000; Dwinell et al., 2000). This secondary respiratory response, referred to as ventilatory acclimatization to hypoxia (VAH), represents an important form of plasticity involving time-dependent remodeling of multiple cellular/synaptic mechanisms within the respiratory control system (Powell et al., 1998). The increased HVR

results from both increases in the O_2 sensitivity of the carotid body chemoreceptors (Bisgard, 2000; Smith et al., 1986) as well as changes in the central neural integration and processing of chemoafferent inputs (Dwinell et al., 2000; Powell et al., 2000).

VAH requires sustained hypoxic exposure lasting hours to months, and as such it has been proposed that the mechanisms underlying it are coordinated by changes at the gene level. Indeed, HIF1α protein expression has been shown to increase in the carotid body and CNS respiratory centers of mice after as little as 1 hour of hypoxic exposure (Kline et al., 2002; Pascual et al., 2001). Support for a role of HIF1α in mediating the HVR comes from studies demonstrating mice partially deficient in HIF1α (*Hif*$^{+/-}$) exhibit impaired O_2 sensing by the carotid body, characterized by a reduction in f_R and a depressed neural response to sustained hypoxia (Kline et al., 2002). Furthermore, transgenic mice with a CNS-specific knockout of the HIF1α gene but with fully functional carotid body exhibit a normal acute HVR, but do not experience changes in ventilatory drive or respiratory sensitivity following chronic exposure suggesting HIF1α in the CNS is necessary to VAH (Bavis et al., 2007; Helton et al., 2005).

HIF1α likely contributes to the anatomical remodeling of the chemoreceptor organ through increased transcription of VEGF, receptors associated with VEGF actions, and platelet derived endothelial cell growth factor expression (Jyung et al., 2000; Semenza, 2000b), causing the carotid body to double in size following the hyperplasia, hypertrophy, and increased neovascularization of type I cells (Dhillon et al., 1984; McGregor et al., 1984). VEGF has been suggested to play a role in neural plasticity during VAH through increasing blood vessel density and by eliciting its own downstream pathways (Murakami et al., 2003) which stimulate similar cellular signaling pathways in the brain. Increased VEGF therefore further contributes to ventilatory plasticity during sustained hypoxia (Baker-Herman et al., 2004; Chen et al., 2005).

In theory, these changes are beneficial because they decrease diffusion distance between arterial blood and carotid bodies and therefore increase the speed of responses to hypoxia however this remains to be demonstrated experimentally.

Carotid bodies also express a variety of proteins allegedly involved in O_2 signal transduction, including nitric oxide synthase (NOS) and haem-oxygenase 2 (HO-2). Previous investigations have reported increases in NO production in the carotid body following chronic sustained hypoxia (Di Giulio et al., 1998; Ye et al., 2002). Basal NO released from nerve endings exerts an inhibitory influence on sensory discharge, likely through retrograde signaling on Ca^{2+} channels and subsequent downregulation of carotid body activity. Thus, increased levels of NO—which have been shown to be inducible through HIF1α and its effect on neuronal NOS (nNOS)(Ward et al., 2005)—yield depressive effects on the O_2 sensitivity of the carotid body. The HIF1α-nNOS pathway would therefore contribute to the hypoxic desensitization of the carotid body, which has been documented in several species following chronic hypoxic exposure (Bisgard, 2000; Powell et al., 1998).

It is recognized that carbon monoxide (CO) can act as a chemical messenger to increase carotid body activity and subsequently ventilatory drive in hypoxia, through upregulation of HO-2. This antioxidant enzyme requires nicotinamide adenine dinucleotide phosphate (NADPH) and O_2 as co-factors to catabolize haem into CO, biliverdin, and iron (Williams et al., 2004). Under hypoxic conditions, CO generation through HO-2 haem degradation decreases, leading to a reduction in channel activity, channel closure, membrane potential depolarization, and finally neurotransmitter release (Prabhakar et al., 1995). HIF1α has been shown to mediate a decrease in HO-2 expression while promoting increases in the expression of inducible HO (HO-1), which

would lead to a decrease in CO production, and consequently an increase in respiration (Dawn and Bolli, 2005; Lee et al., 1997; Neubauer and Sunderram, 2012).

ET-1 is a vasoconstrictor that increases in the carotid body (Chen et al., 2002a) as well as the pulmonary artery (Li et al., 1994) following chronic hypoxia. ET-1 and its receptor ET_A are widely distributed throughout the CNS (Giaid et al., 1989; Lee et al., 1990; Takahashi et al., 1991; Yoshizawa et al., 1990) and has been to shown to release various neuropeptides (Levin, 1995; Masaki, 1995; Webb et al., 1998) involved in neurotransmission and/or neuromodulation within the CNS. ET-1 may therefore potentiate chemoreceptor responses by activating second messenger systems which promote hypoxia-evoked intracellular Ca^{2+} responses and voltage-gated Ca^{2+} currents (Chen et al., 2000) and which may enhance future hypersensitivity and ventilatory drive. Under the influence of HIF1α, ET-1 expression increases and markedly augments the hypoxic sensory response (Chen et al., 2002b). For example, treatment with an ET_A inhibitor in isolated rat carotid bodies reduced chronic hypoxia-induced increases in chemosensitivity by 50% (Chen et al., 2002a). Moreover, ET-1 heterozygous knockouts exhibit a blunted HVR (Kuwaki et al., 1996).

A growing body of evidence implicates HIF1α as a transcriptional regulator of the adenosine receptor, A2B (Eckle et al., 2014; Kong et al., 2006; Sitkovsky et al., 2004). Adenosine is a purine nucleoside synthesized within mammalian cells and released into the extracellular fluid where it acts as either a respiratory stimulant or depressant during conditions of hypoxic stress (Griffiths and Holgate, 1990). For example, the activation of adenosine receptors in the carotid body has a stimulant effect and increases ventilation in the cat (McQueen and Ribeiro, 1986) human (Watt and Routledge, 1985) and rabbits (Buss et al., 1986). In contrast, increased concentrations of adenosine in the CNS have been demonstrated to exert

depressive effects on pulmonary ventilation including decreases in both f_R, V_T, and ventilatory drive (Hedner et al., 1982; Heitzmann et al., 2016). These effects are mediated by specific adenosine receptors (A1 and A2) located on the outer surface of the cell membrane (Fredholm, 1982). In awake rats, A1 and A2 agonism reduced $\dot{V}_E$ by 65-75%, whereas antagonism of these receptors reversed their respiratory depressant effects (Murphy et al., 1993).

Chuvash polycythemia

Mutations in the VHL-HIF signaling pathway are historically associated with an increase in ventilatory activity. For example, these mutations characterize an autosomal recessive disorder in humans called chuvash polycythemia (CP). The mutations underlying CP diminish the binding affinity of VHL for hydroxylated HIF1α, partially inhibiting its normoxic degradation (Ang et al., 2002). As a consequence of chronic systemic elevation of HIF, CP is characterized by elevated basal $\dot{V}_E$ and an enhanced acute HVR without prior exposure to hypoxia (Smith et al., 2006). For example, in CP-engineered mice, hypoxia (10% O_2) elicits a significant 2.2-fold increase in $\dot{V}_E$ relative to controls, similar to mice exposed to episodic or chronic hypoxia (Hickey et al., 2010; Slingo et al., 2014). The ventilatory changes observed in CP mice are accompanied by structural alterations in carotid-body morphology including the number and size of type I cells (Slingo et al., 2014), further demonstrating a role for HIF1α in HVR.

1.5 African Naked Mole Rats

Subterranean mammals possess multiple highly specialized physiological and biochemical systems to cope with life underground. Sealed burrows offer protection from predators and harsh weather conditions but expose inhabitants, particularly social species, to varying degrees of

hypoxic and hypercapnic challenge due to group respiration and limited soil permeability (Jarvis et al., 1991; Shams et al., 2005; Withers, 1978). As a result, common adaptations among fossorial mammals include low basal metabolic rates, high ranges of thermoneutrality and low T_bs , and often poor thermoregulatory capacity (Bennett et al., 1993; Bennett et al., 1994; Contreras and McNab, 1990; McNab, 1979; McNab, 1983). In adapting to the subterranean niche, these animals have also evolved complex adaptive respiratory and blood-gas properties that allow them to optimize O_2 delivery during hypoxic exposure (Johansen et al., 1976; Shams et al., 2004; Weber et al., 2017).

African naked mole rats are one such underground rodent native to Eastern Africa which have received significant attention from researchers studying hypoxia tolerance. Contrary to reports from other subterranean burrows, such as those of the middle east blind mole rat which experience chronic hypoxia as low as 6% (Shams et al., 2005), naked mole rats live in well-ventilated burrow systems where O_2 tensions are closer to ambient air (Holtze et al., 2017). Instead, naked mole rats likely encounter acute or sustained hypoxic episodes during digging activity, or during conspecific huddling in their large colony sizes of up to 280 members (Jarvis et al., 1991). Despite these reports, naked mole rats have been reported to withstand 3%-5% O_2 (Nathaniel et al., 2012; Pamenter et al., 2018; Park et al., 2017) and 80% CO_2 (Park et al., 2017) for several hours in a laboratory setting, suggesting they are one of the most hypoxia-tolerant mammal described to date (Johansen et al., 1976; Pamenter et al., 2015; Park et al., 2017).

African naked mole rats possess a number of physiological and biochemical defense strategies which prevent otherwise lethal hypoxic cellular injury including a modified haemoglobin structure that increases the O_2 binding affinity and unloading efficiency of red blood cells (a P_{50} of 23 mmHg compared to 33 mmHg in mice) (Johansen et al., 1976; Weber et

al., 2017), mass-specific metabolic rates around 30% lower than what would be predicted from allometry (Buffenstein and Yahav, 1991), lower T_bs relative to similar sized rodents (Nathaniel et al., 2012), and blunted neuronal Ca^{2+} influx during hypoxia (Peterson et al., 2012).

Similar to other hypoxia-tolerant species, naked mole rats respond to low O_2 availability with a substantial and reversible suppression of metabolic rate, thereby reducing ATP consumption and O_2 demand (Kirby et al., 2018; Pamenter et al., 2015). Remarkably, these animals also undergo a matched *decrease* in total $\dot{V}_E$ and therefore do not express the hypoxia-mediated increase in their air convection requirement (ACR; $\dot{V}_E:\dot{V}O_2$) typical to other mammals (Pamenter et al., 2015): i.e. do not hyperventilate in sustained hypoxia. This respiratory response would thereby reduce the high metabolic cost associated with increased ventilatory activity.

Recent genomic analysis conducted by Kim *et al.* (2011) may provide insight into the ability of naked mole rats to downregulate $\dot{V}_E$ and metabolism in response to hypoxia. The team uncovered two point mutations within the functional site of the VHL binding domain of naked mole rats. Both threonine at position 407 as well as valine at position 166 have both been substituted for leucine (Kim et al., 2011), suggesting a relaxation of the ubiquitin-dependent degradation of HIF1α, and a subsequent increase in the stabilization of HIF1α (Figure 1.3). In theory, HIF1α downstream gene targets would then be chronically upregulated in normoxia similar to that observed in a close relative (middle east blind mole rat), which possess higher normoxic HIF1α and EPO protein expression relative to hypoxia-intolerant rats (Shams et al., 2004). This elevated expression of HIF1α may thus contribute to the atypical adaptive responses of naked mole rats through transcriptional regulation of downstream genes.

1.6 Objectives and Hypotheses

Naked mole rats present an invaluable model in which to study hypoxic adaptation. As their basic physiological responses to hypoxic exposure become better characterized, we turn our attention toward the mechanisms underlying those responses and how they might contribute to our understanding of hypoxic illness and injury. Specifically, naked mole rats may provide insight into how elevated HIF1α expression translates acute hypoxic stress into beneficial metabolic and respiratory responses. This thesis aims to determine: a) the functional effect of the VHL mutation possessed by naked mole rats compared to mice, b) the degree of involvement of HIF1α in the acute HVR and HMR of naked mole rats, and c) the effect of HIF1α stabilization on the HVR and HMR of mice.

1.3.1 ***Objective 1:*** *Profile baseline expression of HIF1α in African naked mole rats relative to mice*

Hypothesis 1: Naked mole rats express elevated baseline HIF1α protein levels relative to mice due to a pVHL mutation.

The following thesis tests this hypothesis by measuring basal HIF1α protein expression in naked mole rats and mice using immunoblotting. One of the goals of this study is to determine if the mutations presented by Kim *et al*. correspond to compromised VHL activity and increased HIF1α protein levels in normoxia.

1.3.2 ***Objective 2:*** *Profile the role of HIF1α in the HVR and HMR in naked mole rats through pharmacological inhibition*

Naked mole rats, which may possess elevated HIF1α levels, do not hyperventilate in hypoxia and instead experience ventilatory decline accompanied by matched reductions in their metabolic rate (Kirby et al., 2018; Pamenter et al., 2015). Previous studies have demonstrated inhibitory adenosinergic signaling likely mediates the HVR of naked mole rats (Pamenter et al., 2015), but this mechanism has been ruled out as contributing to the HMR. Other studies have also ruled out GABAergic signaling as mediating acute hypoxic metabolic changes (Chung et al., 2016), although it may inhibit metabolic plasticity in animals breathing normoxic air following exposure to chronic sustained hypoxia. Therefore, an opportunity exists to better characterize the underlying mechanisms governing the HMR of naked mole rats.

Hypothesis 2: Endogenous expression of HIF1α contributes to the ventilatory and metabolic responses of naked mole rats through increased baseline expression of downstream targets. We predict that ventilatory and metabolic compensation to acute hypoxia will be altered in mole rats treated with a pharmacological HIF1α inhibitor prior to exposure to hypoxia.

This thesis tests this hypothesis by measuring ventilatory and metabolic changes in naked mole rats treated with either saline or a HIF1α antagonist and subsequently challenged with acute hypoxic stress (7% O_2 for 1 hour). We also measure changes in HIF1α mRNA expression, as well as downstream targets: VEGF, glucose transporter 1 (GLUT-1), and endothelin-1 (ET-1) through qPCR to validate drug efficacy.

1.3.3 ***Objective 3*****:** *Characterize HIF1α involvement in the HVR and HMR through pharmacological* HIF1α *stabilization in mice*

We sought to determine if normoxic stabilization of HIF1α would yield a naked mole rat-like HVR or HMR. Research shows HIF1α increases in the carotid body and CNS respiratory centers of mice after as little as 1 hour of hypoxia (Pascual et al., 2001). Furthermore, mice partially deficient for HIF1α show reduced O_2 sensing and signal transduction ability as well as decreased ventilatory drive to sustained hypoxia (Kline et al., 2002; Peng et al., 2006). Conversely, systemic treatment of mice with a PHD inhibitor (ethyl-3,4 dihydroxybenzoate (EDHB)) leads to an increase in ventilation as a result of changes in V_T (Hodson et al., 2016) as well as decreases in normoxic metabolism (Aragonés et al., 2008).

Hypothesis 3: Normoxic stabilization of HIF1α will mimic hypoxic preconditioning and either cause a progressive increase in ventilatory activity or lead to hypoxic desensitization due to an upregulation of HIF1α downstream targets. PHD inhibition will affect normoxic metabolism and may, to a lesser extent, result in changes in the HMR.

This thesis tests this hypothesis by measuring ventilatory and metabolic changes in mice treated with either saline or EDHB and subsequently exposed to an acute hypoxic stress (7% O_2 for 1 hour). We also measure changes in HIF1α mRNA expression, as well as downstream targets: VEGF, GLUT-1, and ET-1 through qPCR to validate drug efficacy.

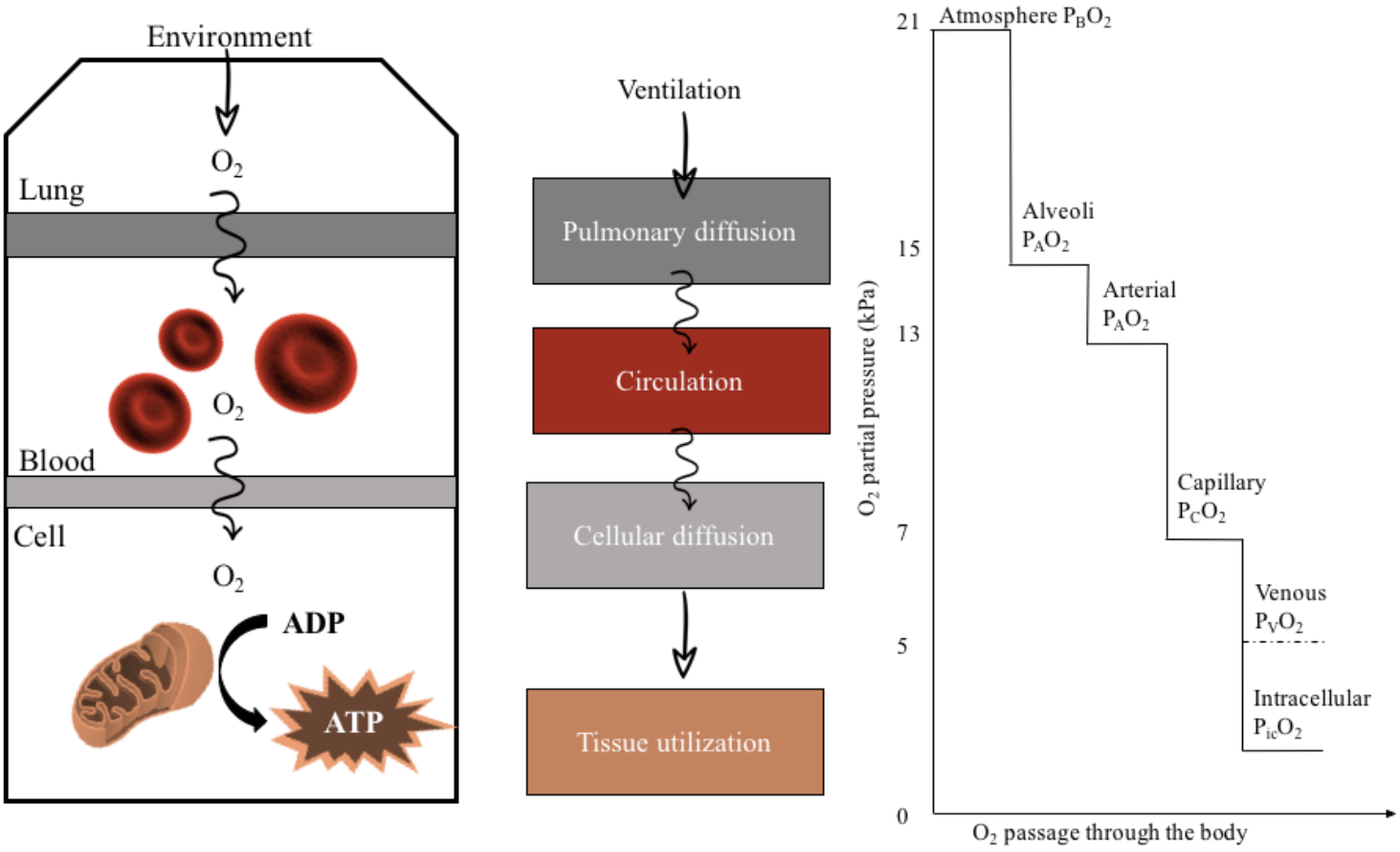

Figure 1.1 The O_2 transport cascade (adapted from Storz *et al.*, 2010). O_2 is passively transported from air to mitochondria along a pathway of convective, diffusive, and biochemical barriers with each step progressively lowering O_2 tensions until they are utilized by tissues to generate ATP.

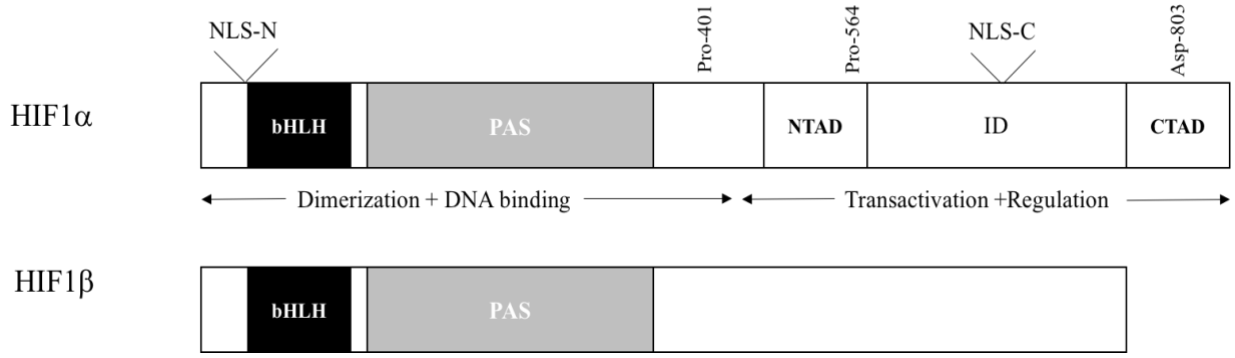

Figure 1.2 Structure of (human) HIF1 modified from (Semenza, 2000a). Functional domains of α and β subunits: bHLH and PAS domains, hydroxylation sites of prolyl and asparagyl hydroxylases Pro-401 and Pro-564, Asp 803.

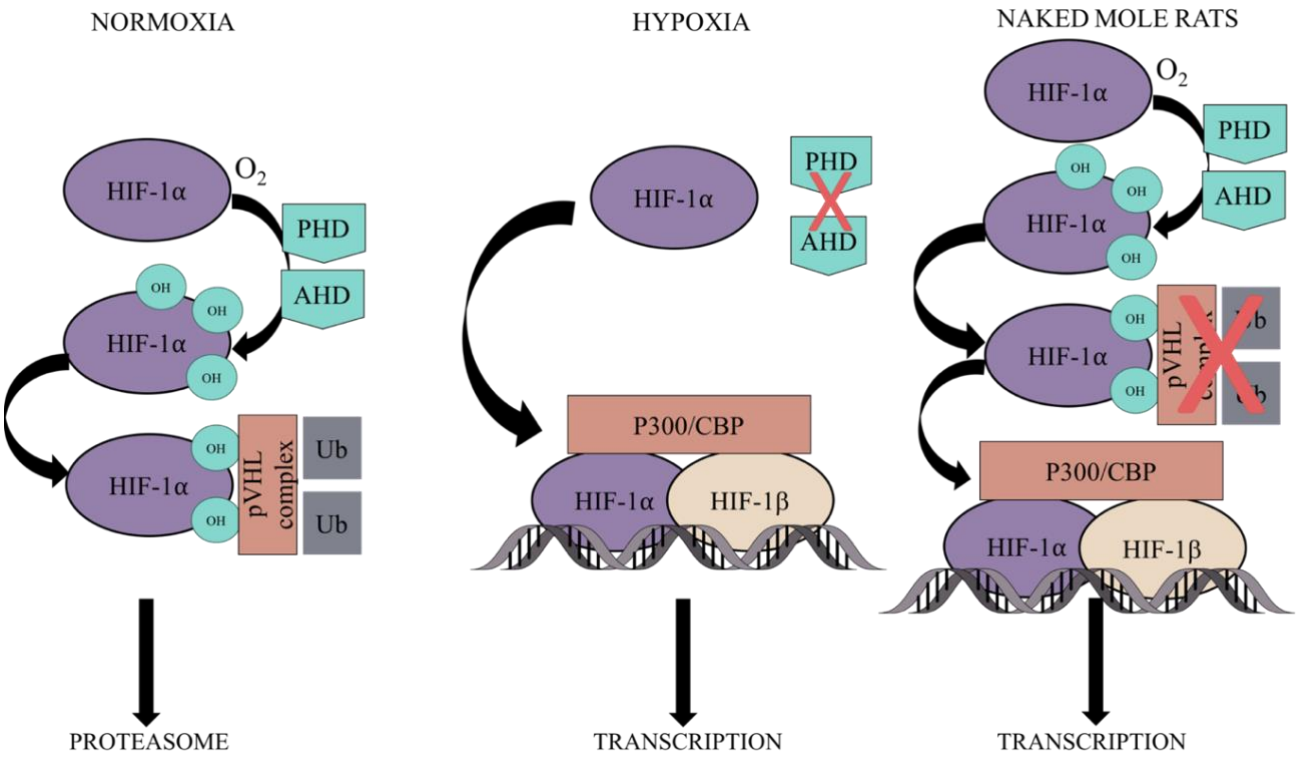

Figure 1.3 Hypoxia-inducible factor (HIF) degradation in normoxia (a), compared with HIF stabilization in hypoxia (b), and putative mechanism of stabilization in normoxia in naked mole rats (c) (Borecky and Pamenter, 2017). HIFα subunits are hydroxylated by prolyl hydroxylase (PHDs) in normal O_2 tensions and subsequently bound by the pVHL-E3 ligase complex, triggering their degradation by the proteasome. During hypoxia, hydroxylation of HIFα cannot take place sparing it from destruction. In turn, HIF is translocated into the cellular nucleus where it dimerizes with HIFβ before binding to hypoxic response elements (HREs) within DNA to facilitate transcription. In naked mole rats, a mutation in their von Hippel Lindau protein (pVHL) binding domain suggests a relaxation of HIF-pVHL binding and thereby increased HIFα stabilization in normoxia.

Chapter 2

MATERIALS AND METHODS

2.1 Animals and Ethics

Captive colonies of African naked mole rats (*Heterocephalus glaber)* were bred and maintained within the Animal Care and Veterinary Services center at the University of Ottawa, Canada. Animals were group-housed within artificial burrow systems in rooms held at 28°C in 70% humidity under a 12:12 hour dim light-dark photoperiod. The burrow systems consist of multiple, interconnected cages to simulate their natural underground burrow environment. Naked mole rats were fed a Pronutro cereal supplement containing vitamins and minerals, as well as fresh fruit, vegetables, and tubers, *ad libitum*. Animals were identified using micro LifeChip Bio-Thermo Technology (Destron Fearing^{TM}, Eagan, MN, USA), which also allowed for regular temperature sampling (see below).

Male and female BALB/c mice of 8 to 10 weeks of age, bred in the animal care facilities at the University of Ottawa were used for tissue analysis and plethysmography experiments. Mice were housed in standard ventilated cages in groups of two to four and held at room temperature under a 12:12 hour light-dark photoperiod according to institutional guidelines. Mice were fed Purina Rodent Chow (Purina LabDiet, St. Louis, MO). Mice were identified on a per-cage, per-treatment basis or using permanent marker as required, remarked when needed.

All pharmacological procedures and experimental protocol (#BL-2535) were in compliance with the requirements established by Canadian Council on Animal Care and approved by the University of Ottawa Animal Care Committee.

2.2 Experimental design and pharmacology

In total, 26 male and female non-breeding, adult naked mole rats weighing 41.5 ± 0.8 g were randomly divided into three experimental groups and intraperitoneally administered either

(i) saline (n = 8), (ii) echinomycin dissolved in 5.0% DMSO diluted with saline (0.5 mg kg^{-1}, n = 8 and 1.0 mg kg^{-1}, n = 6), or (iii) PX-478 dissolved in saline (80.0 mg kg^{-1}, n = 4) every two days for a period of seven days (total of three injections). All drugs were made up to ensure a volume of 0.3-0.4 mL. Echinomycin was purchased from Sigma-Aldrich (SML0477, St.Louis, MO, USA).

Originally isolated from *Streptomyces echinatus*, echinomycin is a cyclic peptide belonging to the family of quinoxaline antibiotics. Echinomycin selectively inhibits HIF1 dimer recognition of HRE promoter region sequences through sequence-specific DNA intercalation (Fox and Kentebe, 1990; Kong et al., 2005; Onnis et al., 2009). Echinomycin has been shown to block lymphoma and acute myelogenous leukemia growth (Wang et al., 2014) as well as HIF-mediated induction of ovulation in rats (Wang et al., 2012), making it a promising pharmacological agent for use in this study The dosing strategy for echinomycin was chosen based on similar literature values used to inhibit HIF1 activity in mice (Pan et al., 2015; Wang et al., 2012; Wang et al., 2014). A second, lower dose was selected to address and minimize toxicity symptoms observed in our high dose dataset (0.5 mg kg^{-1}). PX-478 (Cat. #: S7612, Selleckchem, Houston, TX, USA) was selected to validate echinomycin trials. PX-478 was initially identified through a screen for compounds that lowered cellular HIF1α levels. Although its mechanism of action is unknown, it is believed to operate through translational inhibition similar to echinomycin and independently of O_2, pVHL, or p53 (Koh et al., 2008). Decreased HIFα protein levels have also been observed following treatment with PX-478 (Koh et al., 2008) and echinomycin (Vlaminck et al., 2007).

In total, 20 mice weighing on average 30.5 g ± 0.8 g were divided into two groups and received intraperitoneal injections of either (i) saline (n = 12), or (ii) EDHB dissolved in 5.0%

DMSO diluted with saline (180.0 mg kg^{-1}, n = 8) up to a maximum volume of 0.5 mL every second day for one week (total of three injections). EDHB (Cat. #: 23223, Sigma Aldrich) is a polyphenolic compound found in common plants which acts as an analog of the substrate α-ketoglutarate. By virtue of its competition for PHD, EDHB acts as an inhibitor of PHD activity and thus prevents HIF1α degradation by VHL-E3 ligase complex and therein promotes transcription of HIF1α downstream targets in normoxia. EDHB and associated dosing strategies were selected based on a previous study which demonstrated increased viability and enhanced exercise performance in EDHB-treated mice subjected to sub-lethal and lethal levels of hypoxia (8% and 5% respectively) (Kasiganesan et al., 2007).

2.3 Plethysmography and respirometry

Ventilatory responses to sustained hypoxia were monitored using a whole-body plethysmograph consisting of two rectangular 450.0 mL Plexiglas chambers connected via a differential pressure transducer (DP103, Validyne, Northridge, CA, USA). Following pretreatment, unrestrained, un-anaesthetized animals were placed into the experimental apparatus. These chambers were flushed with 21% O_2 and were set inside a controlled environmental chamber to maintain temperature at ~28°C for naked mole rats, and ~21°C for mice. Ambient temperature was continuously recorded throughout the experiment using a thermocouple (University of Ottawa, ON, CA) designed specifically for the purposes of this experiment. T_b readings were taken every fifteen minutes using a RFID reader on microchips (Allflex USA Inc., Dallas, TX, USA) subcutaneously implanted in mole rats, and at the end of each treatment period using a rectal thermometer for mice.

Naked mole rats and mice were acclimated to holding conditions for 20-60 minutes prior to beginning the experiment while supplied with air (21% O_2, balance N_2) at a rate necessary to ensure O_2 and/or CO_2 levels did not deviate more than 1.5% as a product of the animal's metabolism (~110 mL min^{-1} for naked mole rats, ~200-300 mL min^{-1} for mice) (Alicat gas mass flow meter, Tuscon, AZ, USA), until they were noticeably relaxed with a stable breathing pattern. Baseline measurements were then made for 1 hour at 21% O_2, after which animals were exposed to hypoxia (7% O_2) for 1 hour, and left to recover (21% O_2) for 1 hour. Each experimental trial took a total of ~4 hours.

As the animal respired, changes in pressure between the experimental and reference chamber representing V_T were amplified, recorded, and stored for further analysis. f_R was determined directly from oscillatory activity caused by the animal's ventilation (average cyclic frequency, multiplied by 60). Prior to each experiment, known volumes of air (0.2, 0.3, and 0.4 mL) were forced into the animal chamber to produce pressure changes (P_{cal}) which were then used in calculations of V_T using equations for the barometric method adapted for continuous flow by Jacky (1980), originally described by Drorbaugh and Fenn (1955).

Excurrent gas from the experimental chamber was passed through a desiccant media before entering the two fuel cell analyzers for O_2 and CO_2 (FC-10 and CA-10 respectively, Sable Systems, Las Vegas, NV, USA). The gas analyzers were calibrated for O_2 and CO_2 before each trial with a premixed gas (21% O_2; 1.6% CO_2 balanced with NO_2). Flow rate was measured using mass flow meters (Alicat Scientific, Tuscan, AZ, USA). Gas exited the chamber by passive flow, and both inflowing and outflowing gas concentrations were measured by the gas analyzers (Sable Systems). Incurrent gas concentrations were checked at the end of each treatment period.

2.4 Tissue collection

The first four animals in each treatment group were euthanized 12-24 hours following experimentation to account for potential hypoxia-induced increases in HIF1α. Eight naked mole rats (control, n = 4; low dose echinomycin, n = 4) euthanized by cervical dislocation. Eight mice (control, n = 4; EDHB, n = 4) were euthanized via CO_2. Tissues were collected and immediately snap-frozen in liquid N_2 and stored at -80°C until processing.

To prepare soluble protein extracts, frozen tissues were ground into a powder over liquid N_2 using a mortar and pestle. Samples were then weighed and 100.0 mg of tissue was added to 200 µl RIPA© buffer (Cat. #: 89901, ThermoFisher Scientific, Waltham, MA, USA). Samples were homogenized using a handheld Tissue Master 125 with 5 mm generator probe (OMNI International, Kennesaw, GA, USA) and centrifuged for 10 minutes at a speed of 13,500 rpm at 4°C. Supernatant was transferred into fresh tubes and stored at -80°C. Extracted protein concentrations were determined via triplicate readings on a microplate reader using Pierce© BioRad Protein Assay (Cat. #: 23223, ThermoFisher Scientific) with Bovine Serum Albumin as the standards. Absorbance readings were measured at 562 nm using BioTek Epoch (Winooski, Vermont, USA) and Gen5 software.

2.5 Immunoblotting

Samples containing 100.0 µg protein mixed with equal parts (1:1 v:v ratio) 2x LaemmLi Sample Buffer (Cat.#: 1610737, BioRad, Hercules, CA, USA) and 10% v:v -mercaptoethanol were heated at 95°C for 3 minutes to denature the proteins. Proteins were loaded onto a 10% SDS-page gel and subsequently separated via electrophoresis at 150 V and ~50 mA in a 1x Tris-glycine resolving buffer (24 mM Tris-HCl, 2 M glycine, 3.5 mM SDS) using a BioRad Mini-

Protean System for 60-90 minutes (BioRad). Aliquots of 10 µl of pre-stained protein molecular weight ladders (Precision Plus Protein™ Standards, Cat. #1610363, BioRad) were run on a gel concurrently with the samples, serving as a molecular weight reference.

Following electrophoresis, protein was transferred onto 0.45 µm PVDF membranes (Immun-Blot, Cat. #: 162-0177, BioRad) fully submerged in 1x transfer buffer (26 mM Tris-HCl, 15 mM glycine, 800 mL methanol,) at 180 mA overnight using BioRad transfer cells. After transfer, PVDF membrane was washed once with 10 mL 1x TBST (20 mM Tris-HCl, 137 mM NaCl, .1% v/v Tween-20, pH 7.6) for 5 minutes at room temperature before blocking membrane in 5% milk for one hour at room temperature. Following blocking, membrane was washed three times for 5 minutes each in 10 mL 1x TBST (10 mM Tris, 150 mM NaCl, 0.1% v/v Tween-20, pH 7.5). Membrane was then incubated with 10 mL HIF1α rabbit mAb (Cat. #: D2U3T, Cell Signalling Technology, Danvers, MA, USA) primary antibody at a dilution of 1:500 v:v antibody: TBST overnight (16-24 hours) at 4°C. Membrane was subsequently washed three times for 5 minutes each in 10 mL of 1x TBST and then incubated with Anti-rabbit IgG, HRP-linked antibody at a concentration of 1:2000 with gentle agitation at room temperature (Cat.#: 7074, Cell Signaling Technology). Membrane was washed again in 10 mL TBST three times, for 5 minutes. Membrane was then exposed to a 600 µL mixture of enhanced luminol reagent and H_2O_2 (1:1 v:v) (Clarity™ Western, Cat.#:170-5060, BioRad) for 5 minutes and then imaged in a Vilber Lourmat Fusion FX (Marne-la-Vallée, Collégien, France) with Fusion 3Mega software.

Membrane was then stripped using mild stripping buffer (20 mM glycine, .3 mM SDS, 5mL Tween 20, pH 2.2) and probed for ß-tubulin (E7-s) (Developmental Studies Hybridoma Bank, Iowa City, IA, USA) at a dilution of 1:5000 v/v antibody: TBST for 30 minutes at room temperature. Membrane was washed three times in 1x TBST and probed with polyclonal goat

anti-mouse HRP (Cat. #: P0447, Agilent, Santa Clara, USA). Membrane was again exposed to 600 μL ECL (Clarity™ Western, Cat. #:170-5060, BioRad) for 5 minutes and imaged. Following imaging, HIF1 bands were quantified through densitometry using AlphaEaseFC software (Alpha Innotech, San Leandro, California).

2.6 qPCR

Control and treatment RNA was isolated using TRIzol™ Reagent (Cat. #: 15596026, ThermoFisher Scientific) as described in the manufacturer's protocol. 1 mL of TRIzol™ Reagent was added to 100mg of tissue and homogenized using a 1 mL syringe with 20-gauge needle, drawing sample up and down until completely homogenized. Samples were then centrifuged for 5 minutes at 13,500 rpm at 4°C and the supernatant was transferred to fresh tubes with 200 μL of chloroform. Sample was hand vortexed for 3 minutes at room temperature before centrifuging again, this time for 15 minutes at 13, 500 rpm at 4°C. The resulting colourless aqueous phase was subsequently transferred to a fresh set of tubes with 500 μL isopropanol and the solution was incubated for 10 minutes on ice. Samples were once again centrifuged at 13, 500 rpm at 4°C after which supernatant was discarded, and pellet was washed in 1 mL of 75% ethanol. Pellets were washed two more times, this time centrifuged at 10,000 rpm. Remaining RNA pellet was air dried for 10 minutes before re-suspending it in 20-50 μL of RNase-free water. RNA samples were stored at -80°C.

RNA concentrations of the samples were determined by OD_{260} measurements using a NanoDrop™ 2000/2000c Spectrophotometer (ThermFisher Sceintific, ND-2000). A total of 2 μg RNA mixed with 375.0 ng random hexamers [Integrated DNA Technologies(IDT), Coralville, IA, USA], 125.0 ng oligo dTs (IDT), and dNTPs (Invitrogen; 0.5 mM final concentration) was

treated with DNase I (Cat#.18068015, ThermoFisher Scientific) and incubated at 65°C for 5 minutes. The reaction was then chilled on ice for 5 minutes and 5x first-strand reaction buffer, dithiothreitol (5 mM final concentration), RNase Out, and nuclease-free water (0.5 µL) (SuperScript™ II Reverse Transcriptase kit, Cat. #: 18064-022, ThermoFisher Scientific) were added before incubating at 42°C for 2 minutes. SuperScript™ II reverse transcriptase (SuperScript™ II Reverse Transcriptase, Cat. #: 18064-022, ThermoFisher Scientific) was added to a total volume of 20 µL, incubated at 42°C for 50 minutes, and inactivated at 72°C for 15 minutes.

Following reverse transcription, the cDNA yield was amplified by adding 1 µL of diluted template (1:5) to a 25 µL total reaction volume containing PCR reaction buffer (Denville Scientific, Holliston, MA, USA; 1× final concentration), dNTPs (ThermoFisher Scientific; 0.2 mM final concentration), 0.15 µl Choice Taq (Denville Scientific), and gene-specific sense and antisense primers (IDT; 0.2 µM final concentrations). Primers for each gene were designed using the National Center for Biotechnology's gene database (Altschul et al., 1990). Primers suitable for qPCR –fragment length 60-150 bp, optimal T_m 65°C, and primer length 19-26 bp were designed within the sequence (Table 2.1). The final qPCR amplicons were sequenced and searched against BLAST to ensure the correct product was amplified.

For PCR, 1 µL of diluted template was added to a 12.5 µl total reaction volume containing 6.25 µL Rotor-Gene SYBR Green PCR master mix (Cat. # 4309155, ThermoFisher Scientific) and 200 nM each gene-specific sense and antisense primer (Table 2.1). Template groups were run in technical duplicate with no template negative controls. For each primer pair, annealing temperature was optimized by gradient PCR. Fluorescence was detected using a Rotor-Gene Q Real Time PCR cycler (Qiagen, Hilden, Germany). Amplification by qPCR was carried out for

40 cycles of 95°C for 5 seconds and 60°C for 10 seconds, and fluorescence readings were acquired at the end of each amplification cycle at 60°C. Melting curve analysis was performed with continuous fluorescence acquisition from 60°C to 95°C. The fold change in expression of each target mRNA (HIF1α, VEGF, GLUT1, ET-1) relative to four additional 'reference' genes (EEF, EIF RPL, ß-Actin) were calculated based on the threshold cycle (C_T), normalized using the data-driven NORMAgene method (Heckmann et al., 2011).

Primers	Naked mole rat	Mice
HIF1α	F: TGCGAACCTATTCCTCATCC R: CCTGTGGTGACCTGTCCTTT	F: TCAAGTCAGCAACGTGGAAG R: TATCGAGGCTGTGTCGACTG
Glut	F: GCTGCCTTGGATGTCCTATC R: CATGCCCACAATGAAGTTTG	F: GCTGTGCTTATGGGCTTCTC R: ACACCTGGGCAATAAGGATG
VEGF	F: TCTTCAAGCCATCCTGTGTG R: AACTCATCTCCCCAATGTGC	F: AGACACGGTGGTGGAAGAAG R: GGAAGGGAAGATGAGGAAGG
ET1	F: TGCCAATGTGCTAACCAAAA R: TGTTTTCCTTCCCTTCACCA	F: CTGCCAAGCAGGAAAAGAAC R: TTGTGCGTCAACTTCTGGTC
Actin	F: GGCTACAGCTTCACCACCAC R: GGGCAGCTCGTAGCTCTTCT	F: ACTGGGACGACATGGAGAAG R: GGGGTGTTGAAGGTCTCAAA
EEF_2	F: CTGCCAGCTCATCCTAGACC R: CTTGTCCTTGTCCTCGCTGT	F: GGAGATCCAGTGTCCTGAGC R: GGACTCATTGACAGGCAGGT
EIF	F: TCTCTTCTTCGGGGCATCTA R: TGCTTGGGTCTCCTTGAACT	F: GATTTGGGAGGAAAGGTGTG R: TATTCAGCAACAGCGAGCAC
RPL	F: GAGGGCATCAACATTTCTGG R: TCTTGTGTGGCAGCATACCT	F: GAGGGGCAGGTTCTGGTATT R: GGGAGGGGTTGGTATTCATC

Table 2.1 Sequences of primers used in qPCR reactions for both naked mole rat and mice, including hypoxia-inducible factor 1α (HIF1α), glucose transporter-1 (GLUT1), vascular endothelin growth factor (VEGF), and endothelin-1 (ET-1). Actin, eukaryotic elongation factor 2 (EEF_2), eukaryotic translation initiation factor (EIF), and ribosomal protein (RPL) were quantified and used for NORMAgene analysis.

2.7 Data Collection and Statistical analysis

Total ventilation ($\dot{V}_E$) was determined as the product of f_R and V_T. Rates of O_2 consumption $\dot{V}_{O2}$) and CO_2 production ($\dot{V}_{CO2}$) were calculated as follows:

$$\dot{V}O_2 = (F_IO_2 - F_EO_2) \bullet \text{flow rate (mL min}^{-1}\text{)/ bodyweight (kg)}$$

$$\dot{V}CO_2 = (F_ICO_2 - F_ECO_2) \bullet \text{flow rate (mL min}^{-1}\text{) / bodyweight (kg)}$$

wherein F denotes fractional concentration of inspired (i), and expired (e) gases (Frappell et al., 1992). The respiratory exchange ratio (RER) was calculated as the quotient of $\dot{V}CO_2$ and $\dot{V}O_2$. Air convection requirement (ACR) was calculated as the quotient of $\dot{V}_E$ and $\dot{V}O_2$. Lung extraction efficiency was calculated as the quotient of $\dot{V}O_2$ and $\dot{V}_E$ multiplied by 100. Average values were calculated for each variable during the last 10 minutes of steady state at each experimental O_2 level. In pilot experiments we determined all parameters reach steady state within 30 minutes of exposure to a change in O_2 level. For ventilatory measurements, a series of no fewer than 5 sets of 10 or more consecutive breaths when the animal was awake but not active were selected for analysis. The activity of the animal could be confirmed visually during experimentation, as well as using the shape of the breathing trace. All data output was converted to analog signal via PowerLab 8/35 and recorded with digital data acquisition system (LabChart).

All statistical analysis was performed using GraphPad Prism 7 statistical software (La Jolla, CA, USA). For all experiments, individual *n* values correspond to a single animal treated with either saline, echinomycin (1.0 or 0.5 mg kg $^{-1}$), PX-478 (80.0 mg kg^{-1}), or EDHB (180.0 mg kg^{-1}) dissolved in DMSO as described above, before and after exposure to 21% O_2 and then acute hypoxia (7% O_2). Values are presented as mean ± S.E.M and $p < 0.05$ was considered to achieve statistical significance. All data sets were tested for normality (Shapiro-Wilk test), homogeneity of variance (Bartlett's test) and were found to meet these assumptions. A fixed-effect, repeated measures ANOVA was used to assess the main effects and interactions between the two independent variables: (1) the treatment (saline vs. pharmacological agent) and (2) acute inspired O_2 level (21% vs. 7%). All two-way interactions were tested between O_2 level and

treatment type. A Tukey's HSD post-hoc multiple comparisons test corrected for violations of sphericity (Greenhouse-Geisser epsilon hat method) was run on each of the dependent variables (f_R, $\dot{V}_E$, V_T, $\dot{V}O_2$, $\dot{V}CO_2$, $ACRVO_2$, RER, and EO_2) to determine where statistical difference occurred and to correct for multiple comparisons. A Welch's unpaired t-test was performed on qPCR and Western results to assess differences between treatment groups and between species respectively. Undetectable bands were assumed to be zero for the purposes of statistical analysis.

Chapter 3

RESULTS

3.1 Naked mole rats possess elevated endogenous HIF1α

We compared HIF1α relative protein expression in samples of brain and liver from naked mole rats and mice using immunoblotting techniques (Figure 3.1, n = 4 each). Naked mole rats have previously been reported to possess two point mutations within their pVHL binding site, suggesting its decreased affinity for and capacity to degrade HIF1α in normoxia. Following immunoblotting, we find HIF1α expression was 3-fold higher in naked mole rat brain than mouse brain ($p < 0.0001$). HIF1α was undetectable in mouse liver and therefore its expression was assumed to be zero for statistical analysis. HIF1α was therefore found to be 4-fold higher in naked mole rat liver relative to mouse liver tissue ($p < 0.0001$).

3.2 Pharmacological manipulation of HIF1α and downstream gene changes

To confirm the efficacy of pharmacological agents, HIF1α and downstream target mRNA levels were measured using qPCR on isolated tissues from mice and naked mole rats. Although echinomycin was not expected to influence HIF1α mRNA levels, HIF1α mRNA expression was assessed to validate mechanism of action as well as possible off-target effects. We also measured VEGF, GLUT1, and ET-1 mRNA expression as well as several housekeeping genes to aid in NORMAgene analysis. Animals chosen for sampling were echinomycin (0.5 mg kg^{-1}) treated naked mole rats, and EDHB treated mice. Our results demonstrate echinomycin had no effect on HIF1α and downstream mRNA levels in muscle but caused HIF1α and all gene target mRNA to increase 6-8 fold in liver (ET-1, $p = 0.0002$; GLUT1, $p = 0.0004$; HIF1α, $p < 0.0001$; VEGF, $p = 0.004$; Figure 3.2). No significant changes were observed in either tissue in mice post-EDHB treatment (Figure 3.3).

3.3 HIF1 antagonism alters normoxic metabolism in naked mole rats

Steady-state metabolism ($\dot{V}O_2$, and $\dot{V}CO_2$), $\dot{V}_E$, and T_b were measured in naked mole rats treated with either i.p saline, echinomycin at one of two doses, or PX-478 at ambient O_2, subsequently challenged with 7%. Consistent with previous findings (Pamenter et al., 2014), saline-treated animals breathing 7% O_2 exhibited a reversible ~70% reduction in O_2 consumption and CO_2 production respectively (from 40.1 ± 5.0 to 11.9 ± 0.9 mL O_2 min^{-1} kg^{-1} , and 29.2 ± 3.7 to 11.3 ± 0.9 mL CO_2 min^{-1} kg^{-1}; $p < 0.0001$; Figure 3.4*a*,*c*). Conversely, none of our naked mole rat treatment groups experienced a change in their hypoxic metabolic rate relative to saline-controls. However, HIF1α antagonism with both echinomycin (1.0 mg kg^{-1}) and PX-478 (80.0 mg kg^{-1}) reduced normoxic metabolic rates by ~ 45% ($p = 0.0011$ and 0.0034 respectively; Figure 3.4*a, c*). A similar decrease in metabolic rate was observed at the end of the recovery period in these two treatment groups, indicating these animals fully recovered to their respective normoxic baseline (Echinomycin HD, 16.3 ± 1.1 mL O_2 min^{-1} kg^{-1}, $p = 0.0011$; PX-478, 18.0 ± 4.4 mL O_2 min^{-1} kg^{-1}, $p = 0.0070$; Figure 3.4*a, c*). Due to changes in baseline metabolism, the magnitude of the HMR (determined by the change in $\dot{V}O_2$ or $\dot{V}CO_2$ between hypoxia and normoxia) was reduced in PX-478 treated animals (-28.1 ± 4.6 to 13.0 ± 1.2 $\Delta\dot{V}O_2$; $p = 0.0457$; Figure 3.4*d*).

3.4 HIF1α may mediate a metabolic fuel switch

Recent studies demonstrate high-altitude rodents undergo a fuel switch and metabolize carbohydrates as opposed to lipids in hypoxia (Schippers et al., 2012). Previous studies have observed a similar switch to fructose-fueled metabolism in naked mole rats exposed to anoxia although it is unclear how this switch affects their respiratory quotient or RER (Park et al.,

2017). To determine the role of HIF1α in this pathway we calculated the RER (Figure 3.5)—which acts as an indirect measure of the balance between metabolic fuel substrates—for naked mole rats exposed to each level of O_2. Consistent with studies in other rodents (McClelland et al., 1998; Schippers et al., 2012; Schippers et al., 2014) we observed a reversible fuel substrate switch from primarily lipid-based metabolism (RER = 0.7 ± 0.0) toward a greater reliance on carbohydrates (RER = 1.0 ± 0.1; $p < 0.0001$; Figure 3.5) in acute hypoxia. Conversely, treatment with both high and low dose echinomycin significantly blunted this response in naked mole rats (hypoxic RER = 0.8 ± 0.01; $p = 0.0378$ and 0.0260, respectively), suggesting hypoxic carbohydrate utilization might have been restricted following HIF1α antagonism

3.5 HIF1α antagonism does not affect hypoxic ventilatory depression of naked mole rats

In saline-treated animals, the hypoxia-induced reduction in metabolic rate was accompanied by a non-significant 32% decrease in $\dot{V}_E$ when challenged with 7% O_2 (1298.3 ± 188.52 to 882.6 ± 117.0 mL min^{-1} kg^{-1}; Figure 3.6*c*). This hypoxic decline in $\dot{V}_E$ was a result of a 12% reduction in f_R (from 105.5 ± 9.8 to 93.6 ± 9.2 breaths min^{-1}; Figure 3.6*a*) and a 15% reduction in V_T (from 11.8 ± 0.0 to 10.0 ± 1.5 mL kg^{-1}; Figure 3.6*b*). Naked mole rats treated with high dose echinomycin (1.0 mg kg^{-1}) exhibited a 50% decline in f_R in normoxia, hypoxia, and recovery relative to our control group (from 105.9 ± 9.8, 93.6 ±9.2, 98.4 ± 11.5 breaths min^{-1} in saline-treated animals to 44.8 ± 5.8, 47.1 ± 3.2, and 41.9 ± 5.2, $p = 0.0002$, 0.0059, and 0.0007, respectively), which did not translate into significant changes in $\dot{V}_E$ due to offsetting, but insignificant changes in V_T in this treatment group (Figure 3.6*b, c*). Conversely, naked mole rats treated with low dose echinomycin (0.5 mg kg^{-1}) experienced this same 50% reduction in f_R (91.3 ± 13.3 to 45.0 ± 6.2; $p = 0.0008$) when challenged with 7% O_2 which did not completely

reverse upon reentry into normoxia (64.6 breaths min^{-1}, p = 0.0260; Figure 3.6*a*). Following treatment with low dose echinomycin, we observed significant increases in V_T across all O_2 exposures (from 11.8 ± 0.9, 10.0 ± 1.5, and 9.4 ± 1.9 to 26.0 ± 2.6, 16.4 ± 2.2, and 35.1 ± 2.0; p = 0.0235, 0.0080, and 0.0001, respectively). This change was most pronounced in 21% O_2, whereby increases in V_T lead to corresponding increases in $\dot{V}_E$ during normoxia and recovery (from 1298.3 ± 188.5 to 2239.5 ± 196.0 and 906.8 ± 235.3 to 2330.4 ± 543.4 mL min^{-1} kg^{-1}, respectively; p = 0.0311 and 0.0006, respectively; Figure 3.6*c*) despite a decrease in f_R. In general, animals treated with echinomycin took fewer, but deeper breaths. However, this change was not reflected by significant changes to hypoxic $\dot{V}_E$ in any of our treatment groups (Figure 3.6*c, d*).

3.6 Naked mole rats do not hyperventilate in hypoxia

The ACR for O_2 consumption in sham naked mole rats did not change significantly between normoxia and hypoxia, indicating these animals do not hyperventilate in hypoxia (Figure 3.7). This was anticipated, as previous studies have demonstrated the HVR and HMR are typically equal in magnitude in these animals (Chung et al., 2016). Conversely, the hypoxic ACR of mole rats treated with a HIF1α antagonist significantly increased relative to each group's normoxic ACR. This change reached its highest in the low-dose echinomycin group (from 71.8 ± 11.3 to 159.2 ± 34.6; p = 0.0072) and the PX-478 treatment group (from 58.3 ± 20.7 to 171.3 ± 104.4; p = 0.0143).

3.7 Naked mole rats do not experience an increase in lung extraction efficiency

During normoxia, lung extraction efficiency (EO_2) was 17% in saline-treated naked mole rats which did not change significantly after an hour of exposure to 7% O_2 (Figure 3.8). HIF1α antagonism did not significantly affect EO_2 in either normoxia or hypoxia, although EO_2 during the recovery period was significantly affected following treatment with both high and low doses of echinomycin (from 26.7 ± 6.9 to 11.43 ± 1.5 and 12.52 ± 4.9; $p = 0.0497$ and 0.0337, respectively; Figure 3.8).

3.8 Naked mole rats do not experience a decline in T_b

Changes in T_b were measured in naked mole rats throughout the course of the experiment using subcutaneously implanted microchips. Reductions in metabolic rate are commonly associated with decreases in T_b owing to the Q_{10} effect on metabolic rate. Here we find T_b was not affected during hypoxic challenge, an observation which was not affected in naked mole rats by either drug treatment (Figure 3.9).

3.9 Elevated HIF1α expression has little effect on the HMR of mice

To determine if increased HIF1α availability plays a role in the HMR, we attempted to reproduce the HIF1α profile of naked mole rats by treating mice with a PHD inhibitor (EDHB). Consistent with other studies (Peng et al., 2011), saline-treated mice exhibited a 64% decrease in O_2 consumption (from 60.3 ± 1.9 to 21.8 ± 1.8 mL O_2 min^{-1} kg^{-1}; $p < 0.0001$; Figure 3.10*a*,*b*) and CO_2 production (40.3 ± 1.8 to 15.5 ± 1.8 mL CO_2 min^{-1} kg^{-1}; $p < 0.0001$; Figure 3.10*c*,*d*). Normoxic $\dot{V}O_2$ decreased slightly in mice following treatment with EDHB, leading to a significant decrease in the magnitude of O_2 consumption represented by $\Delta\dot{V}O_2$ (from-39.7 ± 1.2

to -27.8 ± 4.0; $p = 0.0132$; Figure 3.10*a,b*). No significant changes were observed in hypoxia in EDHB-treated mice.

3.10 Elevated HIF1α expression has no effect on hypoxic fuel selection in mice

To again assess substrate-use in hypoxia, we calculated the RER in mice treated with saline or EDHB breathing normoxic and hypoxic gas mixtures. In contrast to naked mole rats, our saline control mice did not exhibit a hypoxia-induced increase in their RER relative to normoxia. Interestingly, mice treated with EDHB exhibited a 16% increase in their baseline RER (from 0.6 ± 0.0 to 0.8 ± 0.0; $p = 0.0481$; Figure 3.11). EDHB-treatment did not affect hypoxic RER values.

3.11 HIF1α agonism affects f_R in mice

In saline-treated animals, acute exposure to 7% O_2 caused a 27% increase in f_R relative to breathing normoxic gas mixtures (157.1 ± 9.5 to 200.4 ± 10.8 breaths min^{-1}; $p = 0.0035$)(Figure 3.12*a*), which was not accompanied by a significant increase in V_T (Figure 3.12*b*) or $\dot{V}_E$ (Figure 3.12*c,d*). Conversely, i.p. injection with EDHB caused an 18% increase in f_R during challenge with 7% O_2 (from 200.4 ± 10.8 to 236.5 ± 14.1 breaths min^{-1}; $p < 0.0003$). This increase in f_R was offset by a reduction in V_T resulting in no significant change in $\dot{V}_E$ or $\Delta\dot{V}_E$ (Figure 3.12*c, d*).

3.12 The ACR of mice is unaffected by EDHB

Contrary to naked mole rats, saline-control mice experienced a 3.5-fold increase in their ACR$\dot{V}O_2$ during exposure to 7% O_2 relative to normoxia (from 40 ± 3.9 to 144.7 ± 12.1; $p <$ 0.0001; Figure 3.12). Despite significant changes in f_R in EDHB-treated mice, the ACR$\dot{V}O_2$ of these animals was unaffected due to a strong compensation of V_T (Figure 3.12*b*).

3.13 EO_2 does not increase in mice exposed to hypoxia

Interestingly, control mice experienced a hypoxia-induced decrease in EO_2 relative to normoxia (from 12.2% ± 1.1% to 8.7% ± 0.7%; $p = 0.0249$; Figure 3.14). Treatment with EDHB did not significantly affect EO_2 in any O_2 level (Figure 3.14).

3.14 Elevated HIF1α expression has no effect on T_b regulation in mice

As expected, the decrease in metabolic rate observed in saline-treated mice was accompanied by a 2.6ºC decrease in T_b when challenged with the same level of hypoxia (36.0 ± 0.3 to 33.4 ± 0.3, $p < 0.0001$; Figure 3.15). Treatment with EDHB did not affect T_b in any O_2 level.

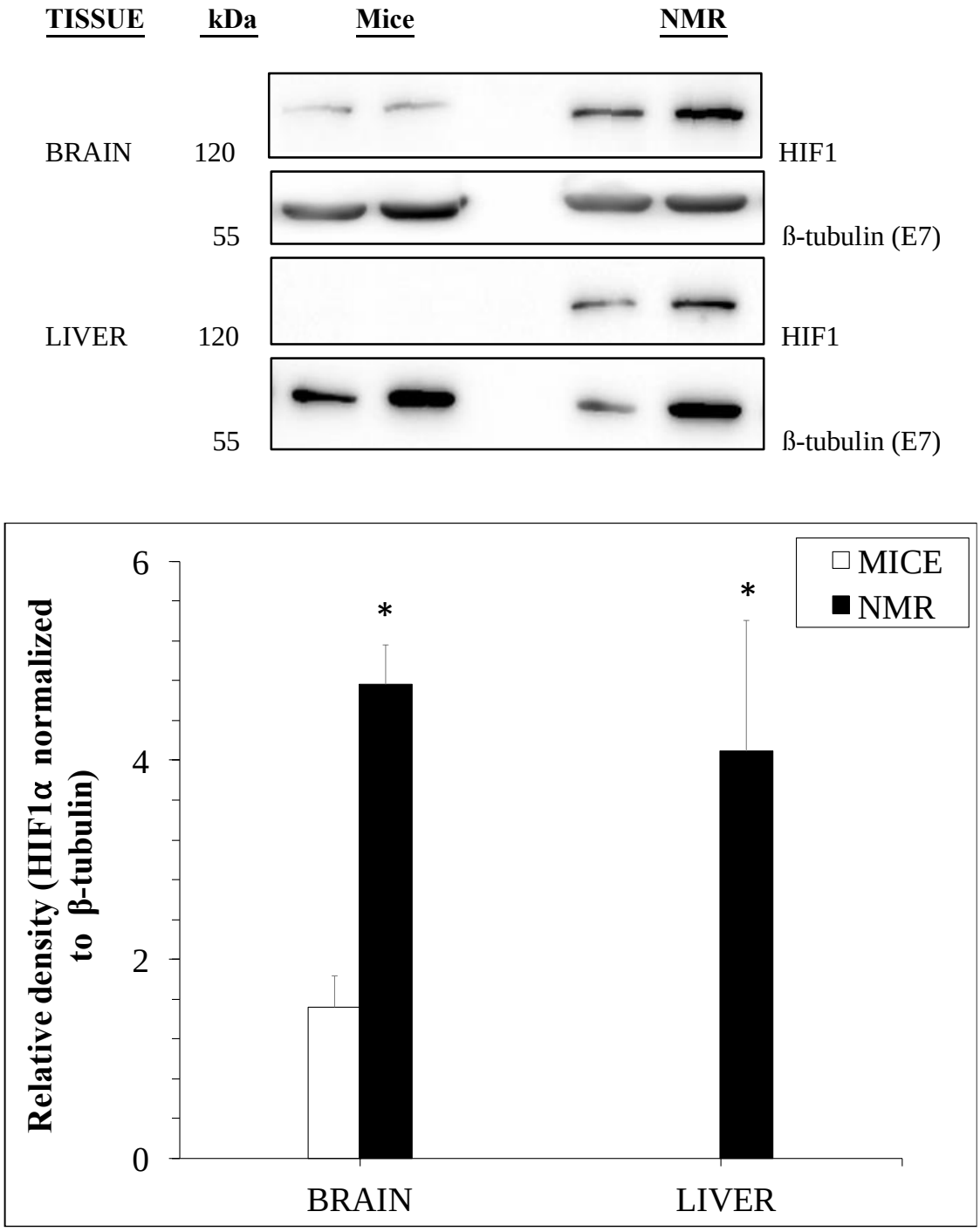

Figure 3.1 Western blot analysis of HIF1α protein levels in brain and liver of mice and naked mole rats. Animals were untreated controls housed in normoxic conditions. Mean ± S.E.M. were calculated from *n = 4*. A Student's *t* test was performed ($p < 0.05$).

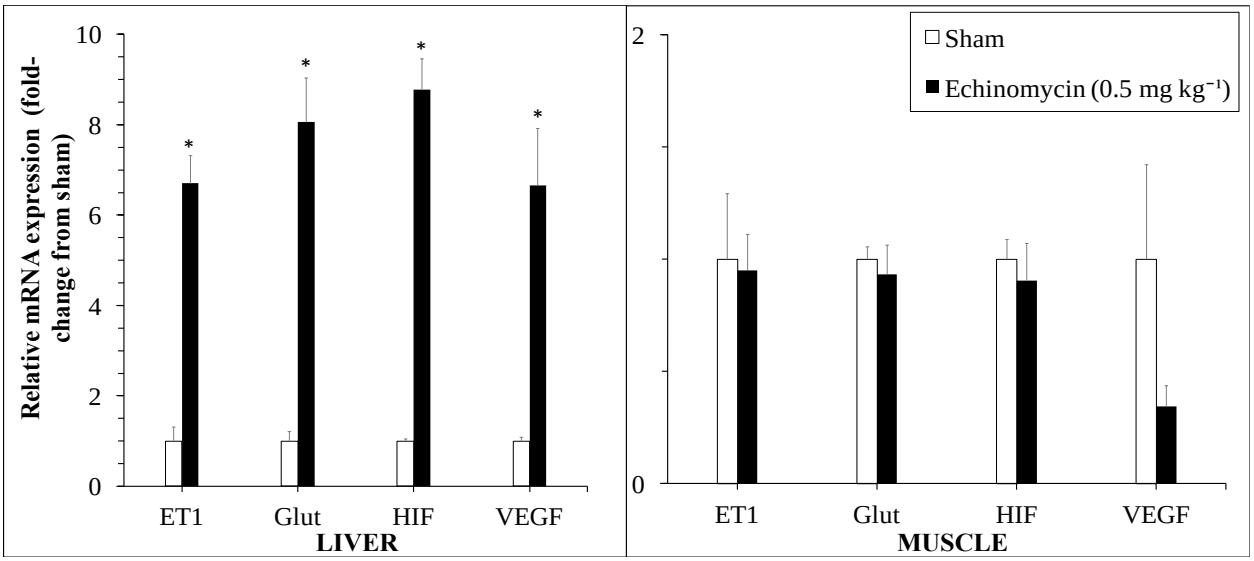

Figure 3.2 Naked mole rats were treated with echinomycin (1.0 mg kg^{-1}) and qPCR was performed on isolated liver and muscle tissue from both control (*n = 4*) and treatment animals (*n = 4*). Graphs depict fold changes in Endothelin 1 (ET1), Glucose transporter 1 (GLUT1), HIF1α, and vascular endothelial growth factor (VEGF) in treated animals relative to controls, normalized using data-driven NORMAgene. Mean ± S.E.M. is shown. A Student's *t* test was performed ($p < 0.05$). Asterisks (*) indicate significant differences between control and treatment groups.

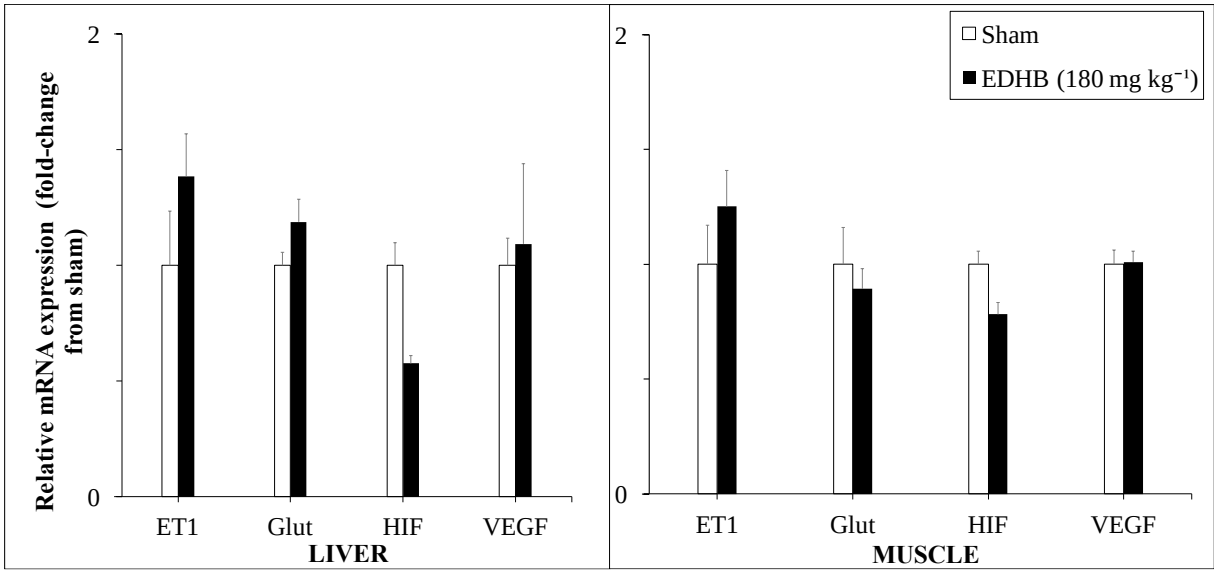

Figure 3.3 Mice were treated with ethyl-3,4-dihydroxybenzoae (EDHB; 180 mg kg^{-1}), and qPCR was performed on isolated liver and muscle tissue. Graphs depict fold changes in Endothelin 1 (ET-1), Glucose transporter 1 (GLUT1), HIF1α, and vascular endothelial growth factor (VEGF) in treated animals relative to controls, normalized using data-driven NORMAgene. Mean ± S.E.M were calculated from *n = 4*. A Student's *t* test was performed ($p < 0.05$).

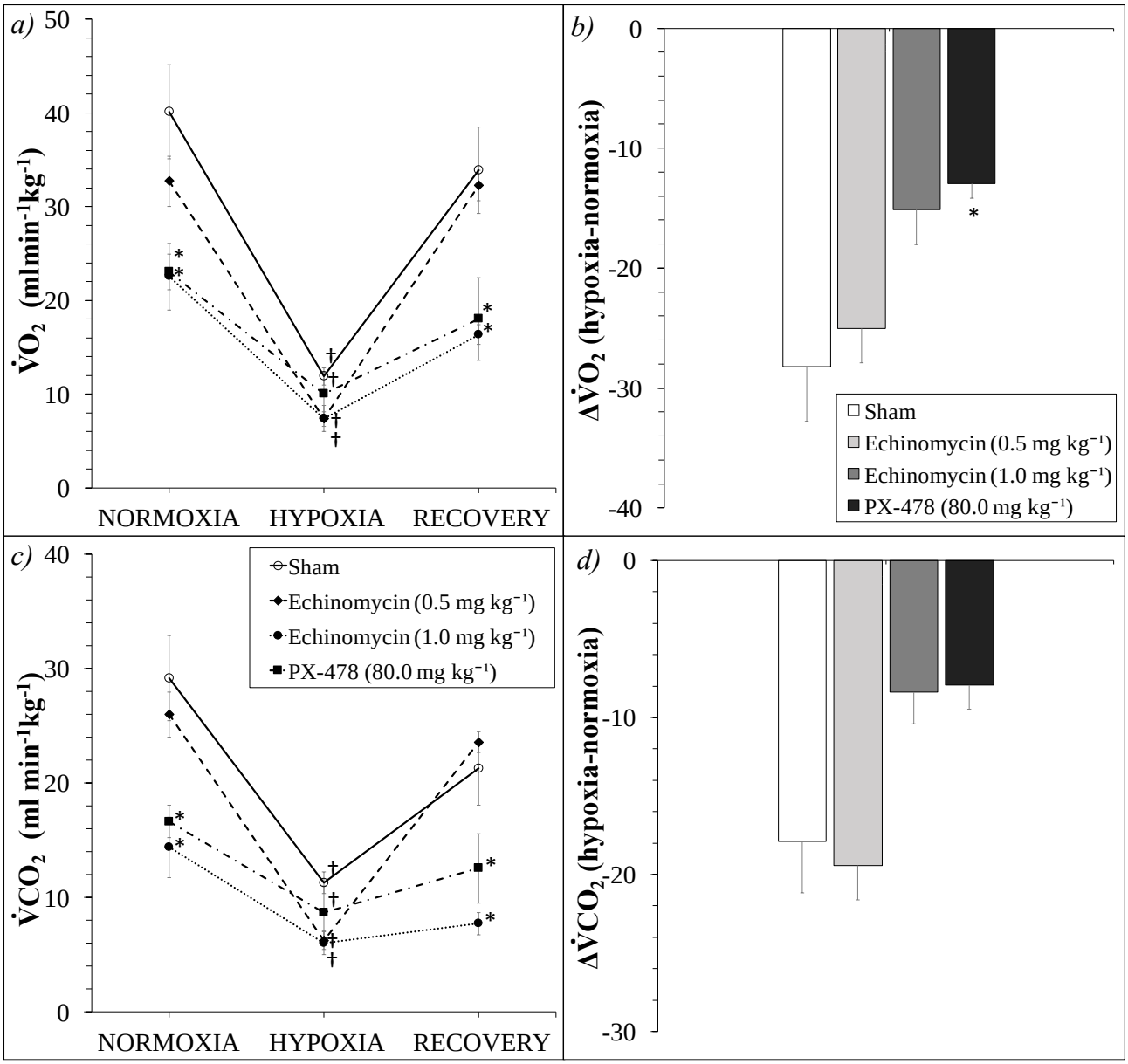

Figure 3.4 Average metabolic rate (O_2 consumption and CO_2 production) in naked mole rats exposed to normoxic (21%) or hypoxic (7%) gas mixtures and treated intraperitoneally with saline (solid line, open circles and left most bar), echinomycin (0.5 mg kg^{-1}; dotted line, closed diamond and second bar from the left), echinomycin (1.0 mg kg^{-1}; dotted line, closed circles and third bar from the left), or PX-478 (80.0 mg kg^{-1}; dotted line, closed square and right most bar) (*a*, *c*). Average difference ($\Delta\dot{V}O_2$, $\Delta\dot{V}CO_2$) between metabolic rate (*b*, *d*). Data are mean ± S.E.M, from *n = 9, n = 5, n = 8, n = 4* respectively. A two-way repeated measures ANOVA was used. Asterisks (*) denote significant differences between drug treatments relative to sham, daggers (†) represent significant within-treatment differences between O_2 levels relative to normoxia ($p < 0.05$).

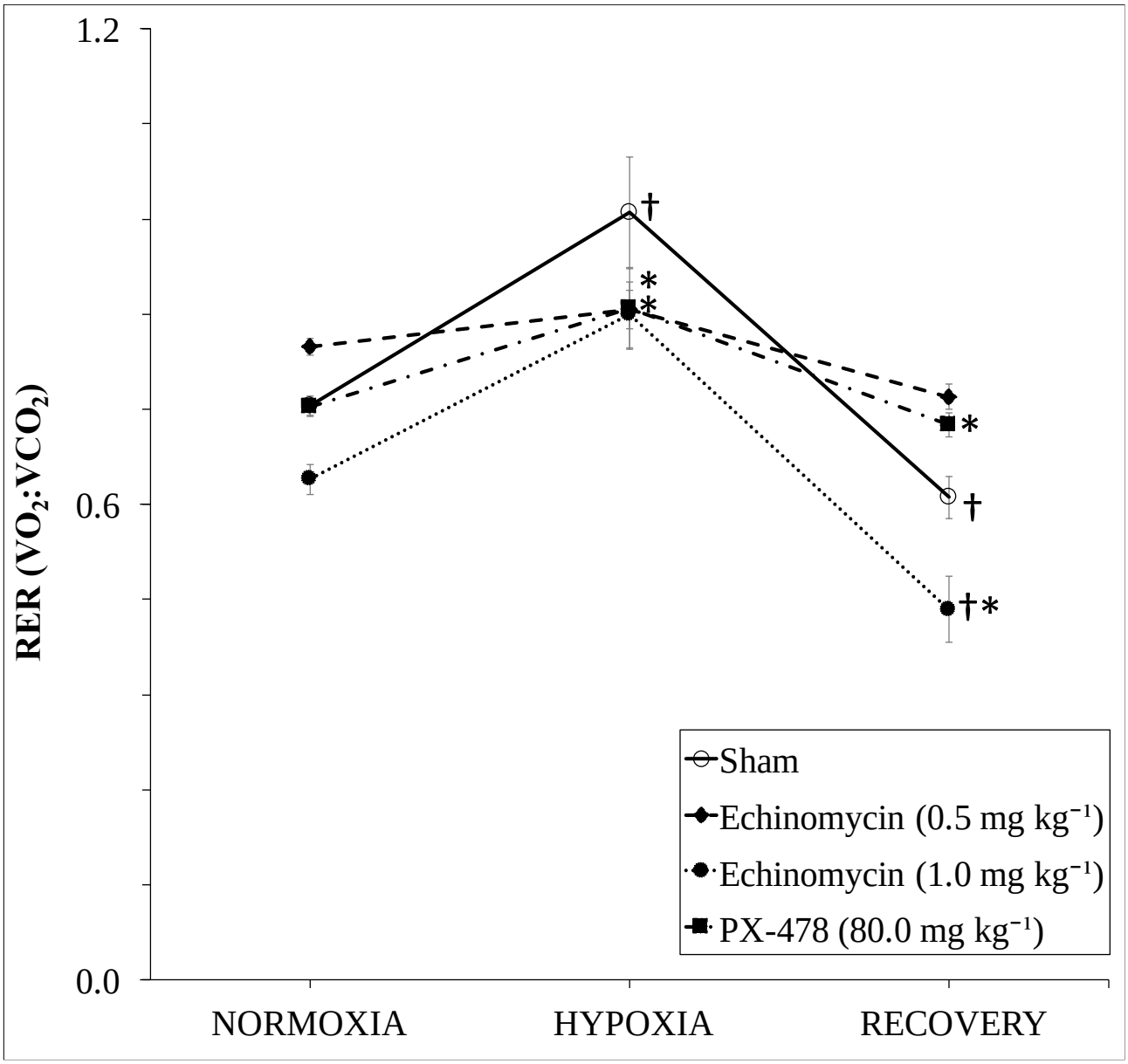

Figure 3.5 Respiratory exchange ratio (RER; $\dot{V}CO_2$: $\dot{V}O_2$) across O_2 levels in naked mole rats treated intraperitoneally with one of saline (left most bar), echinomycin (0.5 mg kg^{-1}; second bar from the left), echinomycin (1.0 mg kg^{-1}; third bar from the left), or PX-478 (80.0 mg kg^{-1}; right most bar). Data are mean ± S.E.M, from *n = 9, n = 5, n = 8, n = 4* respectively. A two-way repeated measures ANOVA was used. Asterisk (*) denote significant differences between drug treatments relative to sham, daggers (†) represent significant within-treatment differences between O_2 levels relative to normoxia ($p < 0.05$).

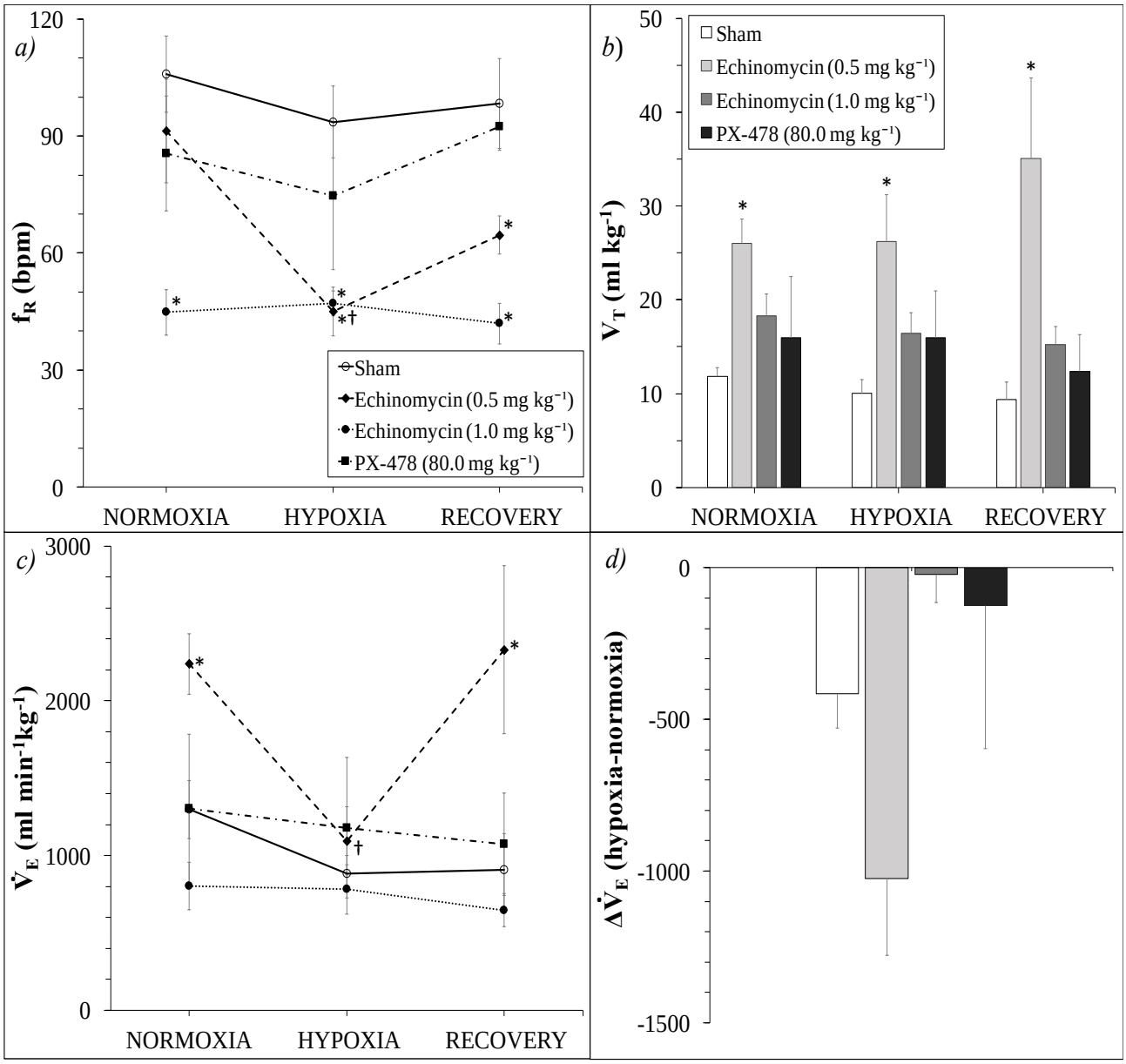

Figure 3.6 Effect of HIF1α inhibition on ventilatory parameters in acute hypoxia (7% O_2): (*a*) breathing frequency (f_R), (*b*) tidal volume (V_T), (*c*) total minute ventilation ($\dot{V}_E$). Animals were treated intraperitoneally with one of saline (solid line, open circles and left most bar), echinomycin (0.5 mg kg^{-1}; dotted line, closed diamond and second bar from the left), echinomycin (1.0 mg kg^{-1}; dotted line, closed circles and third bar from the left), or PX-478 (80.0 mg kg^{-1}; dotted line, closed square and right most bar). Data are mean ± S.E.M., from *n = 9, n = 5, n = 8, n = 4* respectively. A two-way repeated measures ANOVA was used. Asterisks (*) denote significant differences between drug treatments relative to sham, daggers (†) represent significant within-treatment differences between O_2 levels relative to normoxia ($p < 0.05$).

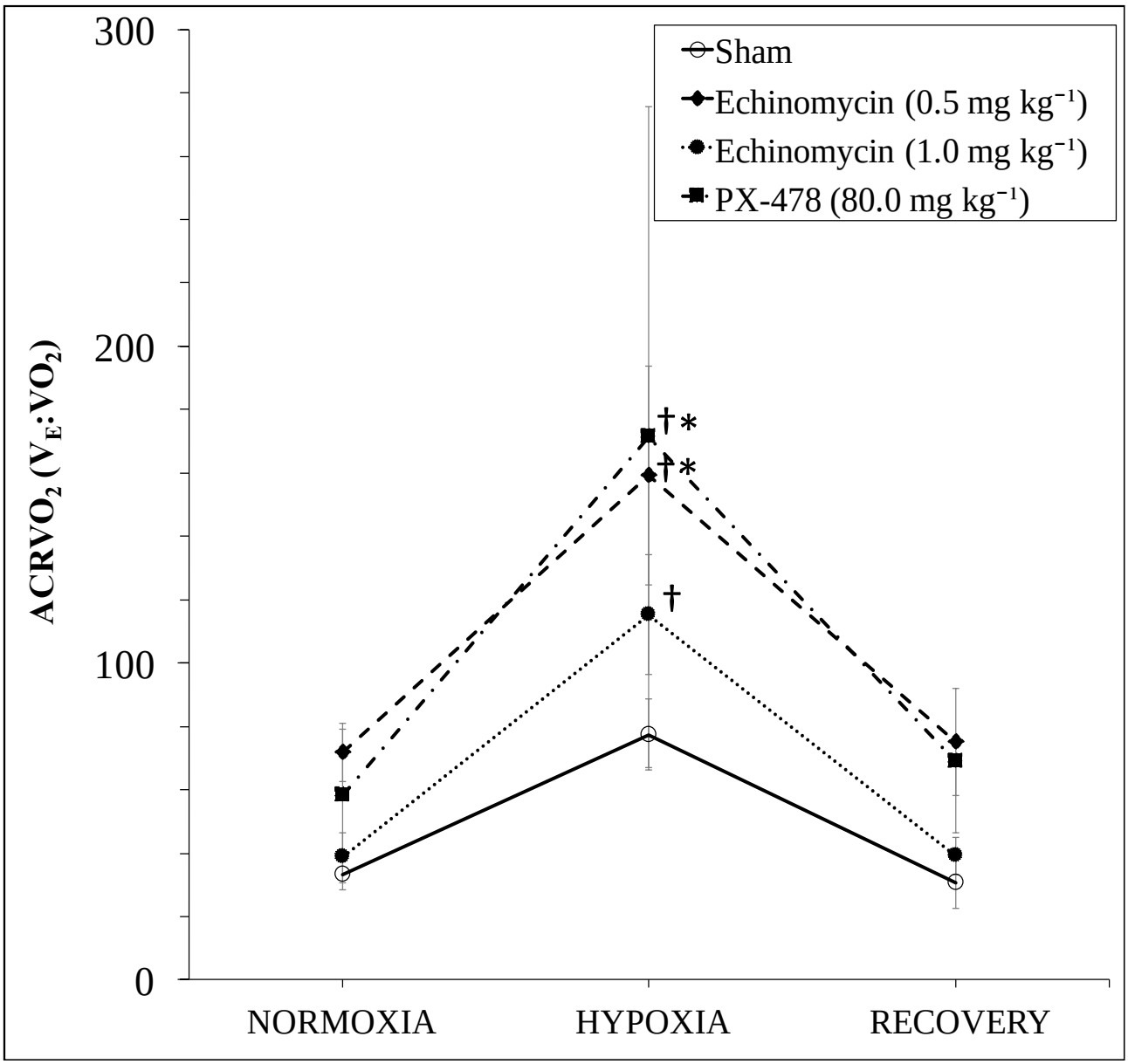

Figure 3.7 Hyperventilation responses as reflected by the air convection requirement ($ACRVO_2$; $\dot{V}_E$: $\dot{V}O_2$) in naked mole rats treated intraperitoneally with one of saline (left most bar), echinomycin (0.5 mg kg^{-1}; second bar from the left), echinomycin (1.0 mg kg^{-1}; third bar from the left), or PX-478 (80.0 mg kg^{-1}; right most bar). Data are mean ± S.E.M., from *n = 9, n = 5, n = 8, n = 4*, respectively. A two-way repeated measures ANOVA was used. Asterisk (*) denote significant differences between drug treatments relative to sham, daggers (†) represent significant within-treatment differences between O_2 levels relative to normoxia ($p < 0.05$).

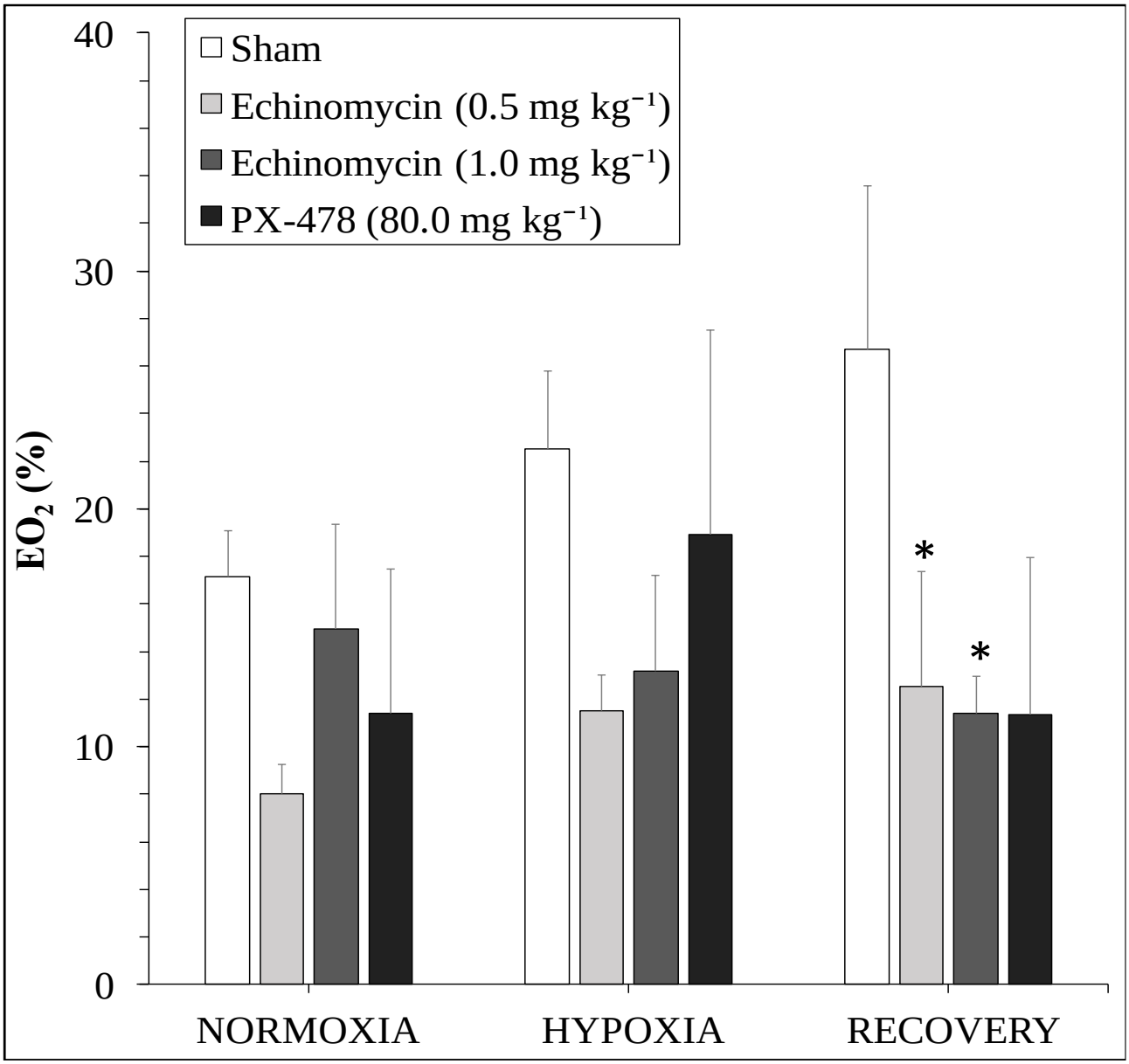

Figure 3.8 O_2 extraction efficiency (EO_2; %) in naked mole rats treated intraperitoneally with one of saline (left most bar), echinomycin (0.5 mg kg^{-1}; second bar from the left), echinomycin (1.0 mg kg^{-1}; third bar from the left), or PX-478 (80.0 mg kg^{-1}; right most bar). Data are mean ± S.E.M., from *n = 9, n = 6, n = 8, n = 4,* respectively. A two-way repeated measures ANOVA was used. Asterisks (*) denote significant differences between drug treatments relative to sham, daggers (†) represent significant within-treatment differences between O_2 levels relative to normoxia ($p < 0.05$).

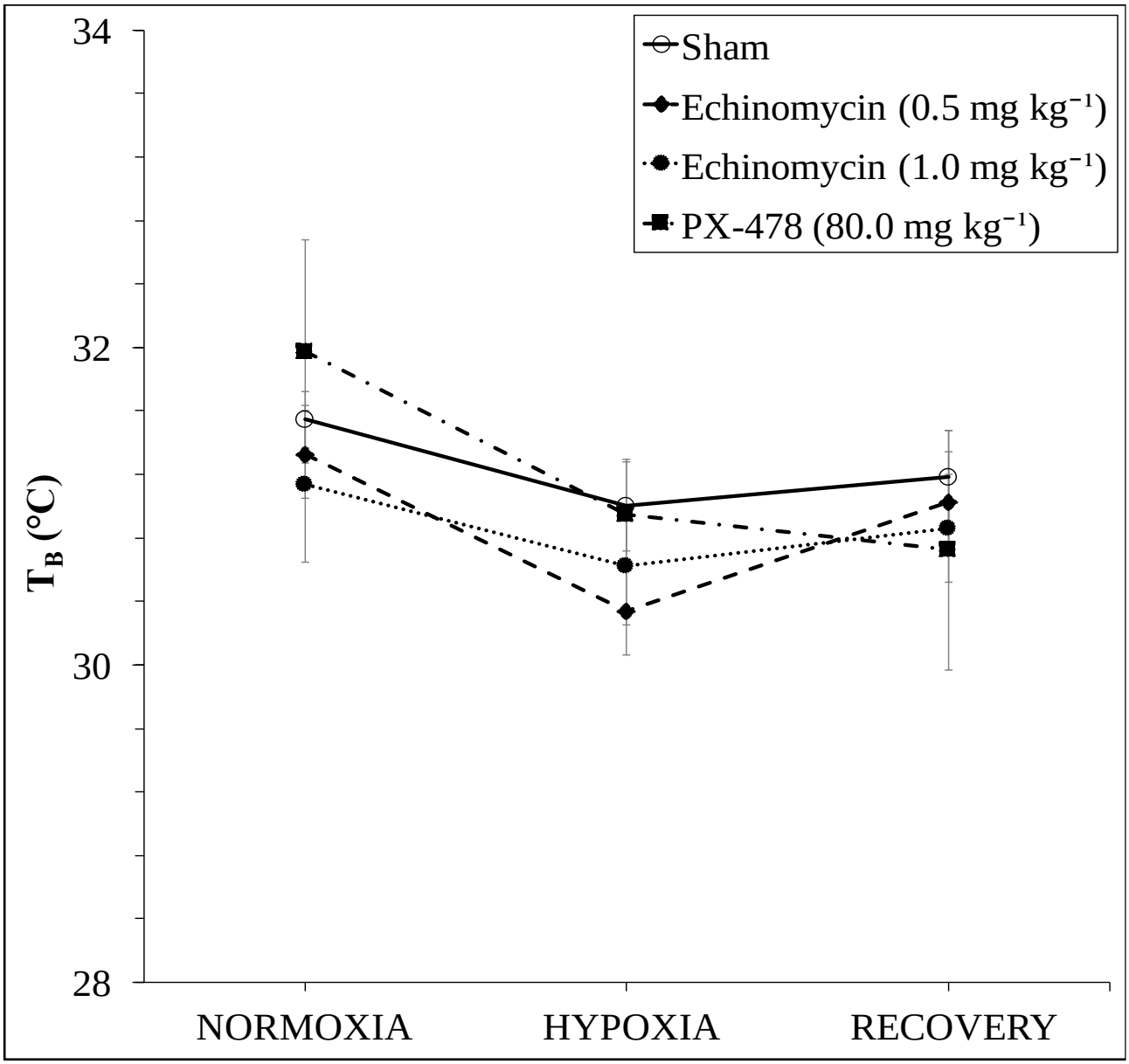

Figure 3.9 Body temperature (T_b) across O_2 levels in naked mole rats treated intraperitoneally with one of saline (left most bar), echinomycin (0.5 mg kg^{-1}; second bar from the left), echinomycin (1.0 mg kg^{-1}; third bar from the left), or PX-478 (80.0 mg kg^{-1}; right most bar). Data are mean ± S.E.M., from *n = 9, n = 6, n = 8, n = 4* respectively. A two-way repeated measures ANOVA was used. Asterisks (*) denote significant differences between drug treatments relative to sham, daggers (†) represent significant within-treatment differences between O_2 levels relative to normoxia ($p < 0.05$).

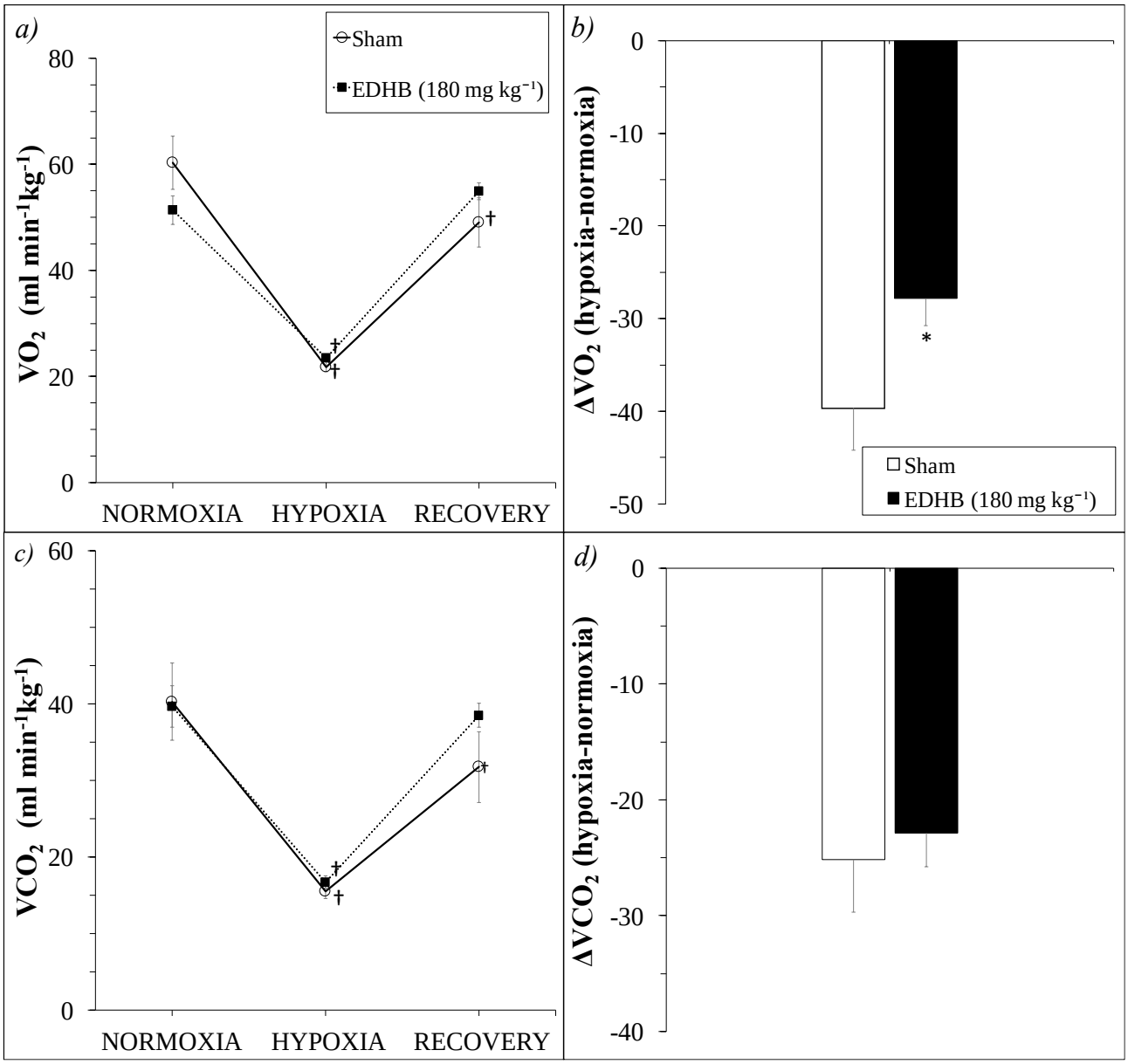

Figure 3.10 Average metabolic rate in mice exposed to normoxic (21%) or hypoxic (7%) gas mixtures and treated intraperitoneally with saline (solid line, open circles; white bar), or ethyl-3,4-dihydroxybenzoate (EDHB; 180.0 mg kg^{-1}) (dotted line, closed circles; black bar) (*a*, *c*). Average difference ($\Delta\dot{V}O_2$, $\Delta\ \dot{V}CO_2$) between metabolic rate (*b*, *d*). Data are mean ± S.E.M, from *n = 10*, *n = 8* respectively. A two-way repeated measures ANOVA was used. Asterisk (*) denote significant differences between drug treatments relative to sham, daggers (†) represent significant within-treatment differences between O_2 levels relative to normoxia ($p < 0.05$).

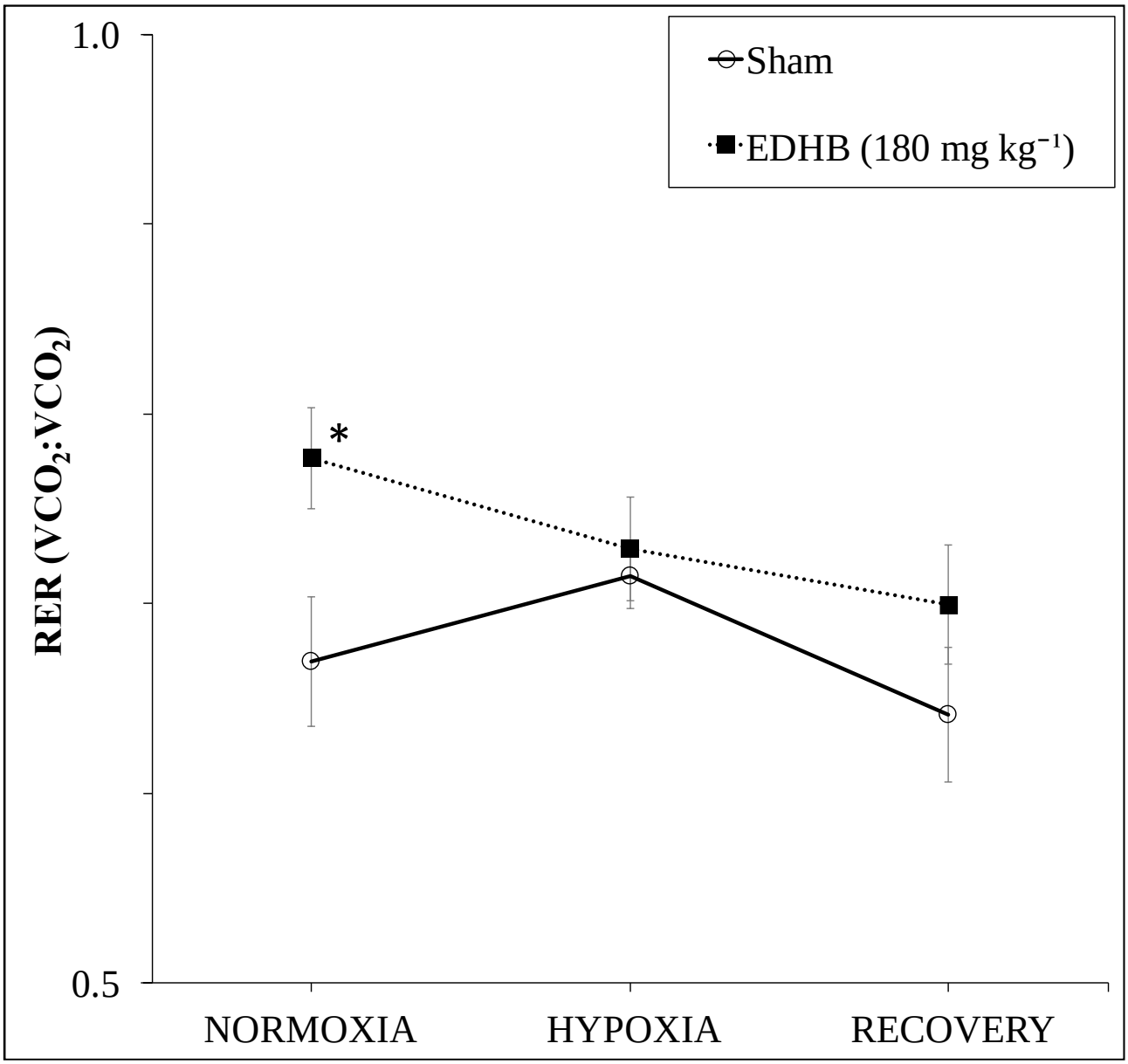

Figure 3.11 Average respiratory exchange ratio (RER) in mice exposed to normoxic (21%) or hypoxic (7%) gas mixtures and treated intraperitoneally with saline (white bar), or ethyl-3,4-dihydroxybenzoate (EDHB; 180.0 mg kg^{-1}) (black bar). Data are mean ± S.E.M, from *n = 10, n = 8* respectively. A two-way repeated measures ANOVA was used. Asterisk (*) denote significant differences between drug treatments relative to sham ($p < 0.05$).

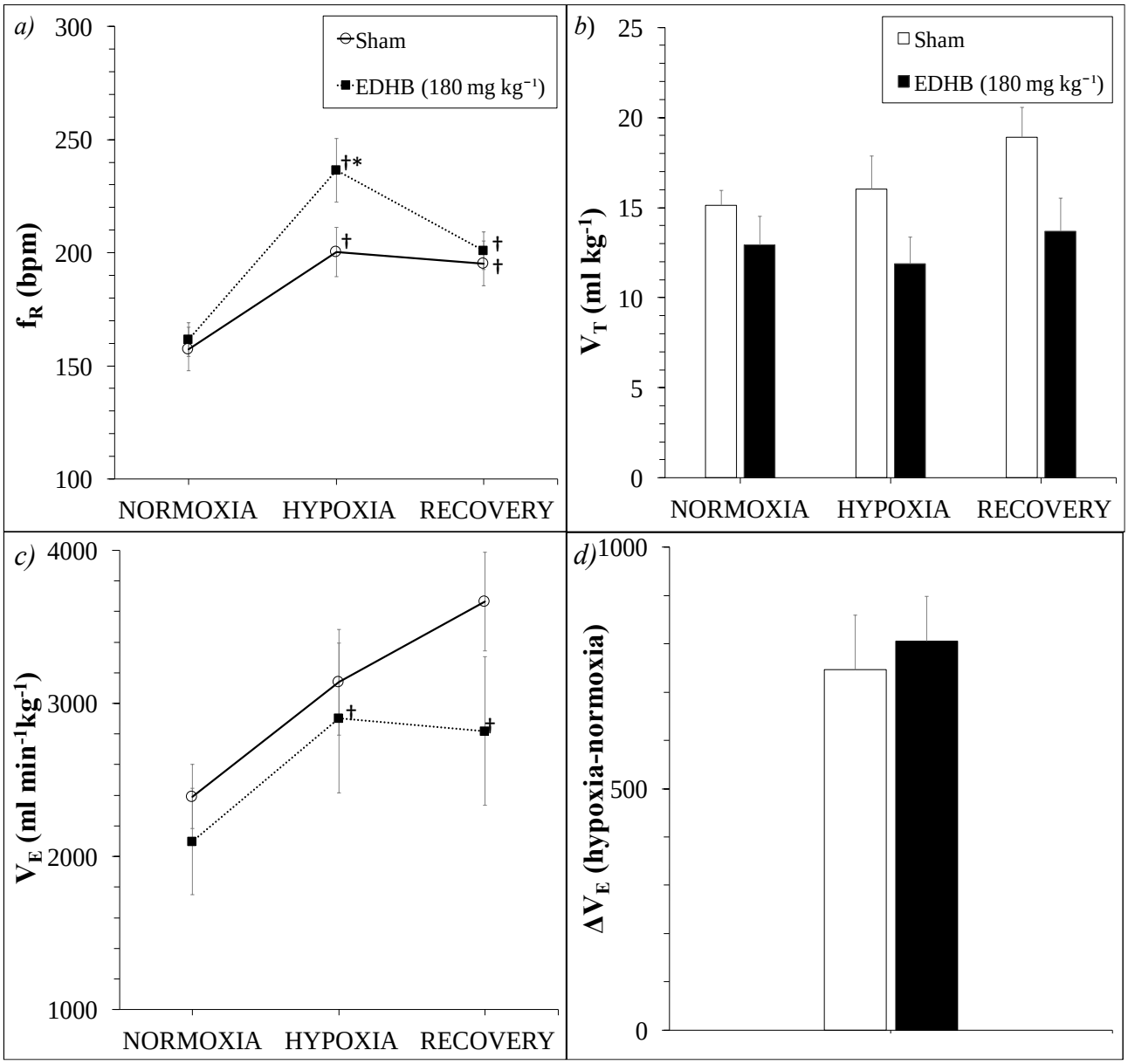

Figure 3.12 Hypoxia-induced ventilatory changes in mice treated with saline (solid line, open circles or white bar), or ethyl-3,4-dihydroxybenzoate (EDHB; 180.0 mg kg^{-1}) (dotted line, closed circles or black bar) (*a*) breathing frequency (f_R), (*b*) tidal volume (V_T), (*c*) total minute ventilation ($\dot{V}_E$), (*d*) $\Delta\dot{V}_E$. Data are mean ± S.E.M, from *n = 10*, *n = 8* respectively. A two-way repeated measures ANOVA was used. Asterisk (*) denote significant differences between drug treatments relative to sham, daggers (†) represent significant within-treatment differences between O_2 levels relative to normoxia ($p < 0.05$).

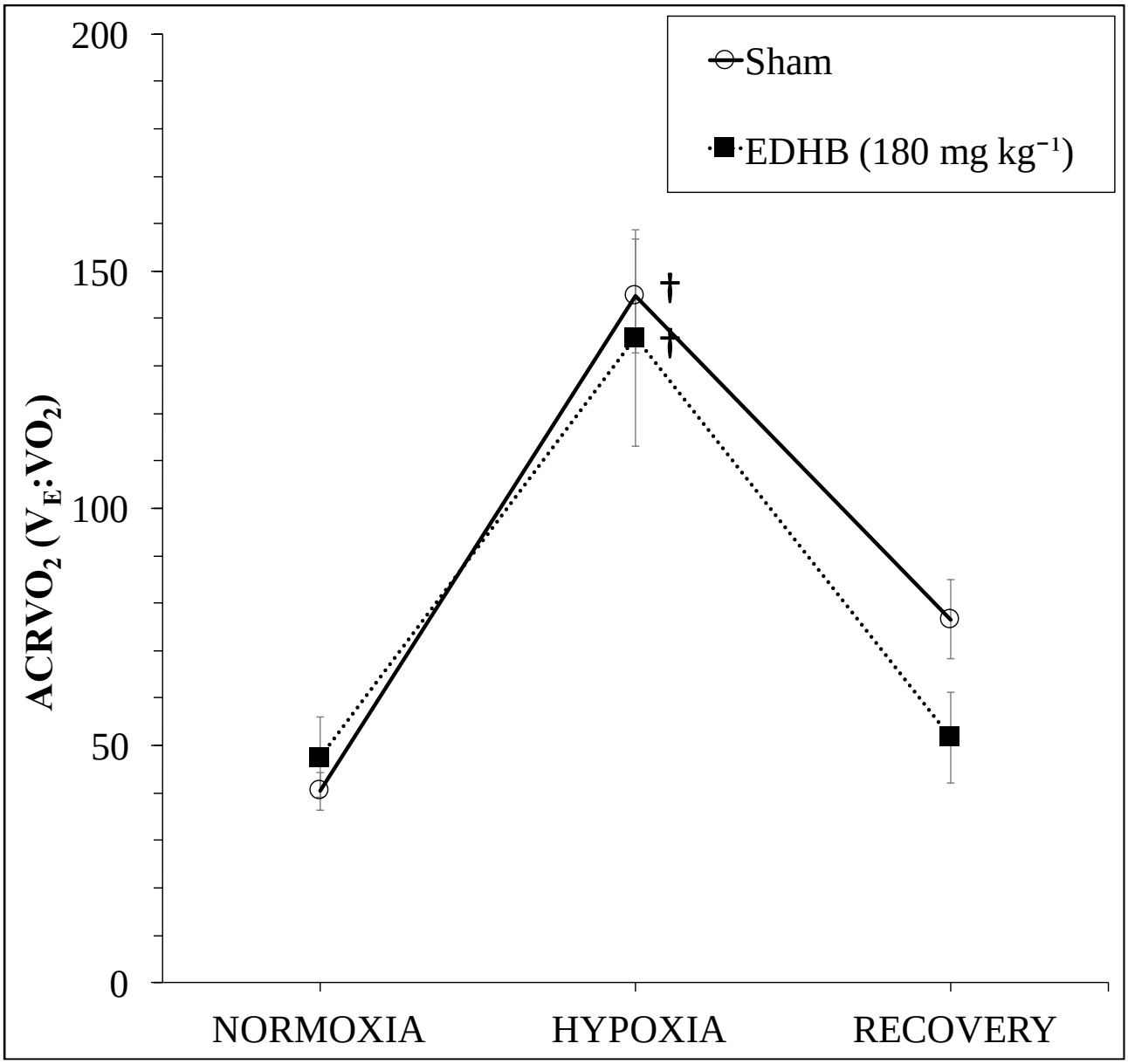

Figure 3.13 Mice hyperventilatory responses in response to hypoxia as reflected by their air convection requirement (ACR; $\dot{V}_E$: $\dot{V}O_2$). Animals were treated intraperitoneally with one of saline (white bar), or ethyl-3,4-dihydroxybenzoate (EDHB; 180.0 mg kg^{-1}) (black bar). Data are mean ± S.E.M, from *n = 10, n = 8* respectively. A two-way repeated measures ANOVA was used. Daggers (†) represent significant within-treatment differences between O_2 levels relative to normoxia ($p < 0.05$).

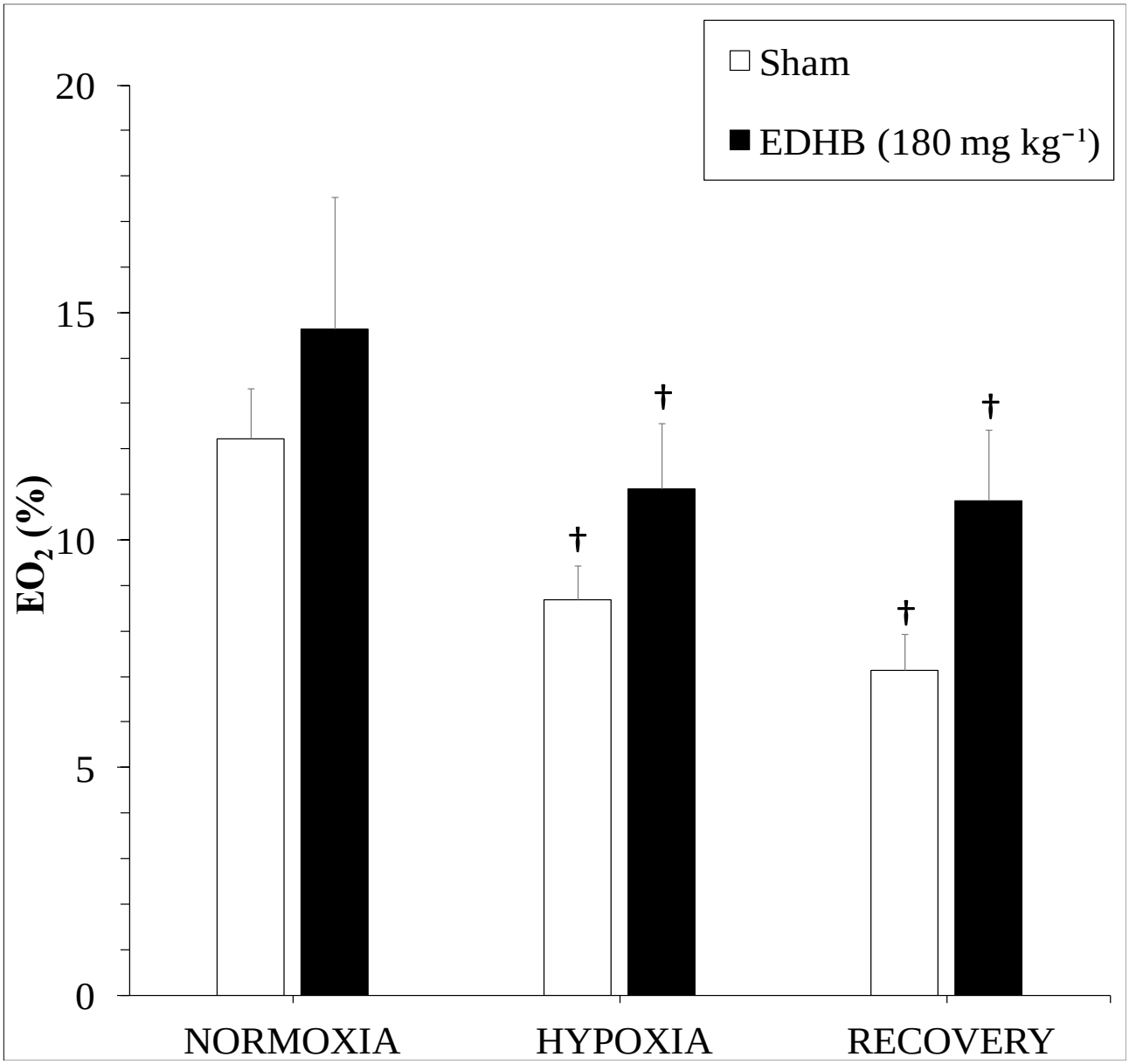

Figure 3.14 Lung extraction efficiency (EO_2) in mice treated intraperitoneally with one of saline (white bar) or ethyl-3,4-dihydroxybenzoate (EDHB; 180.0 mg kg^{-1}) (black bar)—data sets are presented as mean ± S.E.M. from *n = 10 and n = 8* respectively. A two-way repeated measures ANOVA was used. Daggers (†) represent significant within-treatment differences between O_2 levels relative to normoxia ($p < 0.05$).

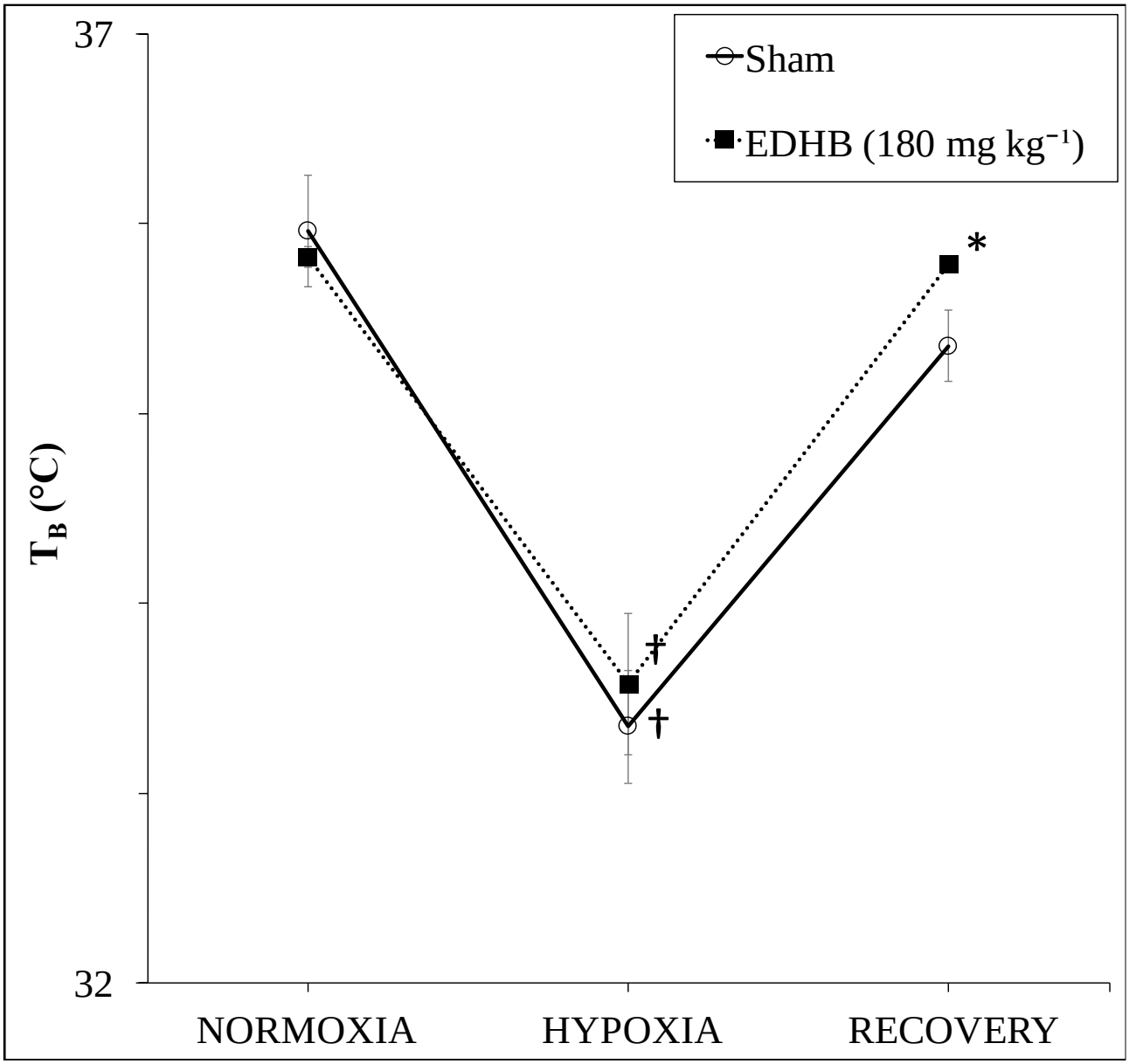

Figure 3.15 Body temperature (T_b) of mice treated intraperitoneally with one of saline (white bar) or ethyl-3,4-dihydroxybenzoate (EDHB; 180.0 mg kg^{-1}) (black bar)—data sets are presented as mean ± S.E.M. from *n = 10 and n = 8* respectively. A two-way repeated measures ANOVA was used ($p < 0.05$).

Chapter 4

Discussion

In this thesis we explored a role for HIF1α in regulating metabolic and respiratory parameters of naked mole rats and mice in normoxia and sustained hypoxia. Although we experienced significant study limitations, hinging on the difficulties surrounding pharmacological manipulation and plethysmography in poikilothermic species, our study yielded six findings: 1) we confirm naked mole rats possess elevated HIF1α relative to mice secondary to mutations within their VHL binding domain (Kim et al., 2011), 2) consistent with previous measurements of hypoxic physiological responses, naked mole rats experience a robust reduction in metabolic rate when exposed to sustained hypoxia accompanied by a small and unmatched reduction in $\dot{V}_E$, 3) increased endogenous HIF1α may affect metabolic set points in normoxia in both naked mole rats and mice, but likely has minimal effect on metabolic rate in hypoxia, 4) HIF1α may contribute to hypoxia-induced metabolic remodelling in naked mole rats through alterations in substrate use as reflected by the observed decrease in RER following HIF1α antagonism, 5) HIF1α inhibition leads to a reduction in f_R in some treatment groups of naked mole rats which was countered by an increase in V_T, potentially compromising the ability of naked mole rats to match O_2 supply and demand in sustained hypoxia, and 6) forced HIF1α in normoxia mimics hypoxic preconditioning by causing a progressive increase in f_R in hypoxia-naïve mice.

4.1 The HMR of mice and naked mole rats is independent of HIF1α

Consistent with other measurements in this species from other laboratories (Goldman et al., 1999; O'Connor et al., 2002), as well as from our own research team (Chung et al., 2016; Kirby et al., 2018; Pamenter et al., 2015), we report that naked mole rats exhibit a robust (70%) reduction in metabolic rate. While other studies have reported significant reductions in T_b in

naked mole rats challenged with 7% O_2 (Ilacqua et al., 2017; Kirby et al., 2018), the reduction in metabolic rate observed here was only accompanied by a small decrease in T_b (~0.5°C ± 0.35) when exposed to that same level of hypoxia (7% O_2 for 1 hour). We turned our attention toward HIF1α based on its known role as a global regulator of O_2 homeostasis in metazoans. Research shows HIF1α protein accumulates inside the cellular nucleus in as little as 2 minutes of hypoxic exposure (0.02-5.0% O_2), and continues to increase rapidly for 30 minutes (Jewell *et al.*, 2001) before slowing down and eventually reaching a maximum level after 60 minutes. Furthermore, HIF1α protein expression has been shown to increase in mice *in vivo* after as little as 1 hour of hypoxic exposure (Pascual *et al.*, 2001; Kline *et al.*, 2002). This instantaneous response of HIF1α and the induction of hundreds of known target genes plays a crucial role in surviving hypoxic events, primarily through rapidly increasing O_2 delivery to mitochondria, initiating metabolic rate depression, and supporting it through improved anaerobic glycolysis (Kim et al., 2006; Papandreou et al., 2006).

Our study stemmed from genomic analysis indicating naked mole rats possess a pVHL-mutation, which may lead to a relaxation of HIF1α degradation pathways. Indeed, HIF1α protein expression was found to be 3-4 times higher in brain and liver tissue isolated from naked mole rats relative to mice both held in normoxic conditions. To investigate if elevated endogenous HIF1α contributes to the HVR and HMR, we used two pharmacological agents (echinomycin and PX-478) to inhibit HIF1α binding activity in naked mole rats, and treated mice with a HIF1α stabilizer (EDHB). We subsequently measured changes in ventilation and metabolism in these animals exposed to 7% O_2. Interestingly, HIF1α antagonism (both agents) modified normoxic metabolic rate in naked mole rats but had little effect on hypoxic VO_2 or VCO_2. As a result, naked mole rats treated with a HIF1α inhibitor experienced a decrease in the magnitude of their

HMR from baseline. Interestingly, PHD antagonism in mice also resulted in a non-significant decrease in normoxic metabolic rate. As a result of this trend, the magnitude of their HMR was blunted.

In line with earlier observations exploring the link between metabolic rate and HIF expression (Iyer et al., 1998; Semenza et al., 1996), upregulation of HIF1α through PHD-inhibition is known to elicit decreases in basal O_2 consumption in mice (Aragonés et al., 2008). In contrast, a study two years later determined mice lacking FIH—and therefore possessing higher normoxic HIF1α expression—had higher metabolic rates, improved glucose and lipid homeostasis, and higher rates of ventilation (Zhang et al., 2010). It was therefore unclear how HIF-manipulation would affect metabolic rate in mice or naked mole rats. However, we predicted HIF1α antagonism in naked mole rats would elicit a response opposite to that of HIF1α stabilization in mice. Due to potential study limitations (discussed in following sections), HIF1α agonism had no effect on mice and HIF antagonism in naked mole rats led to reductions in normoxic $\dot{V}O_2$. Hypoxic metabolic rate did not change in either species following pharmacological HIF1α manipulation.

4.2 Naked mole rats undergo a metabolic fuel switch in hypoxia

We evaluated the proportion of lipids and carbohydrates used by naked mole rats through quantifying the RER (the quotient of $\dot{V}CO_2$ and $\dot{V}O_2$). Based on stoichiometry, ATP yield per mole of O_2 is 15% higher from oxidation of carbohydrates compared to lipids (Brand, 2005; Welch et al., 2007) while studies have demonstrated the actual yield of carbohydrate use is approximately 30% higher than that of lipids (Daut et al., 1989; Korvald et al., 2000). Thus, this switch to carbohydrate utilization represents an important O_2-saving adaptation during low

O_2 stress. Consistent with studies in high altitude rodent populations (McClelland et al., 1998; Schippers et al., 2012), naked mole rats shift from a primarily lipid-fueled metabolism toward a greater reliance on carbohydrates during hypoxic exposure, as indicated by an increase in their RER. Conversely, the same level of hypoxia did not elicit an observable switch to carbohydrate metabolism in mice.

Contrary to other studies (Zhang et al., 2010) in which the RER of FIH-mutant mice was unchanged, we observed a shift toward carbohydrate use following HIF1α stabilization in PHD-inhibited mice. In contrast, HIF1α-inhibition prevented the hypoxia-induced increase in carbohydrate use in naked mole rats. This suggests HIF1α stabilization may mediate a metabolic fuel switch during sustained hypoxia. In support of this, HIF1α is known to mediate a metabolic conversion in tumor cells through the induction of facultative glucose transporters GLUT1 and GLUT3 that increases the rate of glucose uptake into the cells (Ebert et al., 1995).

Another candidate behind fuel selection and metabolic remodeling in hypoxia is 5' AMP-activated protein kinase (AMPK) (Hardie and Sakamoto, 2006; Jørgensen et al., 2006). AMPK is a heterotrimeric enzyme complex which is activated by increases in the cellular AMP/ATP ratio (Hardie et al., 1999) resulting from hypoxia-induced reductions in ATP synthesis (Kudo et al., 1995; Marsin et al., 2000) or augmented ATP consumption due to exercise (Hardie and Sakamoto, 2006). In energy-scarce conditions, AMPK rapidly turns on catabolic ATP-generating pathways while inhibiting anabolic ATP-consuming biosynthetic pathways. For example, AMPK has been shown to inhibit gluconeogenesis (Horike et al., 2008) and protein synthesis (Hoppe et al., 2009; Leprivier et al., 2013). Studies have shown AMPK stimulates glucose uptake via increased expression and translocation of GLUT4 to the plasma membrane (Holmes et al., 1999; Kurth-Kraczek et al., 1999; Merrill et al., 1997) and may therefore contribute to an increase in

carbohydrate use in hypoxia. Several physiological functions downstream of HIF1α and AMPK and their stimuli intersect, including protein synthesis (via mTOR), apoptosis, and autophagy pathways (Li et al., 2015). A recent study demonstrated AMPK activation appears to be regulated on some level by optimal HIF1α expression (Li et al., 2015), while AMPK activity was important for determining HIF1α transcriptional activity under hypoxic conditions (Lee et al., 2003). Therefore, HIF1α may contribute to fuel selection patterns through interactions with cellular AMPK.

4.3 HIF1α does not mediate hypoxic ventilatory depression in naked mole rats

Other studies from our research team have previously reported a larger decline in $\dot{V}_E$ than what we report here (Chung et al., 2016; Pamenter et al., 2015). In these studies, control animals breathing 7% O_2 exhibited a 50-70% reduction in $\dot{V}_E$ as a result of significant decreases in both V_T (50%) and f_R (47%). Interestingly, our control naked mole rats exhibited only a 32% reduction $\dot{V}_E$ in hypoxia likely due to study limitations discussed in the following section. Nonetheless, this response is rare among small adult mammals, including other fossorial species such as degus, coruros, plateau pikas, and the middle east blind mole rat, all of which exhibit hypoxia-induced increases in $\dot{V}_E$ (Arieli and Ar, 1979; Frappell et al., 1992; Pichon et al., 2009; Tomasco et al., 2010).

Instead, naked mole rats possess a ventilatory response more similar to that of neonatal mammals (Mortola et al., 1989). In newborn mammals, the HVR is biphasic consisting of an immediate increase in ventilation within seconds followed by a depression of ventilation that often falls below baseline levels. The initial increase in respiration is mediated by activation of carotid chemoreceptors—the main O_2 sensing organ in mammals—while the second phase is

mainly controlled by central inhibitory mechanisms and metabolic changes that overrule the excitatory inputs from peripheral chemoreceptors (Bissonnette, 2000; Blanco et al., 1984a; Blanco et al., 1984b; Eden and Hanson, 1987; Mortola et al., 1989; Rehan et al., 1996). Decreased ventilatory activity in hypoxia may serve as a beneficial adaptation in naked mole rats, reducing the metabolic cost of increased breathing.

In naked mole rats, treatment with HIF1α-antagonists had mixed effects on ventilatory parameters. Echinomycin at either dose reduced f_R during hypoxia, and treatment with the higher dose (1.0 mg kg^{-1}) lead to this same decline in f_R during periods of 21% O_2 (baseline and recovery). Conversely, PX-478 treated naked mole rats did not exhibit this same decrease in f_R. Interestingly, V_T increased in all treatment groups in hypoxia following HIF1α inhibition with the most notable increase observed in low dose echinomycin treatment groups. Due to the unmatched effects on the components of ventilation, no significant change in $\dot{V}_E$ were observed during hypoxia. However, we observed a significant increase in the ACR$\dot{V}O_2$ of treated naked mole rats likely as a result of compounding effects of f_R, V_T, $\dot{V}O_2$, and EO_2. This increase suggests to ability of naked mole rats to match O_2 supply with O_2 demand was compromised following HIF1α inhibition.

The effects of HIF1α antagonism on the components of the HVR are interesting, since similar mutations within the VHL-HIF pathway—like those underlying Chuvash polycythemia—result in higher respiratory rates when first challenged with acute hypoxia. In contrast, naked mole rats, who inherently possess a similar mutation in the VHL-HIF pathway, exhibit hypoxic ventilatory decline during hypoxia, and lack an observable VAH response or hypoxia-induced respiratory plasticity following 10 days of chronic sustained hypoxia (Chung et al., 2016). It remains possible that HIF1α affects respiratory drive in naked mole rats, particularly through its

upregulation of adenosine and adenosine receptors. As mentioned, adenosine mediates the HVR by acting as either a respiratory stimulant or a respiratory depressant. Consistent with this, naked mole rats treated with an adenosine receptor antagonist are less tolerant to hypoxia and experience a reversal of the hypoxia-mediated decrease in $\dot{V}_E$ (Pamenter et al., 2015).

In our HIF stabilization experiments, saline-treated mice experienced significant increases in f_R in response to hypoxia. Treatment with EDHB lead to progressive increases in hypoxic f_R relative to control mice breathing 7%. These findings are consistent with previous studies which demonstrate HIF1α stabilization through PHD inhibition leads to an augmented HVR (Bishop et al., 2013; Hodson et al., 2016). The effects of PHD inhibition on f_R were again counteracted by a decrease in V_T resulting in no clear change in $\dot{V}_E$ in EDHB treated mice. The decrease in V_T also prevented significant changes in the ACR$\dot{V}O_2$ of mice. Interestingly, these results were reported in a study by Soliz et al. which injected mice with EPO, a downstream target of HIF1α. EPO-mice took shallower breaths but respired more frequently than saline-injected controls under severe hypoxia (6% inspiratory O_2) (Soliz et al., 2005; Soliz et al., 2007). This suggests V_T and f_R may be regulated by different physiological pathways, both of which are potentially downstream of the HIF1α pathway.

Study Limitations

Although this research was carefully prepared, we would like to acknowledge a few of its limitations and shortcomings.

Two-species comparisons

Interspecific comparisons are a common approach within comparative physiology—often used to identify which characteristics differ between species, or to establish new models in which

to study a phenomena or unique biomechanical mechanisms. Unfortunately, limiting comparisons to only two-species leads to several logical and statistical problems which often complicate our ability to draw meaningful conclusions about the adaptations in question (Garland and Adolph, 1994). In the context of this study, comparing HIF1α protein expression between mice and naked mole rats may not necessarily reflect the true adaptive landscape. Indeed, it is possible naked mole rats possess levels of HIF1α protein comparable to species not studied here, but which do not possess known genomic mutations in the HIF1α degradation pathway. Therefore, this study would have benefited from additional models in the qualification of HIF1α protein levels.

Similarly, PHD-inhibition in alternative hypoxia-intolerant models may yield ventilatory responses closer to naked mole rats, since the underlying mechanisms and the various time domains which define the HVR differ greatly between species and stage of maturation. Future studies are therefore encouraged to take a multi-species approach when comparing physiological adaptations.

Drug Dosing and Toxicity

Our EDHB dosing strategy was selected based off of previous studies which demonstrated that treatment with EDHB increases whole-animal hypoxia tolerance (Kasiganesan et al., 2007) and enhanced exercise performance in mice (Nimker et al., 2015; Nimker et al., 2016). Both studies confirmed injection with EDHB (50-250 mg kg^{-1}) leads to elevated levels of HIF1α, EPO, and VEGF protein in muscle via immunoblotting analysis (Nimker et al., 2015), and elevated HIF1α in liver and HIF1α-inducible EPO in serum (Kasiganesan et al., 2007). Furthermore, their research determined systemic treatment with EDHB results in significantly

increased survival in lethal hypoxia (5% O_2) and increased performance in sub-lethal hypoxia (8%) (Kasiganesan et al., 2007). The level of hypoxia used by Kasiganesan is normally lethal within 20 minutes (Scremin et al., 1980), however, half of the EDHB-treated animals survived until the termination of experiment at 60 minutes of exposure and fully recovered after 10 minutes following reintroduction of 21% O_2 (Kasiganesan et al., 2007).

The use of EDHB in the present study is therefore justified based on the successful inhibition of normoxic degradation of HIF1α by PHDs in the aforementioned studies. Unfortunately, the results of our qPCR analysis indicate treatment with EDHB did not elicit a significant increase in HIF1α or downstream target mRNA in mouse muscle and liver. It is worth mentioning that the highest administered dose in their experimental protocol (250 mg kg^{-1}) resulted in observable toxicity symptoms such as weight loss and reduced grooming behaviour. To avoid stress and toxicity-induced changes in respiratory and metabolic measurements, we injected mice with a mid-range dose of 180 mg kg^{-1} every second day for one week. It is therefore possible this dosing strategy was insufficient, or inappropriate for our model.

Similarly, mRNA levels for HIF1α-inducible genes did not significantly change in naked mole rat muscle following treatment with echinomycin (0.5 mg kg^{-1}). In contrast, mRNA expression of all genes evaluated by qPCR significantly increased in mole rat liver following treatment with echinomycin. This suggests a failure of echinomycin to inhibit HIF1α transcriptional activity. As well, our experimental animals were likely experiencing symptoms of drug-induced toxicity characterized by acute liver injury. In support of this, naked mole rats treated with high-dose echinomycin exhibited significant weight loss (~10-15%), lethargy, and skin lesions near the injection site. Increased HIF expression has been reported in many instances of hepatic disease in rats (Corpechot et al., 2002; Paternostro et al., 2010; Rosmorduc et al.,

1999) and might therefore explain the increase in HIF1α mRNA expression in liver. No overt toxicity symptoms were observed in naked mole rats administered with PX-478.

Weight loss is also commonly observed following exposure to hypoxia (Levine and Stray-Gundersen, 2001; Moraes and Loscalzo, 1997; Naeije, 1997) The factors contributing to hypoxia-induced weight loss are complex, although may result from HIF1α manipulation and its downstream effects on energy metabolism. For instance, hypoxia modulates insulin and insulin-like growth factor pathway (Agani and Semenza, 1998) which has been shown to induce growth retardation during chronic intrauterine hypoxia in some fetal species (Tazuke et al., 1998). It is therefore unclear if the weight loss observed in naked mole rats represents adverse drug events, or a HIF1α-directed response.

Additionally, our control animals were treated with saline despite both EDHB and echinomycin requiring the use of DMSO as a dissolving agent. While the concentration of DMSO was low (5%, or about 11.7 μg kg^{-1}), it has nevertheless been shown to act as a respiratory depressant (Rowed and De La Torre, 1973; Takeda et al., 2016) and therefore a DMSO control would have been appropriate for the purposes of our experiments.

mRNA expression does not necessarily predict protein expression

In hindsight, our mRNA expression profile between control and treated animals should have been followed up by protein quantification. Transcript expression levels are rarely predictive of protein levels. Studies which have investigated the link between the two often present weak and inconsistent correlations, restricting the use of mRNA quantification as a proxy for protein abundance. For example, Gygi *et al* found certain mRNA expression patterns in yeast were accompanied by substantial variations in protein abundance (Gygi et al., 1999).

Conversely, Greenbaum *et al* found a significant positive correlation (r=0.20-0.89) between protein and mRNA expression by merging many yeast protein abundance datasets (Greenbaum et al., 2003), and Anderson and Seilhamer found a positive correlation (r=0.48) between 19 selected mRNA-protein levels in human liver tissues (Anderson and Seilhamer, 1997). Similarly, a recent study that explored the predictive value of transcript levels in genes specific to human brain tissue found that while transcriptomic analysis was appropriate for certain classes of proteins, other transcription-translation correlations were highly variable (Bauernfeind and Babbitt, 2017).

Another study carried out mRNA-protein correlation analysis on 71 genes in isolated human circulating monocytes and found varied correlation depending on the biological category of gene ontology, with only five of the studied genes showing significant positive correlation across all samples (Guo et al., 2008). The team found a high correlation for genes associated with cellular components within the extracellular region, and a low correlation for genes involved in regulatory pathways. A previous study exploring both HIF mRNA and protein changes in hypoxia observed a decrease in HIF protein despite no variation in HIF mRNA upon exposure to acute or chronic hypoxia (Ginouvès et al., 2008).

Despite a growing body of literature on the topic, it remains difficult to evaluate which biological factor most prominently influences the correlation between mRNA and protein abundance, and therefore we are unable to determine if the results from our qPCR accurately reflect the entire physiological picture following drug-treatment. Furthermore, several studies have revealed HIF-dependent gene expression profiles are cell-type specific (Chi et al., 2006; Xia and Kung, 2009). Stroka *et al.* and Wiesener *et al.* (2003) also demonstrated differential HIFα expression among different organs supporting the model of tissue-specific adaptive protein

synthesis previously proposed (Smith et al., 1996; Stroka et al., 2001; Wiesener et al., 2003), suggesting our collection of data from only two tissues may not have been sufficient to answer the research question.

HIF Isoforms

It has been suggested that the balance of HIF1α, HIF2α and HIF3α, rather than their absolute expression, establishes set points for hypoxic sensing. HIF1α and HIF2α are the best studied HIFα isoforms and share 48% amino acid sequence identity and highly conserved biochemical properties (*i.e* domain architecture, hypoxic protein stabilization, dimerization with ARNT, and overlapping DNA recognition sequences) (Epstein et al., 2001; Semenza et al., 1996). The roles of HIF3α and its splice variants are less understood. HIF1α and HIF2α exhibit clear transcriptional selectivity as well as time and tissue-specific expression patterns restricted to distinct cell types during hypoxic gene regulation (Epstein et al., 2001; Menrad et al., 2010; Raval et al., 2005; Yuan et al., 2013). For instance, in some cell lines HIF1α appears most active during short periods (2-24 h) of intense hypoxia or anoxia (<.1%O_2) while HIF2α seemingly regulates responses to mild physiological hypoxia and/or chronic sustained hypoxia (Holmquist-Mengelbier et al., 2006). While HIF1α and HIF2α possess overlapping functions, its HIF2α that appears to transactivate EPO and mediate erythropoiesis (Gruber et al., 2007) and HIF1α which contributes to the transcription of LDHA or PDK1 (Elvidge et al., 2006; Hu et al., 2006; Raval et al., 2005; Sowter et al., 2003).

Studies of ventilatory control reveal opposing respiratory phenotypes in mice heterozygous for HIF1α versus HIF2α heterozygous mice. Carotid bodies isolated from HIF1α$^{+/-}$ mice manifest reduced sensitivity and response to some, but not all, forms of hypoxic stimulation

(Kline et al., 2002; Peng et al., 2006). Peng *et al* demonstrated mice haplo-insufficient for HIF2α and subjected to hypoxia experienced an exaggerated carotid body response, irregular breathing, hypertension, and elevated plasma norepinephrine levels (Peng et al., 2011). In contrast, HIF2α gain-of-function mutations do not elicit increase ventilatory sensitivity to hypoxia in mice (Formenti et al., 2011; Tan et al., 2013) while the presence of a hypomorphic VHL allele that impairs degradation of both HIF-α subunits in CP mice, leads to basal arterial hypocapnia, and a marked increase in the HVR (Smith et al., 2006). These findings suggest (i) hypoxia exerts different effects on HIF1α and HIF2α and (ii) different HIF α isoforms govern different adaptive responses in hypoxia. The balance of HIF1α and HIF2α during hypoxic exposure and their differential regulation of ventilatory parameters may possibly explain some of our mixed results.

Barometric Method in Poikilotherms

Whole-body plethysmography is a widely- used technique in the field of respiratory physiology. The basis for this method consists of recording pressure oscillations generated as the animal inside the experimental chamber warms and humidifies inspired air, which increases total pressure inside the chamber upon expiration. Converting this pressure signal to ventilatory volumes is commonly done using the barometric pressure method first introduced by Chapin (1954) and Drorbaugh and Fenn (1955), which was later modified by Jacky (1978) and Epstein *et al*. (1980) (Chapin, 1954; Drorbaugh and Fenn, 1955; Jacky, 1978). The barometric method depends upon six measurable parameters: 1) pressure changes within the chamber, 2) chamber water vapor pressure (P_cH_2O), 3) ambient temperature (T_a), 4) body temperature (T_b), 5) airway water vapor pressure (P_aH_2O), and 6) the pressure/volume response of a known volume displacement (pressure calibrations).

Open-chamber, open-flow plethysmography offers an advantage over other techniques because it allows for the non-invasive measurement of various ventilatory parameters, with no requirement for anesthesia, subject cooperation, or need to interfere with the airways or the animal's normal behaviour. However, its accuracy and application in poikilotherms or hibernating mammals has been called into question (Chaui-Berlinck and Bicudo, 1998; Enhorning et al., 1998; Epstein and Epstein, 1978; Malan, 1973; Mortola and Frappell, 1998; Szewczak and Powell, 2003). One major limitation in its use lies in the difficulty of accurately measuring the difference between T_b and T_a, especially when the difference between these temperatures begins to shrink. Studies suggest inaccuracies in T_a and T_b can introduce the largest errors in V_T, with the consequences of these errors being larger with smaller differences in T_a and T_b (Figure 4.1) (Chaui-Berlinck and Bicudo, 1998; Malan, 1973; Mortola and Frappell, 1998). For instance, Mortola and Frappell demonstrated a 1°C error in T_a measurement causes a 7% overestimation in V_T when the difference between T_a and T_b is 13°C. Conversely, when that difference is reduced to only 7°C, the degree of error introduced doubles (+15%) with the same 1°C error (Mortola and Frappell, 1998). Other studies have suggested that in order to keep errors in V_T computation below 5%, a temperature difference above 15°C is required (Chaui-Berlinck and Bicudo, 1998).

Naked mole rats have a unique thermoregulatory profile in that they are endothermic and thus capable endogenous heat production *via* non-shivering thermogenesis (Hislop and Buffenstein, 1994), and also poikilothermic, in that T_b is highly governed by T_a. This introduces a possibility for significant, and in some cases enormous errors (Chaui-Berlinck and Bicudo, 1998; Malan, 1973; Mortola and Frappell, 1998). This risk is often the reason why the barometric pressure technique is seldom adopted in animals with limited thermoregulatory capacity to maintain T_b

well above T_a (Malan, 1973). Therefore, the comparison between a homeothermic mouse and a poikilothermic naked mole rat using plethysmography may occlude our ability to identify the effects of HIFα manipulation by our pharmacological agents. It is likely some of our temperature measurements do not reflect true core temperature, due to migration of the subdermal microchips to the side of the animal, while others remained closer to the heat-generating interscapular brown adipose tissue (Goldman et al., 1999). Unfortunately, we also did not quantify relative humidity inside the chamber and instead assumed 100% saturation in our calculation of P_cH_2O. If the chamber is fully saturated, errors in P_cH_2O are only caused by errors in the measurements of T_a. However, a relative humidity lower than that assumed leads to an overestimation in V_T as much as 34% when the difference between T_b-T_a is small (6°C) (Mortola and Frappell, 1998). Since the T_b-T_a in mole rats was on average 2.7°C, it is likely that we significantly overestimated V_T.

Conclusion and Future Directions

The prominent role of the PHD-HIF signaling cascade in O_2 homeostasis has made it an attractive target in the study of comparative physiology and human disease. Indeed, manipulation of HIF activity has become a focal point in the treatment of cancer and ischemic injury (Hirota and Semenza, 2006; Kido et al., 2005; Pugh and Ratcliffe, 2003). Interestingly, naked mole rats possess elevated HIF1α levels in normoxia without any of the detriments seen in humans with VHL disease or Chuvash polycythemia. In fact, this fossorial species displays remarkable tolerance to hypoxic exposure because of their ability to match O_2 demand with O_2 supply through adjustments in metabolism and ventilation.

Both HIF1α-antagonists had mixed effects on ventilatory and metabolic parameters in naked mole rats breathing both 21% and 7% O_2. It is possible that HIF1-mediated transcription of

downstream targets contributes to metabolic set points in normoxia, overall ventilatory drive, and hypoxic fuel switching in naked mole rats, however, the true nature of its effects are masked by the challenges of pharmacological manipulation. The use of pharmaceuticals, especially in new species, poses a problem in that it is difficult to assess drug-specificity and off-target effects. Inhibiting PHD enzymes in particular is challenging, due to its involvement in many different physiological pathways (Cao et al., 1997; Teodoro et al., 2006; Vuori et al., 1992). While we attempted to reconcile this challenge by comparing the effects of two different HIF-inhibitors, a larger data set and pharmacological agents which may be better suited to naked mole rat physiology would be valuable in determining the true effect of HIF-manipulation on the HVR and HMR. Alternatively, with the advent and improvement of promising genetic techniques like CRISPR, HIF1α genetic knockdowns may be much more reliable in determining HIF-mediated metabolic and ventilatory responses in naked mole rats.

In acknowledging the difficulties associated with plethysmography use in poikilotherms, we first attempted to assess ventilatory parameters by way of pneumotach, which removes the suite of errors intrinsic to the barometric method and allows for more accurate interspecies comparison. Unfortunately, the available apparatuses are designed for rodents with conical snouts. The flat-faces and externally-located teeth of naked mole rats present a barrier to the use of this equipment in that a tight-seal cannot be maintained. Furthermore, these devices require animal-restraint which typically induces a stress-response that may confound measurements of f_R. Future studies may wish to develop a pneumotach better adapted to naked mole rats, although they should consider the trade-offs to either approach.

In hindsight, protein analysis may have been more informative in determining drug-efficacy and future studies are advised to perform both. Future research may also wish to investigate the

degree of contribution from each HIFα isoforms on the HVR and HMR and narrow down the possible downstream targets which may mediate these responses. The opposing effects of HIFα on V_T and f_R are particularly interesting and represent an area which may benefit from additional research.

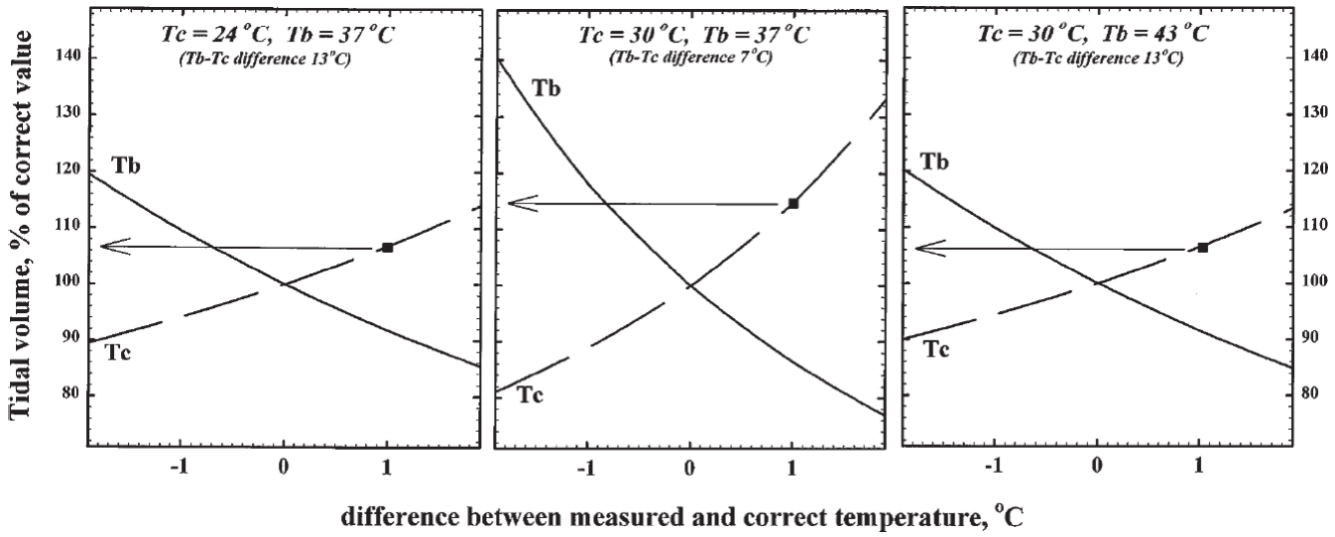

Figure 4.1 Effect of introduced measurement errors in either body temperature or chamber temperature on tidal volume (Mortola and Frappell, 1998).

References

Agani, F. and Semenza, G. L. (1998). Mersalyl is a novel inducer of vascular endothelial growth factor gene expression and hypoxia-inducible factor 1 activity. *Mol. Pharmacol.* **54**, 749–754.

Ainscow, E. K. and Brand, M. D. (1999). Top-down control analysis of ATP turnover, glycolysis and oxidative phosphorylation in rat hepatocytes. *Eur. J. Biochem.* **263**, 671–685.

Altschul, S. F., Gish, W., Miller, W., Myers, E. W. and Lipman, D. J. (1990). Basic local alignment search tool. *J. Mol. Biol.* **215**, 403–410.

Anderson, L. and Seilhamer, J. (1997). A comparison of selected mRNA and protein abundances in human liver. In *Electrophoresis*, pp. 533–537.

Ang, S. O., Chen, H., Hirota, K., Gordeuk, V. R., Jelinek, J., Guan, Y., Liu, E., Sergueeva, A. I., Miasnikova, G. Y., Mole, D., et al. (2002). Disruption of oxygen homeostasis underlies congenital Chuvash polycythemia. *Nat. Genet.* **32**, 614–21.

Aragonés, J., Schneider, M., Van Geyte, K., Fraisl, P., Dresselaers, T., Mazzone, M., Dirkx, R., Zacchigna, S., Lemieux, H., Jeoung, N. H., et al. (2008). Deficiency or inhibition of oxygen sensor Phd1 induces hypoxia tolerance by reprogramming basal metabolism. *Nat. Genet.* **40**, 170–180.

Arieli, R. and Ar, A. (1979). Ventilation of a fossorial mammal (*Spalax ehrenbergi*) in hypoxic and hypercapnic conditions. *J. Appl. Physiol.* **47**, 1011–1017.

Baker-Herman, T. L., Fuller, D. D., Bavis, R. W., Zabka, A. G., Golder, F. J., Doperalski, N. J., Johnson, R. A., Watters, J. J. and Mitchell, G. S. (2004). BDNF is necessary and sufficient for spinal respiratory plasticity following intermittent hypoxia. *Nat. Neurosci.* **7**, 48–55.

Barros, R. C., Zimmer, M. E., Branco, L. G. and Milsom, W. K. (2001). Hypoxic metabolic

response of the golden-mantled ground squirrel. *J. Appl. Physiol.* **91**, 603–12.

Bauernfeind, A. L. and Babbitt, C. C. (2017). The predictive nature of transcript expression levels on protein expression in adult human brain. *BMC Genomics* **18**,.

Bavis, R. W., Powell, F. L., Bradford, A., Hsia, C. C. W., Peltonen, J. E., Soliz, J., Zeis, B., Fergusson, E. K., Fu, Z., Gassmann, M., et al. (2007). Respiratory plasticity in response to changes in oxygen supply and demand. *Integr. Comp. Biol.* **47**, 532–551.

Benderro, G. F. and Lamanna, J. C. (2011). Hypoxia-induced angiogenesis is delayed in aging mouse brain. *Brain Res.* **1389**, 50–60.

Bennett, N. C., Jarvis, J. U. M. and Cotterili, F. P. D. (1993). Poikilothermic traits and thermoregulation in the Afrotropical social subterranean Mashona mole-rat (Cryptomys hottentotus darlingi) (Rodentia: Bathyergidae). *J. Zool.* **231**, 179–186.

Bennett, N. C., Aguilar, G. H., Jarvis, J. U. M. and Faulkes, C. G. (1994). Thermoregulation in three species of Afrotropical subterranean mole-rats (Rodentia: Bathyergidae) from Zambia and Angola and scaling within the genus Cryptomys. *Oecologia* **97**, 222–227.

Bickler, P. E. and Buck, L. T. (2007). Hypoxia tolerance in reptiles, amphibians, and fishes: life with variable oxygen availability. *Annu Rev Physiol* **69**, 145–170.

Bisgard, G. E. (2000). Carotid body mechanisms in acclimatization to hypoxia. *Respir. Physiol.* **121**, 237–246.

Bishop, T., Talbot, N. P., Turner, P. J., Nicholls, L. G., Pascual, A., Hodson, E. J., Douglas, G., Fielding, J. W., Smith, T. G., Demetriades, M., et al. (2013). Carotid body hyperplasia and enhanced ventilatory responses to hypoxia in mice with heterozygous deficiency of PHD2. *J. Physiol.* **591**, 3565–77.

Bissonnette, J. M. (2000). Mechanisms regulating hypoxic respiratory depression during fetal

and postnatal life. *Am. J. Physiol. Regul. Integr. Comp. Physiol.* **278**, R1391-400.

Blanco, C. E., Dawes, G. S., Hanson, M. A. and McCooke, H. B. (1984a). The response to hypoxia of arterial chemoreceptors in fetal sheep and new???born lambs. *J. Physiol.* **351**, 25–37.

Blanco, C. E., Hanson, M. a, Johnson, P. and Rigatto, H. (1984b). Breathing pattern of kittens during hypoxia. *J. Appl. Physiol.* **56**, 12–7.

Bocharova, L. S., Gordon, R. Y. and Arkhipov, V. I. (1992). Uridine uptake and RNA synthesis in the brain of torpid and awakened ground squirrels. *Comp. Biochem. Physiol. -- Part B Biochem.* **101**, 189–192.

Borecky, L. and Pamenter, M. (2017). Oxygen sensing and transcriptional regulation of adaptive hypoxic responses. In *Chemosensory Sensors and Systems: Evolutionary Significance, Biological Effects and New Insights*, pp. 1–72.

Bosch-Marce, M., Okuyama, H., Wesley, J. B., Sarkar, K., Kimura, H., Liu, Y. V., Zhang, H., Strazza, M., Rey, S., Savino, L., et al. (2007). Effects of aging and hypoxia-inducible factor-1 activity on angiogenic cell mobilization and recovery of perfusion after limb ischemia. *Circ. Res.* **101**, 1310–1318.

Bouverot, P. and Hildwein, G. (1978). Combined effects of hypoxia and moderate heat load on ventilation in awake Pekin ducks. *Respir. Physiol.* **35**, 373–383.

Brand, M. D. (2005). The efficiency and plasticity of mitochondrial energy transduction. *Biochem. Soc. Trans.* **33**, 897–904.

Brooks, G. a, Butterfield, G. E., Wolfe, R. R., Groves, B. M., Mazzeo, R. S., Sutton, J. R., Wolfel, E. E. and Reeves, J. T. (1991). Increased dependence on blood glucose after acclimatization to 4,300 m. *J. Appl. Physiol.* **70**, 919–927.

Brugarolas, J., Lei, K., Hurley, R. L., Manning, B. D., Reiling, J. H., Hafen, E., Witters, L. A., Ellisen, L. W. and Kaelin, W. G. (2004). Regulation of mTOR function in response to hypoxia by REDD1 and the TSC1/TSC2 tumor suppressor complex. *Genes Dev.* **18**, 2893–2904.

Bryan, J. D., Hill, L. G. and Neill, W. H. (1984). Interdependence of acute temperature preference and respiration in the plains minnow. *Trans. Am. Fish. Soc.* **113**, 557–562.

Buc-Calderon, P., Lefebvre, V. and Steenbrugge, M. (1993). Inhibition of protein synthesis in isolated hepatocytes as an immediate response to oxygen limitation. In *Surviving Hypoxia*, pp. 271–280.

Buck, L. T. and Bickler, P. E. (1995). Role of adenosine in NMDA receptor modulation in the cerebral cortex of an anoxia-tolerant turtle (Chrysemys picta belli). *J. Exp. Biol.* **198**, 1621–1628.

Buck, L. T. and Hochachka, P. W. (1993). Anoxic suppression of Na(+)-K(+)-ATPase and constant membrane potential in hepatocytes: support for channel arrest. *Am. J. Physiol.* **265**, R1020–R1025.

Buck, L. T., Land, S. C. and Hochachka, P. W. (1993). Anoxia-tolerant hepatocytes: model system for study of reversible metabolic suppression. *Am. J. Physiol.* **265**, R49–R56.

Buffenstein, R. and Yahav, S. (1991). Is the naked mole-rat Hererocephalus glaber an endothermic yet poikilothermic mammal? *J. Therm. Biol.* **16**, 227–232.

Buss, D., Routledge, P. and Watt, A. (1986). Intravenous adenosine stimulates respiration in conscious adult rabbits. *Br. J. Pharmacol.* **87**, 182.

Buttgereit, F. and Brand, M. D. (1995). A hierarchy of ATP-consuming processes in mammalian cells. *Biochem. J.* **312 (Pt 1**, 163–167.

Cam, H., Easton, J. B., High, A. and Houghton, P. J. (2010). mTORC1 signaling under hypoxic conditions is controlled by atm-dependent phosphorylation of HIF-1α. *Mol. Cell* **40**, 509–520.

Cao, M., Westerhausen-Larson, a, Niyibizi, C., Kavalkovich, K., Georgescu, H. I., Rizzo, C. F., Hebda, P. a, Stefanovic-Racic, M. and Evans, C. H. (1997). Nitric oxide inhibits the synthesis of type-II collagen without altering Col2A1 mRNA abundance: prolyl hydroxylase as a possible target. *Biochem. J.* **324 (Pt 1**, 305–10.

Chance, B. and Williams, G. R. (1956). The respiratory chain and oxidative phosphorylation. *Advan Enzym. Relat Areas Mol Biol* **17**, 65–135.

Chapin, J. L. (1954). Ventilatory Response of the Unrestraned and Unanesthetized Hamster to CO2. *Am. J. Physiol. Content* **179**, 146–148.

Chaui-Berlinck, J. G. and Bicudo, J. E. P. W. (1998). The signal in total-body plethysmography: Errors due to adiabatic-isothermic difference. *Respir. Physiol.* **113**, 259–270.

Chen, J., He, L., Dinger, B. and Fidone, S. (2000). Cellular mechanisms involved in rabbit carotid body excitation elicited by endothelin peptides. *Respir. Physiol.* **121**, 13–23.

Chen, J., He, L., Dinger, B., Stensaas, L. and Fidone, S. (2002a). Role of endothelin and endothelin A-type receptor in adaptation of the carotid body to chronic hypoxia. *Am. J. Physiol. Lung Cell. Mol. Physiol.* **282**, L1314-23.

Chen, Y., Tipoe, G. L., Liong, E., Leung, P., Lam, S. Y., Iwase, R., Tjong, Y. W. and Fung, M. L. (2002b). Chronic hypoxia enhances endothelin-1-induced intracellular calcium elevation in rat carotid body chemoreceptors and up-regulates ETA receptor expression. *Pflugers Arch. Eur. J. Physiol.* **443**, 565–573.

Chen, J., Zhang, C., Jiang, H., Li, Y., Zhang, L., Robin, A., Katakowski, M., Lu, M. and Chopp, M. (2005). Atorvastatin induction of VEGF and BDNF promotes brain plasticity after stroke in mice. *J. Cereb. Blood Flow Metab.* **25**, 281–290.

Cheviron, Z. A., Bachman, G. C., Connaty, A. D., McClelland, G. B. and Storz, J. F. (2012). Regulatory changes contribute to the adaptive enhancement of thermogenic capacity in high-altitude deer mice. *Proc. Natl. Acad. Sci.* **109**, 8635–8640.

Chi, J.-T., Wang, Z., Nuyten, D. S. A., Rodriguez, E. H., Schaner, M. E., Salim, A., Wang, Y., Kristensen, G. B., Helland, Å., Børresen-Dale, A.-L., et al. (2006). Gene Expression Programs in Response to Hypoxia: Cell Type Specificity and Prognostic Significance in Human Cancers. *PLoS Med* **3**, e47.

Chidekel, A. S., Friedman, J. E. and Haddad, G. G. (1997). Anoxia-Induced Neuronal Injury : Role of Na+ Entry and Na+-Dependent Transport. *Exp. Neurol.* **413**, 403–413.

Chung, D., Dzal, Y. A., Seow, A., Milsom, W. K. and Pamenter, M. E. (2016). Naked mole rats exhibit metabolic but not ventilatory plasticity following chronic sustained hypoxia. *Proc. R. Soc. B* **283**,.

Colom, L. V, Diaz, M. E., Beers, D. R., Neely, a, Xie, W. J. and Appel, S. H. (1998). Role of potassium channels in amyloid-induced cell death. *J. Neurochem.* **70**, 1925–1934.

Contreras, L. C. and McNab, B. K. (1990). Thermoregulation and energetics in subterranean mammals. *Prog. Clin. Biol. Res.* **335**, 231–50.

Corpechot, C., Barbu, V., Wendum, D., Kinnman, N., Rey, C., Poupon, R., Housset, C. and Rosmorduc, O. (2002). Hypoxia-induced VEGF and collagen I expressions are associated with angiogenesis and fibrogenesis in experimental cirrhosis. *Hepatology* **35**, 1010–1021.

Corradetti, M. N., Inoki, K. and Guan, K. L. (2005). The stress-inducted proteins RTP801 and

RTP801L are negative regulators of the mammalian target of rapamycin pathway. *J. Biol. Chem.* **280**, 9769–9772.

Dallaporta, B., Hirsch, T., Susin, S. A., Zamzami, N., Larochette, N., Brenner, C., Marzo, I. and Kroemer, G. (1998). Potassium leakage during the apoptotic degradation phase. *J. Immunol.* **160**, 5605–15.

Dang, C. V., Kim, J. W., Gao, P. and Yustein, J. (2008). The interplay between MYC and HIF in cancer. *Nat. Rev. Cancer* **8**, 51–56.

Daut, B. J., Elzinga, G. and Ut, J. DA (1989). SUBSTRATE DEPENDENCE OF ENERGY METABOLISM IN ISOLATED GUINEA-PIG CARDIAC MUSCLE: A MICROCALORIMETRIC STUDY. *J. Physiol.* **413**, 379–397.

Dawn, B. and Bolli, R. (2005). HO-1 induction by HIF-1: a new mechanism for delayed cardioprotection? *Am. J. Physiol. Circ. Physiol.* **289**, H522–H524.

Dhani, N., Fyles, A., Hedley, D. and Milosevic, M. (2015). The clinical significance of hypoxia in human cancers. *Semin. Nucl. Med.* **45**, 110–121.

Dhillon, D. P., Barer, G. R. and Walsh, M. (1984). The enlarged carotid body of the chronically hypoxic and chronically hypoxic and hypercapnic rat: a morphometric analysis . *Q. J. Exp. Physiol.* **69**, 301–317.

Di Giulio, C., Grilli, A., De Lutiis, M. A., Di Natale, F., Sabatino, G. and Felaco, M. (1998). Does chronic hypoxia increase rat carotid body nitric oxide? *Comp. Biochem. Physiol. - A Mol. Integr. Physiol.* **120**, 243–247.

Dirnagl, U., Iadecola, C. and Moskowitz, M. A. (1999). Pathobiology of ischaemic stroke: An integrated view. *Trends Neurosci.* **22**, 391–397.

Doll, C. J., Hochachka, P. W. and Reiner, P. B. (1991). Channel arrest: implications from

membrane resistance in turtle neurons. *Am. J. Physiol.* **261**, R1321–R1324.

Dominguez-Sola, D., Ying, C. Y., Grandori, C., Ruggiero, L., Chen, B., Li, M., Galloway, D. A., Gu, W., Gautier, J. and Dalla-Favera, R. (2007). Non-transcriptional control of DNA replication by c-Myc. *Nature* **448**, 445–451.

Drorbaugh, J. E. and Fenn, W. O. (1955). A barometric method for measuring ventilation in newborn infants. *Pediatrics* **16**, 81–7.

Dwinell, M. R., Huey, K. a and Powell, F. L. (2000). Chronic hypoxia induces changes in the central nervous system processing of arterial chemoreceptor input. *Adv. Exp. Med. Biol.* **475**, 477–84.

Ebert, B. L., Firth, J. D. and Ratcliffe, P. J. (1995). Hypoxia and mitochondrial inhibitors regulate expression of glucose transporter-1 via distinct cis-acting sequences. *J. Biol. Chem.* **270**, 29083–29089.

Eckle, T., Kewley, E. M., Brodsky, K. S., Tak, E., Bonney, S., Gobel, M., Anderson, D., Glover, L. E., Riegel, A. K., Colgan, S. P., et al. (2014). Identification of Hypoxia-Inducible Factor HIF-1A as Transcriptional Regulator of the A2B Adenosine Receptor during Acute Lung Injury. *J. Immunol.* **192**, 1249–1256.

Eden, G. J. and Hanson, M. A. (1987). Maturation of the respiratory response to acute hypoxia in the newborn rat. *J. Physiol.* **392**, 1–9.

Elvidge, G. P., Glenny, L., Appelhoff, R. J., Ratcliffe, P. J., Ragoussis, J. and Gleadle, J. M. (2006). Concordant regulation of gene expression by hypoxia and 2-oxoglutarate-dependent dioxygenase inhibition: The role of HIF-1α, HIF-2α, and other pathways. *J. Biol. Chem.* **281**, 15215–15226.

Enhorning, G., van Schaik, S., Lundgren, C. and Vargas, I. (1998). Whole-body

plethysmography, does it measure tidal volume of small animals? *Can. J. Physiol. Pharmacol.* **76**, 945–51.

Epstein, M. A. farrell and Epstein, R. A. (1978). A theoretical analysis of the barometric method for measurement of tidal volume. *Respir. Physiol.* **32**, 105–120.

Epstein, A. C., Gleadle, J. M., McNeill, L. A., Hewitson, K. S., O'Rourke, J., Mole, D. R., Mukherji, M., Metzen, E., Wilson, M. I., Dhanda, A., et al. (2001). C. elegans EGL-9 and mammalian homologs define a family of dioxygenases that regulate HIF by prolyl hydroxylation. *Cell* **107**, 43–54.

Fingar, D. C. and Blenis, J. (2004). Target of rapamycin (TOR): An integrator of nutrient and growth factor signals and coordinator of cell growth and cell cycle progression. *Oncogene* **23**, 3151–3171.

Firth, J. D., Ebert, B. L. and Ratcliffe, P. J. (1995). Hypoxic regulation of lactate dehydrogenase A: Interaction between hypoxia-inducible factor 1 and cAMP response elements. *J. Biol. Chem.* **270**, 21021–21027.

Formenti, F., Beer, P. A., Croft, Q. P. P., Dorrington, K. L., Gale, D. P., Lappin, T. R. J., Lucas, G. S., Maher, E. R., Maxwell, P. H., McMullin, M. F., et al. (2011). Cardiopulmonary function in two human disorders of the hypoxia-inducible factor (HIF) pathway: von Hippel-Lindau disease and HIF-2alpha gain-of-function mutation. *FASEB J.* **25**, 2001–11.

Fox, K. R. and Kentebe, E. (1990). Echinomycin binding to the sequence CG(AT) $_n$ CG alters the structure of the central AT region. *Nucleic Acids Res.* **18**, 1957–1963.

Frappell, P., Saiki, C. and Mortola, J. P. (1991). Metabolism during normoxia, hypoxia and recovery in the newborn kitten. *Respir. Physiol.* **86**, 115–124.

Frappell, P., Lanthier, C., Baudinette, R. V and Mortola, J. P. (1992). Metabolism and ventilation in acute hypoxia: a comparative analysis in small mammalian species. *Am. J. Physiol.* **262**, R1040–R1046.

Fraser, K. P., Houlihan, D. F., Lutz, P. L., Leone-Kabler, S., Manuel, L. and Brechin, J. G. (2001). Complete suppression of protein synthesis during anoxia with no post-anoxia protein synthesis debt in the red-eared slider turtle *Trachemys scripta elegans*. *J. Exp. Biol.* **204**, 4353–4360.

Fredholm, B. (1982). Adenosine receptors. *Med. Biol.* **60**, 289.

Friedman, J. E. and Haddad, G. G. (1994). Anoxia induces an increase in intracellular sodium in rat central neurons in vitro. *Brain Res.* **663**, 329–34.

Garland, T. and Adolph, S. C. (1994). Why Not To Do 2-Species Comparative-Studies - Limitations on Inferring Adaptation. *Physiol. Zool.* **67**, 797–828.

Gautier, H., Bonora, M. and Remmers, J. E. (1989). Effects of hypoxia on metabolic rate of conscious adult cats during cold exposure. *J. Appl. Physiol.* **67**, 32–8.

Giaid, A., Gibson, S. J., Ibrahim, B. N., Legon, S., Bloom, S. R., Yanagisawa, M., Masaki, T., Varndell, I. M. and Polak, J. M. (1989). Endothelin 1, an endothelium-derived peptide, is expressed in neurons of the human spinal cord and dorsal root ganglia. *Proc. Natl. Acad. Sci. U. S. A.* **86**, 7634–8.

Ginouvès, A., Ilc, K., Macías, N., Pouysségur, J. and Berra, E. (2008). PHDs overactivation during chronic hypoxia "desensitizes" HIFalpha and protects cells from necrosis. *Proc. Natl. Acad. Sci. U. S. A.* **105**, 4745–4750.

Giussani, D. A., Spencer, J. A., Moore, P. J., Bennet, L. and Hanson, M. A. (1993). Afferent and efferent components of the cardiovascular reflex responses to acute hypoxia in term

fetal sheep. *J. Physiol.* **461**, 431–49.

Goldman, B. D., Goldman, S. L., Lanz, T., Magaurin, A. and Maurice, A. (1999). Factors influencing metabolic rate in naked mole-rats (Heterocephalus glaber). *Physiol. Behav.* **66**, 447–459.

Golstein, P. and Kroemer, G. (2007). Cell death by necrosis: towards a molecular definition. *Trends Biochem. Sci.* **32**, 37–43.

Gordan, J. D., Thompson, C. B. and Simon, M. C. (2007). HIF and c-Myc: Sibling Rivals for Control of Cancer Cell Metabolism and Proliferation. *Cancer Cell* **12**, 108–113.

Gordon, C. J. and Fogelson, L. (1991). Comparative effects of hypoxia on behavioral thermoregulation in rats, hamsters, and mice. *Am. J. Physiol.* **260**, R120–R125.

Greenbaum, D., Colangelo, C., Williams, K. and Gerstein, M. (2003). Comparing protein abundance and mRNA expression levels on a genomic scale. *Genome Biol.* **4**,.

Grieshaber, M. K., Hardewig, I., Kreutzer, U. and Pörtner, H.-O. (1994). Physiological and Metabolic Responses to Hypoxia in Invertebrates. *Rev. Physiol. Biochem. Pharmacol.* **125**,.

Griffiths, T. L. and Holgate, S. (1990). The role of adenosine in respiratory physiology. In *Adenosine and adenosine receptors*, pp. 381–422. Humana Press.

Gruber, M., Hu, C.-J., Johnson, R. S., Brown, E. J., Keith, B. and Simon, M. C. (2007). Acute postnatal ablation of Hif-2alpha results in anemia. *Proc. Natl. Acad. Sci. U. S. A.* **104**, 2301–6.

Guo, Y., Xiao, P., Lei, S., Deng, F., Xiao, G. G., Liu, Y., Chen, X., Li, L., Wu, S., Chen, Y., et al. (2008). How is mRNA expression predictive for protein expression? A correlation study on human circulating monocytes. *Acta Biochim. Biophys. Sin. (Shanghai).* **40**, 426–436.

Guppy, M. and Withers, P. (1999). Metabolic depression in animals: physiological perspectives and biochemical generalizations. *Biol. Rev. Camb. Philos. Soc.* **74**, 1–40.

Guppy, M., Fuery, C. J. and Flanigan, J. E. (1994). Biochemical principles of metabolic depression. *Comp. Biochem. Physiol. -- Part B Biochem.* **109**, 175–189.

Guzy, R. D., Hoyos, B., Robin, E., Chen, H., Liu, L., Mansfield, K. D., Simon, M. C., Hammerling, U. and Schumacker, P. T. (2005). Mitochondrial complex III is required for hypoxia-induced ROS production and cellular oxygen sensing. *Cell Metab.* **1**, 401–408.

Gygi, S. P., Rochon, Y., Franza, B. R. and Aebersold, R. (1999). Correlation between Protein and mRNA Abundance in Yeast. *Mol. Cell. Biol.* **19**, 1720–1730.

Hardie, D. G. and Sakamoto, K. (2006). AMPK: A Key Sensor of Fuel and Energy Status in Skeletal Muscle. *Physiology* **21**, 48–60.

Hardie, D. G., Salt, I. P., Hawley, S. A. and Davies, S. P. (1999). AMP-activated protein kinase: an ultrasensitive system for monitoring cellular energy charge. *Biochem. J.* **722**, 717–22.

Heckmann, L.-H., Sørensen, P. B., Krogh, P. and Sørensen, J. G. (2011). NORMA-Gene: A simple and robust method for qPCR normalization based on target gene data. *BMC Bioinformatics* **12**, 250.

Hedner, T., Hedner, J., Wessberg, P. and Jonason, J. (1982). Regulation of breathing in the rat: indications for a role of central adenosine mechanisms. *Neurosci. Lett.* **33**, 147–151.

Heitzmann, D., Buehler, P., Schweda, F., Georgieff, M., Warth, R. and Thomas, J. (2016). The in vivo respiratory phenotype of the adenosine A1 receptor knockout mouse. *Respir. Physiol. Neurobiol.* **222**, 16–28.

Helton, R., Cui, J., Scheel, J. R., Ellison, J. a, Ames, C., Gibson, C., Blouw, B., Ouyang, L.,

Dragatsis, I., Zeitlin, S., et al. (2005). Brain-specific knock-out of hypoxia-inducible factor-1alpha reduces rather than increases hypoxic-ischemic damage. *J. Neurosci.* **25**, 4099–4107.

Hervouet, E., Demont, J., Pecina, P., Vojtísková, A., Houstek, J., Simonnet, H. and Godinot, C. (2005). A new role for the von Hippel-Lindau tumor suppressor protein: Stimulation of mitochondrial oxidative phosphorylation complex biogenesis. *Carcinogenesis* **26**, 531–539.

Hewitson, K. S., McNeill, L. A., Riordan, M. V., Tian, Y. M., Bullock, A. N., Welford, R. W., Elkins, J. M., Oldham, N. J., Bhattacharya, S., Gleadle, J. M., et al. (2002). Hypoxia-inducible factor (HIF) asparagine hydroxylase is identical to factor inhibiting HIF (FIH) and is related to the cupin structural family. *J. Biol. Chem.* **277**, 26351–26355.

Hickey, M. M., Richardson, T., Wang, T., Mosqueira, M., Arguiri, E., Yu, H., Yu, Q. C., Solomides, C. C., Morrisey, E. E., Khurana, T. S., et al. (2010). The von Hippel-Lindau Chuvash mutation promotes pulmonary hypertension and fibrosis in mice. *J. Clin. Invest.* **120**, 827–839.

Hicks, J. W. and Wood, S. C. (1985). Temperature regulation in lizards: effects of hypoxia. *Am. J. Physiol.* **248**, R595-600.

Hirota, K. and Semenza, G. L. (2006). Regulation of angiogenesis by hypoxia-inducible factor 1. *Crit. Rev. Oncol. Hematol.* **59**, 15–26.

Hislop, M. S. and Buffenstein, R. (1994). Noradrenaline induces nonshivering thermogenesis in both the naked mole-rat (Heterocephalus glaber) and the Damara mole-rat (Cryptomys damarensis) despite very different modes of thermoregulation. *J. Therm. Biol.* **19**, 25–32.

Hoback, W. W. and Stanley, D. W. (2001). Insects in hypoxia. *J. Insect Physiol.* **47**, 533–542.

Hochachka, P. W. (1986). Defense strategies against hypoxia and hypothermia. *Science* **231**, 234–41.

Hochachka, P. W. and Lutz, P. L. (2001). Mechanism, origin, and evolution of anoxia tolerance in animals. In *Comparative Biochemistry and Physiology - B Biochemistry and Molecular Biology*, pp. 435–459.

Hochachka, P. W., Stanley, C., Matheson, G. O., McKenzie, D. C., Allen, P. S. and Parkhouse, W. S. (1991). Metabolic and work efficiencies during exercise in Andean natives. *J. Appl. Physiol.* **70**, 1720–1730.

Hochachka, P. W., Buck, L. T., Doll, C. J. and Land, S. C. (1996). Unifying theory of hypoxia tolerance: molecular/metabolic defense and rescue mechanisms for surviving oxygen lack. *Proc. Natl. Acad. Sci. U. S. A.* **93**, 9493–9498.

Hockel, M., Schlenger, K., Aral, B., Mitze, M., Schaffer, U. and Vaupel, P. (1996). Association between tumor hypoxia and malignant progression in advanced cancer of the uterine cervix. *Cancer Res.* **56**, 4509–4515.

Hodson, E. J., Nicholls, L. G., Turner, P. J., Llyr, R., Fielding, J. W., Douglas, G., Ratnayaka, I., Robbins, P. A., Pugh, C. W., Buckler, K. J., et al. (2016). Regulation of ventilatory sensitivity and carotid body proliferation in hypoxia by the PHD2/HIF-2 pathway. *J. Physiol.* **594**, 1179–1195.

Holmes, B. F., Kurth-Kraczek, E. J. and Winder, W. W. (1999). Chronic activation of 5'-AMP-activated protein kinase increases GLUT-4, hexokinase, and glycogen in muscle. *J. Appl. Physiol.* **87**, 1990–1995.

Holmquist-Mengelbier, L., Fredlund, E., Löfstedt, T., Noguera, R., Navarro, S., Nilsson, H., Pietras, A., Vallon-Christersson, J., Borg, A., Gradin, K., et al. (2006). Recruitment of

HIF-1alpha and HIF-2alpha to common target genes is differentially regulated in neuroblastoma: HIF-2alpha promotes an aggressive phenotype. *Cancer Cell* **10**, 413–23.

Holtze, S., Braude, S., Lemma, A., Koch, R., Morhart, M., Szafranski, K., Platzer, M., Alemayehu, F., Goeritz, F. and Hildebrandt, T. B. (2017). The microenvironment of naked mole-rat burrows in East Africa. *Afr. J. Ecol.*

Hoppe, S., Bierhoff, H., Cado, I., Weber, A., Tiebe, M., Grummt, I. and Voit, R. (2009). AMP-activated protein kinase adapts rRNA synthesis to cellular energy supply. *Proc. Natl. Acad. Sci.* **106**, 17781–17786.

Horike, N., Sakoda, H., Kushiyama, A., Ono, H., Fujishiro, M., Kamata, H., Nishiyama, K., Uchijima, Y., Kurihara, Y., Kurihara, H., et al. (2008). AMP-activated protein kinase activation increases phosphorylation of glycogen synthase kinase 3beta and thereby reduces cAMP-responsive element transcriptional activity and phosphoenolpyruvate carboxykinase C gene expression in the liver. *J. Biol. Chem.* **283**, 33902–10.

Hu, C., Iyer, S., Sataur, A., Covello, K. L., Chodosh, L. A. and Simon, M. C. (2006). Differential regulation of the transcriptional activities of hypoxia-inducible factor 1 alpha (HIF-1α) and HIF-2α in stem cells. *Mol. Cell. Biol.* **26**, 3514–3526.

Ilacqua, A. N., Kirby, A. M. and Pamenter, M. E. (2017). Behavioural responses of naked mole rats to acute hypoxia and anoxia. *Biol. Lett.* **13**,.

Iritani, B. M. and Eisenman, R. N. (1999). c-Myc enhances protein synthesis and cell size during B lymphocyte development. *Proc. Natl. Acad. Sci. U. S. A.* **96**, 13180–13185.

Ivan, M., Kondo, K., Yang, H., Kim, W., Valiando, J., Ohh, M., Salic, A., Asara, J. M., Lane, W. S. and Kaelin, W. G. (2001). HIFalpha targeted for VHL-mediated destruction by proline hydroxylation: implications for O2 sensing. *Science* **292**, 464–468.

Iyer, N. V, Kotch, L. E., Agani, F., Leung, S. W., Laughner, E., Wenger, R. H., Gassmann, M., Gearhart, J. D., Lawler, A. M., Yu, A. Y., et al. (1998). Cellular and developmental control of O2 homeostasis by hypoxia-inducible factor 1 alpha. *Genes Dev* **12**, 149–162.

Jackson, D. C. (1968). Metabolic depression and oxygen depletion in the diving turtle. *J. Appl. Physiol.* **24**, 503–509.

Jackson, D. C., Ramsey, a L., Paulson, J. M., Crocker, C. E. and Ultsch, G. R. (2000). Lactic acid buffering by bone and shell in anoxic softshell and painted turtles. *Physiol. Biochem. Zool.* **73**, 290–7.

Jacky, J. P. (1978). A plethysmograph for long-term measurements of ventilation in unrestrained animals. *J. Appl. Physiol.* **45**, 644–7.

Jarvis, J. U. M., Sherman, P. W. and Alexander, R. D. (1991). *The biology of the naked mole-rat.*

Jiang, C. and Haddad, G. G. (1991). Effect of anoxia on intracellular and extracellular potassium activity in hypoglossal neurons in vitro. *J. Neurophysiol.* **66**, 103–111.

Jiang, B. H., Rue, E., Wang, G. L., Roe, R. and Semenza, G. L. (1996). Dimerization, DNA binding, and transactivation properties of hypoxia-inducible factor 1. *J. Biol. Chem.* **271**, 17771–17778.

Johansen, K., Lykkeboe, G., Weber, R. E. and Maloiy, G. M. O. (1976). Blood respiratory properties in the naked mole rat Heterocephalus glaber, a mammal of low body temperature. *Respir. Physiol.* **28**, 303–314.

Johnston, I. A. and Bernard, L. M. (1983). Utilization of the Ethanol Pathway in Carp Following Exposure To Anoxia. *J . exp . Biol* **104**, 73–78.

Jørgensen, S. B., Richter, E. A. and Wojtaszewski, J. F. P. (2006). Role of AMPK in skeletal

muscle metabolic regulation and adaptation in relation to exercise. *J. Physiol.* **574**, 17–31.

Jyung, R. W., LeClair, E. E., Bernat, R. A., Kang, T. S., Ung, F., McKenna, M. J. and Tuan, R. S. (2000). Expression of angiogenic growth factors in paragangliomas. *Laryngoscope* **110**, 161–167.

Kaelin, W. G. (2005). The von Hippel-Lindau protein, HIF hydroxylation, and oxygen sensing. *Biochem. Biophys. Res. Commun.* **338**, 627–628.

Kaelin, W. G. and Maher, E. R. (1998). The VHL tumour-suppressor gene paradigm. *Trends Genet.* **14**, 423–426.

Kasiganesan, H., Sridharan, V. and Wright, G. (2007). Prolyl hydroxylase inhibitor treatment confers whole-animal hypoxia tolerance. *Acta Physiol.* **190**, 163–169.

Kido, M., Du, L., Sullivan, C. C., Li, X., Deutsch, R., Jamieson, S. W. and Thistlethwaite, P. A. (2005). Hypoxia-inducible factor 1-alpha reduces infarction and attenuates progression of cardiac dysfunction after myocardial infarction in the mouse. *J. Am. Coll. Cardiol.* **46**, 2116–2124.

Kim, J. W., Tchernyshyov, I., Semenza, G. L. and Dang, C. V. (2006). HIF-1-mediated expression of pyruvate dehydrogenase kinase: A metabolic switch required for cellular adaptation to hypoxia. *Cell Metab.* **3**, 177–185.

Kim, E. B., Fang, X., Fushan, A. A., Huang, Z., Lobanov, A. V, Han, L., Marino, S. M., Sun, X., Turanov, A. A., Yang, P., et al. (2011). Genome sequencing reveals insights into physiology and longevity of the naked mole rat. *Nature* **479**, 223–7.

Kirby, A. M., Fairman, G. and Pamenter, M. E. (2018). Atypical behavioural, metabolic, and thermoregulatory responses to hypoxia in the naked mole rat (Heterocephalus glaber). *J. Zool.*

Kline, D. D., Peng, Y. J., Manalo, D. J., Semenza, G. L. and Prabhakar, N. R. (2002). Defective carotid body function and impaired ventilatory responses to chronic hypoxia in mice partially deficient for hypoxia-inducible factor 1 alpha. *Proc Natl Acad Sci U S A* **99**, 821–826.

Koh, M. Y., Spivak-Kroizman, T., Venturini, S., Welsh, S., Williams, R. R., Kirkpatrick, D. L. and Powis, G. (2008). Molecular mechanisms for the activity of PX-478, an antitumor inhibitor of the hypoxia-inducible factor-1α. *Mol. Cancer Ther.* **7**,.

Kong, D., Park, E. J., Stephen, A. G., Calvani, M., Cardellina, J. H., Monks, A., Fisher, R. J., Shoemaker, R. H. and Melillo, G. (2005). Echinomycin, a Small-Molecule Inhibitor of Hypoxia-Inducible Factor-1 DNA-Binding Activity. *Cancer Res.* **65**,.

Kong, T., Westerman, K. A., Faigle, M., Eltzschig, H. K. and Colgan, S. P. (2006). HIF-dependent induction of adenosine A2B receptor in hypoxia. *FASEB J.* **20**, 2242–2250.

Kornitzer, D. and Ciechanover, a (2000). Modes of regulation of ubiquitin-mediated protein degradation. *J. Cell. Physiol.* **182**, 1–11.

Korvald, C., Elvenes, O. P. and Myrmel, T. (2000). Myocardial substrate metabolism influences left ventricular energetics in vivo. *Am. J. Physiol. Heart Circ. Physiol.* **278**, H1345–H1351.

Koshiji, M., Kageyama, Y., Pete, E. A., Horikawa, I., Barrett, J. C. and Huang, L. E. (2004). HIF-1α induces cell cycle arrest by functionally counteracting Myc. *EMBO J.* **23**, 1949–1956.

Krogh, A. (1914). The quantitative relation between temperature and standard metabolism in animals. *Int. Z. Phys. Chem. Biol.* **1**, 491–508.

Kudo, N., Barr, A. J., Barr, R. L., Desai, S. and Lopaschuk, G. D. (1995). High rates of fatty

acid oxidation during reperfusion of ischemic hearts are associated with a decrease in malonyl-CoA levels due to an increase in 5'-AMP-activated protein kinase inhibition of acetyl-CoA carboxylase. *J. Biol. Chem.* **270**, 17513–17520.

Kurth-Kraczek, E. J., Hirshman, M. F., Goodyear, L. J. and Winder, W. W. (1999). 5' AMP-activated protein kinase activation causes GLUT4 translocation in skeletal muscle. *Diabetes* **48**, 1667–71.

Kuwaki, T., Cao, W. H., Kurihara, Y., Kurihara, H., Ling, G. Y., Onodera, M., Ju, K. H., Yazaki, Y. and Kumada, M. (1996). Impaired ventilatory responses to hypoxia and hypercapnia in mutant mice deficient in endothelin-1. *Am. J. Physiol.* **270**, R1279-86.

Larade, K. and Storey, K. B. (2002a). Reversible suppression of protein synthesis in concert with polysome disaggregation during anoxia exposure in Littorina littorea. *Mol. Cell. Biochem.* **232**, 121–127.

Larade, K. and Storey, K. B. (2002b). A profile of the metabolic responses to anoxia in marine invertebrates. *Cell Mol. Response to Stress* **3**, 27–46.

Lee, M. E., De La Monte, S. M., Ng, S. C., Bloch, K. D. and Quertermous, T. (1990). Expression of the potent vasoconstrictor endothelin in the human central nervous system. *J. Clin. Invest.* **86**, 141–147.

Lee, P. J., Jiang, B. H., Chin, B. Y., Iyer, N. V, Alam, J., Semenza, G. L. and Choi, a M. (1997). Hypoxia-inducible factor-1 mediates transcriptional activation of the heme oxygenase-1 gene in response to hypoxia. *J. Biol. Chem.* **272**, 5375–5381.

Lee, M., Hwang, J. T., Lee, H. J., Jung, S. N., Kang, I., Chi, S. G., Kim, S. S. and Ha, J. (2003). AMP-activated protein kinase activity is critical for hypoxia-inducible factor-1 transcriptional activity and its target gene expression under hypoxic conditions in DU145

cells. *J. Biol. Chem.* **278**, 39653–39661.

Leprivier, G., Remke, M., Rotblat, B., Dubuc, A., Mateo, A. R. F., Kool, M., Agnihotri, S., El-Naggar, A., Yu, B., Prakash Somasekharan, S., et al. (2013). The eEF2 kinase confers resistance to nutrient deprivation by blocking translation elongation. *Cell* **153**,.

Levin, E. R. (1995). Endothelins. *N. Engl. J. Med.* **333**, 356–363.

Levine, B. D. and Stray-Gundersen, J. (2001). The effects of altitude training are mediated primarily by acclimatization, rather than by hypoxic exercise. *Adv Exp Med Biol* **502**, 75–88.

Li, H., Chen, S. J., Chen, Y. F., Meng, Q. C., Durand, J., Oparil, S. and Elton, T. S. (1994). Enhanced endothelin-1 and endothelin receptor gene expression in chronic hypoxia. *J Appl Physiol* **77**, 1451–1459.

Li, F., Wang, Y., Zeller, K. I., Potter, J. J., Wonsey, D. R., O'Donnell, K. A., Kim, J.-W., Yustein, J. T., Lee, L. A. and Dang, C. V (2005). Myc stimulates nuclearly encoded mitochondrial genes and mitochondrial biogenesis. *Mol. Cell. Biol.* **25**, 6225–34.

Li, H., Satriano, J., Thomas, J. L., Miyamoto, S., Sharma, K., Pastor-Soler, N. M., Hallows, K. R., Singh, P., H., L., J., S., et al. (2015). Interactions between HIF-1alpha and AMPK in the regulation of cellular hypoxia adaptation in chronic kidney disease. *Am. J. Physiol. - Ren. Physiol.* **309**, F414-28.

Ma, X. M. and Blenis, J. (2009). Molecular mechanisms of mTOR-mediated translational control. *Nat. Rev. Mol. Cell Biol.* **10**, 307–318.

Malan, A. (1973). Ventilation measured by body plethysmography in hibernating mammals and in poikilotherms. *Respir. Physiol.* **17**, 32–44.

Marsin, A.-S., Bertrand†, L., Rider, M. H., Deprez, J., Beauloye, C., Vincent‡, M. F., Van

den Berghe‡, G., Carling, D. and Hue, L. (2000). Phosphorylation and activation of heart PFK-2 by AMPK has a role in the stimulation of glycolysis during ischaemia. *Curr. Biol.* **10**, 1247–1255.

Masaki, T. (1995). Possible Role of Endothelin in Endothelial Regulation of Vascular Tone. *Annu Rev Pharmacol Toxicol* **35**, 235–255.

Maxwell, P. H., Wiesener, M. S., Chang, G. W., Clifford, S. C., Vaux, E. C., Cockman, M. E., Wykoff, C. C., Pugh, C. W., Maher, E. R. and Ratcliffe, P. J. (1999). The tumour suppressor protein VHL targets hypoxia-inducible factors for oxygen-dependent proteolysis. *Nature* **399**, 271–275.

McClelland, G. B., Hochachka, P. W. and Weber, J. M. (1998). Carbohydrate utilization during exercise after high-altitude acclimation: a new perspective. *Proc. Natl. Acad. Sci. U. S. A.* **95**, 10288–10293.

McGregor, K. H., Gil, J. and Lahiri, S. (1984). A morphometric study of the carotid body in chronically hypoxic rats. *J. Appl. Physiol.* **57**, 1430–8.

McNab, B. K. (1979). The Influence of Body Size on the Energetics and Distribution of Fossorial and Burrowing Mammals. *Ecology* **60**, 1010–1021.

McNab, B. K. (1983). Energetics, body size, and the limits to endothermy. *J. Zool.* **199**, 1–29.

McNeill, L. A., Hewitson, K. S., Gleadle, J. M., Horsfall, L. E., Oldham, N. J., Maxwell, P. H., Pugh, C. W., Ratcliffe, P. J. and Schofield, C. J. (2002). The use of dioxygen by HIF prolyl hydroxylase (PHD1). *Bioorganic Med. Chem. Lett.* **12**, 1547–1550.

McQueen, D. S. and Ribeiro, J. A. (1986). Pharmacological characterization of the receptor involved in chemoexcitation induced by adenosine. *Br. J. Pharmacol.* **88**, 615–620.

Menrad, H., Werno, C., Schmid, T., Copanaki, E., Deller, T., Dehne, N. and Brüne, B.

(2010). Roles of hypoxia-inducible factor-1α (HIF-1α) versus HIF-2α in the survival of hepatocellular tumor spheroids. *Hepatology* **51**, 2183–2192.

Merrill, G. F., Kurth, E. J., Hardie, D. G. and Winder, W. W. (1997). AICA riboside increases AMP-activated protein kinase, fatty acid oxidation, and glucose uptake in rat muscle. *Am. J. Physiol.* **273**, E1107-12.

Michiels, C. (2004). Physiological and pathological responses to hypoxia. *Am. J. Pathol.* **164**, 1875–82.

Mitchell, G. S., Powell, F. L., Hopkins, S. R. and Milsom, W. K. (2001). Time domains of the hypoxic ventilatory response in awake ducks: Episodic and continuous hypoxia. *Respir. Physiol.* **124**, 117–128.

Moraes, D. and Loscalzo, J. (1997). Pulmonary hypertension: newer concepts in diagnosis and management. *Clin. Cardiol.* **20**, 676–682.

Mortola, J. P. and Feher, C. (1998). Hypoxia inhibits cold-induced huddling in rat pups. *Respir. Physiol.* **113**, 213–222.

Mortola, J. P. and Frappell, P. B. (1998). On the barometric method for measurements of ventilation, and its use in small animals. *Can. J. Physiol. Pharmacol.* **76**, 937–944.

Mortola, J. P., Rezzonico, R. and Lanthier, C. (1989). Ventilation and oxygen consumption during acute hypoxia in newborn mammals: a comparative analysis. *Respir. Physiol.* **78**, 31–43.

Murakami, T., Ilieva, H., Shiote, M., Nagata, T., Nagano, I., Shoji, M. and Abe, K. (2003). Hypoxic induction of vascular endothelial growth factor is selectively impaired in mice carrying the mutant SOD1 gene. *Brain Res.* **989**, 231–237.

Murphy, D. J., Joran, M. E. and Renninger, J. E. (1993). Effects of adenosine agonists and

antagonists on pulmonary ventilation in conscious rats. *Gen. Pharmacol.* **24**, 943–54.

Naeije, R. (1997). Pulmonary circulation at high altitude. *Respiration.* **64**, 429–34.

Nathaniel, T. I., Otukonyong, E., Abdellatif, A. and Soyinka, J. O. (2012). Effect of hypoxia on metabolic rate, core body temperature, and c-fos expression in the naked mole rat. *Int. J. Dev. Neurosci.* **30**, 539–544.

Nimker, C., Singh, D., Kaur, G., Saxena, S. and Bansal A (2015). Protective efficacy of ethyl 3, 4-dihydroxy benzoate against exercise induced damages: putative role in improving physical performance. *Int. J. Pharm. Sci. Res.* **6**, 2423.

Nimker, C., Singh, D. P., Saraswat, D. and Bansal, A. (2016). Preconditioning with ethyl 3,4-dihydroxybenzoate augments aerobic respiration in rat skeletal muscle. *Hypoxia (Auckland, N.Z.)* **4**, 109–120.

O'Connor, T. P., Lee, A., Jarvis, J. U. M. and Buffenstein, R. (2002). Prolonged longevity in naked mole-rats: Age-related changes in metabolism, body composition and gastrointestinal function. In *Comparative Biochemistry and Physiology - A Molecular and Integrative Physiology*, pp. 835–842.

Onnis, B., Rapisarda, A. and Melillo, G. (2009). Development of HIF-1 inhibitors for cancer therapy. *J. Cell. Mol. Med.* **13**, 2780–2786.

Osborne, P. G., Gao, B. and Hashimoto, M. (2004). Determination in vivo of newly synthesized gene expression in hamsters during phases of the hibernation cycle. *Jpn. J. Physiol.* **54**, 295–305.

Pamenter, M. E. and Powell, F. L. (2016). Time domains of the hypoxic ventilatory response and their molecular basis. *Compr. Physiol.* **6**, 1345–1385.

Pamenter, M. E., Shin, D. S.-H. and Buck, L. T. (2008). AMPA receptors undergo channel

arrest in the anoxic turtle cortex. *Am. J. Physiol. Regul. Integr. Comp. Physiol.* **294**, R606-13.

Pamenter, M. E., Hogg, D. W., Ormond, J., Shin, D. S., Woodin, M. A. and Buck, L. T. (2011). Endogenous GABAA and GABAB receptor-mediated electrical suppression is critical to neuronal anoxia tolerance. *Proc. Natl. Acad. Sci.* **108**, 11274–11279.

Pamenter, M., Dzal, Y. and Milsom, W. (2014). Profound metabolic depression in the hypoxia-tolerant naked mole rat (879.2). *FASEB J* **28**, 879.2-.

Pamenter, M. E., Dzal, Y. A. and Milsom, W. K. (2015). Adenosine receptors mediate the hypoxic ventilatory response but not the hypoxic metabolic response in the naked mole rat during acute hypoxia. *Proceedings. Biol. Sci.* **282**, 20141722.

Pamenter, M. E., Lau, G. Y., Richards, J. G. and Milsom, W. K. (2018). Naked mole rat brain mitochondria electron transport system flux and H + leak are reduced during acute hypoxia. *J. Exp. Biol.* jeb.171397.

Pan, X. Y., Zhang, Z. H., Wu, L. X. and Wang, Z. C. (2015). Effect of HIF-1a/VEGF signaling pathway on plasma progesterone and ovarian prostaglandin F 2a secretion during luteal development of pseudopregnant rats. *funpecrp.com.br Genet. Mol. Res. Genet. Mol. Res* **14**, 8796–8809.

Papandreou, I., Cairns, R. A., Fontana, L., Lim, A. L. and Denko, N. C. (2006). HIF-1 mediates adaptation to hypoxia by actively downregulating mitochondrial oxygen consumption. *Cell Metab.* **3**, 187–197.

Park, T. J., Reznick, J., Peterson, B. L., Blass, G., Omerbašić, D., Bennett, N. C., Kuich, P. H. J. L., Zasada, C., Browe, B. M., Hamann, W., et al. (2017). Fructose-driven glycolysis supports anoxia resistance in the naked mole-rat. *Science (80-.).* **356**, 307–311.

Pascual, O., Denavit-Saubié, M., Dumas, S., Kietzmann, T., Ghilini, G., Mallet, J. and Pequignot, J. M. (2001). Selective cardiorespiratory and catecholaminergic areas express the hypoxia-inducible factor-1α (HIF-1α) under in vivo hypoxia in rat brainstem. *Eur. J. Neurosci.* **14**, 1981–1991.

Paternostro, C., David, E., Novo, E. and Parola, M. (2010). t. *World J. Gastroenterol.* **16**, 281–288.

Peers, C., Pearson, H. A. and Boyle, J. P. (2007). Hypoxia and Alzheimer's disease. *Essays Biochem.* **43**, 153–64.

Pék, M. and Lutz, P. L. (1997). Role for adenosine in channel arrest in the anoxic turtle brain. *J. Exp. Biol.* **200**, 1913–7.

Peng, Y.-J., Yuan, G., Ramakrishnan, D., Sharma, S. D., Bosch-Marce, M., Kumar, G. K., Semenza, G. L. and Prabhakar, N. R. (2006). Heterozygous HIF-1alpha deficiency impairs carotid body-mediated systemic responses and reactive oxygen species generation in mice exposed to intermittent hypoxia. *J. Physiol.* **577**, 705–716.

Peng, Y. J., Nanduri, J., Khan, S. A., Yuan, G., Wang, N., Kinsman, B., Vaddi, D. R., Kumar, G. K., Garcia, J. A., Semenza, G. L., et al. (2011). Hypoxia-inducible factor 2alpha (HIF-2alpha) heterozygous-null mice exhibit exaggerated carotid body sensitivity to hypoxia, breathing instability, and hypertension. *Proc Natl Acad Sci U S A* **108**, 3065–3070.

Peterson, B. L., Larson, J., Buffenstein, R., Park, T. J. and Fall, C. P. (2012). Blunted neuronal calcium response to hypoxia in naked mole-rat hippocampus. *PLoS One* **7**,.

Pichon, A., Zhenzhong, B., Favret, F., Jin, G., Shufeng, H., Marchant, D., Richalet, J.-P. and Ge, R.-L. (2009). Long-term ventilatory adaptation and ventilatory response to hypoxia in plateau pika (Ochotona curzoniae): role of nNOS and dopamine. *Am. J. Physiol.*

Regul. Integr. Comp. Physiol. **297**, R978–R987.

Poortinga, G., Hannan, K. M., Snelling, H., Walkley, C. R., Jenkins, A., Sharkey, K., Wall, M., Brandenburger, Y., Palatsides, M., Pearson, R. B., et al. (2004). MAD1 and c-MYC regulate UBF and rDNA transcription during granulocyte differentiation. *EMBO J.* **23**, 3325–3335.

Powell, F. L., Milsom, W. K. and Mitchell, G. S. (1998). Time domains of the hypoxic ventilatory response. *Respir. Physiol.* **112**, 123–134.

Powell, F. L., Huey, K. A. and Dwinell, M. R. (2000). Central nervous system mechanisms of ventilatory acclimatization to hypoxia. *Respir. Physiol.* **121**, 223–236.

Prabhakar, N. R., Dinerman, J. L., Agani, F. H. and Snyder, S. H. (1995). Carbon monoxide: a role in carotid body chemoreception. *Proc. Natl. Acad. Sci. U. S. A.* **92**, 1994–7.

Pugh, C. W. and Ratcliffe, P. J. (2003). Regulation of angiogenesis by hypoxia: role of the HIF system. *Nat. Med.* **9**, 677–684.

Raval, R. R., Lau, K. W., Tran, M. G. B., Sowter, H. M., Mandriota, S. J., Li, J.-L., Pugh, C. W., Maxwell, P. H., Harris, A. L. and Ratcliffe, P. J. (2005). Contrasting properties of hypoxia-inducible factor 1 (HIF-1) and HIF-2 in von Hippel-Lindau-associated renal cell carcinoma. *Mol. Cell. Biol.* **25**, 5675–86.

Rehan, V., Haider, A. Z., Alvaro, R. E., Nowaczyk, B., Cates, D. B., Kwiatkowski, K. and Rigatto, H. (1996). The biphasic ventilatory response to hypoxia in preterm infants is not due to a decrease in metabolism. *Pediatr. Pulmonol.* **22**, 287–294.

Robey, I. F., Lien, A. D., Welsh, S. J., Baggett, B. K. and Gillies, R. J. (2005). Hypoxia-Inducible Factor-1α and the Glycolytic Phenotype in Tumors. *Neoplasia* **7**, 324–330.

Rolfe, D. F. and Brown, G. C. (1997). Cellular energy utilization and molecular origin of

standard metabolic rate in mammals. *Physiol. Rev.* **77**, 731–58.

Rosmorduc, O., Wendum, D., Corpechot, C., Galy, B., Sebbagh, N., Raleigh, J., Housset, C. and Poupon, R. (1999). Hepatocellular hypoxia-induced vascular endothelial growth factor expression and angiogenesis in experimental biliary cirrhosis. *Am. J. Pathol.* **155**, 1065–1073.

Rowed, D. W. and De La Torre, J. C. (1973). Dimethyl sulfoxide in experimental hypoxic respiratory depression. *Arch. Int. Pharmacodyn. Ther.* **204**,.

Sarbassov, D. D., Ali, S. M. and Sabatini, D. M. (2005). Growing roles for the mTOR pathway. *Curr. Opin. Cell Biol.* **17**, 596–603.

Schippers, M. P., Ramirez, O., Arana, M., Pinedo-Bernal, P. and McClelland, G. B. (2012). Increase in carbohydrate utilization in high-altitude andean mice. *Curr. Biol.* **22**, 2350–2354.

Schippers, M.-P., LeMoine, C. M. R. and McClelland, G. B. (2014). Patterns of fuel use during locomotion in mammals revisited: the importance of aerobic scope. *J. Exp. Biol.* **217**, 3193–6.

Schmidt, E. V. (1999). The role of c-myc in cellular growth control. *Oncogene* **18**, 2988–2996.

Schurmann, H., Steffensen, J. F. and Lomholt, J. P. (1991). The influence of hypoxia on the preferred temperature of rainbow trout Oncorhynchus mykiss. *J. Exp. Biol.* **157**, 75–86.

Scremin, A. M. E., Scremin, O. U. and Brechner, T. (1980). Survival under hypoxia. Age dependence and effect of cholinergic drugs. *Stroke* **11**, 548–552.

Seagroves, T. N., Ryan, H. E., Lu, H., Wouters, B. G., Knapp, M., Thibault, P., Laderoute, K. and Johnson, R. S. (2001). Transcription factor HIF-1 is a necessary mediator of the pasteur effect in mammalian cells. *Mol. Cell. Biol.* **21**, 3436–44.

Semenza, G. L. (1999). Regulation of mammalian O2 homeostasis by hypoxia-inducible factor 1. *Annu. Rev. Cell Dev. Biol.* **15**, 551–578.

Semenza, G. L. (2000b). HIF-1: mediator of physiological and pathophysiological responses to hypoxia. *J. Appl. Physiol.* **88**, 1474–80.

Semenza, G. L. (2000a). Expression of Hypoxia-inducible Factor 1: Mechanisms and Consequences. *Biochem PHARMACOL* **591**, 47–53.

Semenza, G. L., Jiang, B.-H., Leung, S. W., Passantino, R., Concordetţ, J.-P., Mairetţ, P. and Giallongo, A. (1996). Hypoxia Response Elements in the Aldolase A, Enolase 1, and Lactate Dehydrogenase A Gene Promoters Contain Essential Binding Sites for Hypoxia-inducible Factor 1*. *J. Biol. Chem.* **271**, 32529–32537.

Shams, I., Avivi, A. and Nevo, E. (2004). Hypoxic stress tolerance of the blind subterranean mole rat: expression of erythropoietin and hypoxia-inducible factor 1 alpha. *Proc. Natl. Acad. Sci. U. S. A.* **101**, 9698–703.

Shams, I., Avivi, A. and Nevo, E. (2005). Oxygen and carbon dioxide fluctuations in burrows of subterranean blind mole rats indicate tolerance to hypoxic-hypercapnic stresses. *Comp. Biochem. Physiol. - A Mol. Integr. Physiol.* **142**, 376–382.

Shimizu, S., Eguchi, Y., Kamiike, W., Itoh, Y., Hasegawa, J. I., Yamabe, K., Otsuki, Y., Matsuda, H. and Tsujimoto, Y. (1996). Induction of apoptosis as well as necrosis by hypoxia and predominant prevention of apoptosis by Bcl-2 and Bcl-XL. *Cancer Res.* **56**, 2161–2166.

Shoubridge, E. and Hochachka, P. (1980). Ethanol: novel end product of vertebrate anaerobic metabolism. *Science (80-.).* **209**, 308–309.

Sick, T. J., Perez-pinzon, M., Lutz, P. . and Rosenthal, M. (1993). Maintaining coupled

metabolism and membrane function in anoxic brain: a comparison between the turtle and rat. In *Surviving Hypoxia: Mechanisms of Control and Adaptation*, pp. 351–364.

Sitkovsky, M. V, Lukashev, D., Apasov, S., Kojima, H., Koshiba, M., Caldwell, C., Ohta, A. and Thiel, M. (2004). Physiological control of immune response and inflammatory tissue damage by hypoxia-inducible factors and adenosine A2A receptors. *Annu. Rev. Immunol.* **22**, 657–682.

Skovgaard, N., Hicks, J. W. and Wang, T. (2010). Oxygen uptake and transport in air breathers. In *Respiratory Physiology of Vertebrates* (ed. Nilsson, G. E.), pp. 95–128. Cambridge: Cambridge University Press.

Slingo, M. E., Turner, P. J., Christian, H. C., Buckler, K. J. and Robbins, P. A. (2014). The von Hippel-Lindau Chuvash mutation in mice causes carotid-body hyperplasia and enhanced ventilatory sensitivity to hypoxia. *J. Appl. Physiol.* **116**, 885–892.

Smith, C. a, Bisgard, G. E., Nielsen, a M., Daristotle, L., Kressin, N. a, Forster, H. V and Dempsey, J. a (1986). Carotid bodies are required for ventilatory acclimatization to chronic hypoxia. *J. Appl. Physiol.* **60**, 1003–1010.

Smith, R. W., Houlihan, D. F., Nilsson, G. E. and Brechin, J. G. (1996). Tissue-specific changes in protein synthesis rates in vivo during anoxia in crucian carp. *Am J Physiol* **271**, R897-904.

Smith, T. G., Brooks, J. T., Balanos, G. M., Lappin, T. R., Layton, D. M., Leedham, D. L., Liu, C., Maxwell, P. H., McMullin, M. F., McNamara, C. J., et al. (2006). Mutation of von Hippel-Lindau tumour suppressor and human cardiopulmonary physiology. *PLoS Med.* **3**, 1178–1186.

Sofer, A., Lei, K., Johannessen, C. M. and Ellisen, L. W. (2005). Regulation of mTOR and

Cell Growth in Response to Energy Stress by REDD1. *Mol. Cell. Biol.* **25**, 5834–5845.

Soliz, J., Joseph, V., Soulage, C., Becskei, C., Vogel, J., Pequignot, J. M., Ogunshola, O. and Gassmann, M. (2005). Erythropoietin regulates hypoxic ventilation in mice by interacting with brainstem and carotid bodies. *J. Physiol.* **568**, 559–71.

Soliz, J., Soulage, C., Hermann, D. M. and Gassmann, M. (2007). Acute and chronic exposure to hypoxia alters ventilatory pattern but not minute ventilation of mice overexpressing erythropoietin. *Am. J. Physiol. Regul. Integr. Comp. Physiol.* **293**, R1702-10.

Sowter, H. M., Ratcliffe, P. J., Watson, P., Greenberg, A. H. and Harris, A. L. (2001). HIF-1-dependent regulation of hypoxic induction of the cell death factors BNIP3 and NIX in human tumors. *Cancer Res.* **61**, 6669–6673.

Sowter, H. M., Raval, R. R., Moore, J. W., Ratcliffe, P. J. and Harris, A. L. (2003). Predominant role of hypoxia-inducible transcription factor (Hif)-1alpha versus Hif-2alpha in regulation of the transcriptional response to hypoxia. *Cancer Res* **63**, 6130–6134.

Storey, K. B. and Storey, J. M. (2004). Metabolic rate depression in animals: transcriptional and translational controls. *Biol. Rev. Camb. Philos. Soc.* **79**, 207–233.

Storey, K. B. and Storey, J. M. (2007). Putting life on "pause"--molecular regulation of hypometabolism. *J. Exp. Biol.* **210**, 1700–14.

Storz, J. F. and Moriyama, H. (2008). Mechanisms of Hemoglobin Adaptation to High Altitude Hypoxia. *High Alt. Med. Biol.* **9**, 148–157.

Storz, J. F., Scott, G. R. and Cheviron, Z. A. (2010). Phenotypic plasticity and genetic adaptation to high-altitude hypoxia in vertebrates. *J. Exp. Biol.* **213**, 4125–4136.

Stroka, D. M., Burkhardt, T., Desbaillets, I., Wenger, R. H., Neil, D. a, Bauer, C.,

Gassmann, M. and Candinas, D. (2001). HIF-1 is expressed in normoxic tissue and displays an organ-specific regulation under systemic hypoxia. *FASEB J.* **15**, 2445–2453.

Sun, X., He, G., Qing, H., Zhou, W., Dobie, F., Cai, F., Staufenbiel, M., Huang, L. E. and Song, W. (2006). Hypoxia facilitates Alzheimer's disease pathogenesis by up-regulating BACE1 gene expression. *Proc. Natl. Acad. Sci. U. S. A.* **103**, 18727–32.

Szewczak, J. M. and Powell, F. L. (2003). Open-flow plethysmography with pressure-decay compensation. *Respir. Physiol. Neurobiol.* **134**, 57–67.

Takahashi, K., Ghatei, M. A., Jones, P. M., Murphy, J. K., Lam, H. C., O'halloran, D. J. and Bloom, S. R. (1991). Endothelin in human brain and pituitary gland: Presence of immunoreactive endothelin, endothelin messenger ribonucleic acid, and endothelin receptors. *J. Clin. Endocrinol. Metab.* **72**, 693–699.

Takeda, K., Pokorski, M., Sato, Y., Oyamada, Y. and Okada, Y. (2016). Respiratory toxicity of dimethyl sulfoxide. In *Advances in Experimental Medicine and Biology*, pp. 89–96.

Tan, Q., Kerestes, H., Percy, M. J., Pietrofesa, R., Chen, L., Khurana, T. S., Christofidou-Solomidou, M., Lappin, T. R. J. and Lee, F. S. (2013). Erythrocytosis and pulmonary hypertension in a mouse model of human HIF2A gain of function mutation. *J. Biol. Chem.* **288**, 17134–17144.

Tazuke, S. I., Mazure, N. M., Sugawara, J., Carland, G., Faessen, G. H., Suen, L. F., Irwin, J. C., Powell, D. R., Giaccia, a J. and Giudice, L. C. (1998). Hypoxia stimulates insulin-like growth factor binding protein 1 (IGFBP-1) gene expression in HepG2 cells: a possible model for IGFBP-1 expression in fetal hypoxia. *Proc Natl Acad Sci U S A* **95**, 10188–10193.

Teodoro, J. G., Parker, A. E., Zhu, X. and Green, M. R. (2006). p53-mediated inhibition of

angiogenesis through up-regulation of a collagen prolyl hydroxylase. *Science (80-.).* **313**, 968–971.

Tomasco, I. H., del Río, R., Iturriaga, R. and Bozinovic, F. (2010). Comparative respiratory strategies of subterranean and fossorial octodontid rodents to cope with hypoxic and hypercapnic atmospheres. *J. Comp. Physiol. B Biochem. Syst. Environ. Physiol.* **180**, 877–884.

Vaillancourt, E., Haman, F. and Weber, J. M. (2009). Fuel selection in Wistar rats exposed to cold: Shivering thermogenesis diverts fatty acids from re-esterification to oxidation. *J. Physiol.* **587**, 4349–4359.

Van Breukelen, F. and Martin, S. L. (2002). Reversible depression of transcription during hibernation. *J. Comp. Physiol. B Biochem. Syst. Environ. Physiol.* **172**, 355–361.

Van Thillart, G. Den, Via, J. D., Vitali, G. and Cortesi, P. (1994). Influence of long-term hypoxia exposure on the energy metabolism of Solea solea. I. Critical O2 levels for aerobic and anaerobic metabolism. *Mar. Ecol. Prog. Ser.* **104**, 109–117.

Vaupel, P. and Mayer, A. (2007). Hypoxia in cancer: Significance and impact on clinical outcome. *Cancer Metastasis Rev.* **26**, 225–239.

Vizek, M., Pickett, C. K. and Weil, J. V (1987). Increased carotid body hypoxic sensitivity during acclimatization to hypobaric hypoxia. *J. Appl. Physiol.* **63**, 2403–10.

Vlaminck, B., Toffoli, S., Ghislain, B., Demazy, C., Raes, M. and Michiels, C. (2007). Dual effect of echinomycin on hypoxia-inducible factor-1 activity under normoxic and hypoxic conditions. *FEBS J.* **274**, 5533–5542.

Vuori, K., Pihlajaniemi, T., Myllylä, R. and Kivirikko, K. I. (1992). Site-directed mutagenesis of human protein disulphide isomerase: effect on the assembly, activity and

endoplasmic reticulum retention of human prolyl 4-hydroxylase in Spodoptera frugiperda insect cells. *EMBO J.* **11**, 4213–4217.

Wang, G. L. and Semenza, G. L. (1995). Purification and characterization of Hypoxia-inducible Factor 1. *J. Biol. Chem.* **270**, 1230–1237.

Wang, G. L., Jiang, B. H., Rue, E. A. and Semenza, G. L. (1995). Hypoxia-inducible factor 1 is a basic-helix-loop-helix-PAS heterodimer regulated by cellular O2 tension. *Proc. Natl. Acad. Sci. U. S. A.* **92**, 5510–5514.

Wang, Z., Zhang, Z., Wu, Y., Chen, L., Luo, Q., Zhang, J., Chen, J., Luo, Z., Huang, X. and Cheng, Y. (2012). Effects of echinomycin on endothelin-2 expression and ovulation in immature rats primed with gonadotropins. *Exp. Mol. Med.* **44**, 615.

Wang, Y., Liu, Y., Tang, F., Bernot, K. M., Schore, R., Marcucci, G., Caligiuri, M. A., Zheng, P. and Liu, Y. (2014). Echinomycin protects mice against relapsed acute myeloid leukemia without adverse effect on hematopoietic stem cells. *Blood* **124**, 1127–1135.

Ward, M. E., Toporsian, M., Scott, J. A., Teoh, H., Govindaraju, V., Quan, A., Wener, A. D., Wang, G., Bevan, S. C., Newton, D. C., et al. (2005). Hypoxia induces a functionally significant and translationally efficient neuronal NO synthase mRNA variant. *J. Clin. Invest.* **115**, 3128–3139.

Watt, A. and Routledge, P. (1985). Adenosine stimulates respiration in man. *Br. J. Clin. Pharmacol.* **20**, 503–506.

Webb, D. J., Monge, J. C., Rabelink, T. J. and Yanagisawa, M. (1998). Endothelin: New discoveries and rapid progress in the clinic. In *Trends in Pharmacological Sciences*, pp. 5–8.

Webb, J. D., Coleman, M. L. and Pugh, C. W. (2009). Hypoxia, hypoxia-inducible factors

(HIF), HIF hydroxylases and oxygen sensing. *Cell. Mol. Life Sci.* **66**, 3539–3554.

Weber, J. M. and Haman, F. (2005). Fuel selection in shivering humans. In *Acta Physiologica Scandinavica*, pp. 319–329.

Weber, R. E., Jarvis, J. U. M., Fago, A. and Bennett, N. C. (2017). O2 binding and CO2 sensitivity in haemoglobins of subterranean African mole rats. *J. Exp. Biol.* **220**,.

Weibel, E. R. (1984). *The pathway for oxygen: structure and function in the mammalian respiratory system*.

Welch, K. C., Altshuler, D. L. and Suarez, R. K. (2007). Oxygen consumption rates in hovering hummingbirds reflect substrate-dependent differences in P/O ratios: carbohydrate as a `premium fuel'. *J. Exp. Biol.* **210**, 2146–2153.

Wiesener, M. S., Jürgensen, J. S., Rosenberger, C., Scholze, C. K., Hörstrup, J. H., Warnecke, C., Mandriota, S., Bechmann, I., Frei, U. A., Pugh, C. W., et al. (2003). Widespread hypoxia-inducible expression of HIF-2alpha in distinct cell populations of different organs. *FASEB J.* **17**, 271–273.

Wilkie, M. P., Pamenter, M. E., Alkabie, S., Carapic, D., Shin, D. S. H. and Buck, L. T. (2008). Evidence of anoxia-induced channel arrest in the brain of the goldfish (Carassius auratus). *Comp. Biochem. Physiol. - C Toxicol. Pharmacol.* **148**, 355–362.

Williams, S. E. J., Wootton, P., Mason, H. S., Bould, J., Iles, D. E., Riccardi, D., Peers, C. and Kemp, P. J. (2004). Hemoxygenase-2 is an oxygen sensor for a calcium-sensitive potassium channel. *Science* **306**, 2093–7.

Withers, P. C. (1978). Models of Diffusion-Mediated Gas Exchange in Animal Burrows. *Am. Nat.* **112**, 1101–1112.

Wood, S. C. (1991). Interactions between hypoxia and hypothermia. *Annu. Rev. Physiol.* **53**, 71–

85.

Xia, X. and Kung, A. L. (2009). Preferential binding of HIF-1 to transcriptionally active loci determines cell-type specific response to hypoxia. *Genome Biol.* **10**, R113.

Ye, J.-S., Tipoe, G. L., Fung, P. C. W. and Fung, M.-L. (2002). Augmentation of hypoxia-induced nitric oxide generation in the rat carotid body adapted to chronic hypoxia: an involvement of constitutive and inducible nitric oxide synthases. *Pflügers Arch. Eur. J. Physiol.* **444**, 178–85.

Yoshizawa, T., Shinmi, O., Giaid, A., Yanagisawa, M., Gibson, S. J., Kimura, S., Uchiyama, Y., Polak, J. M., Masaki, T. and Kanazawa, I. (1990). Endothelin: a novel peptide in the posterior pituitary system. *Science (80-.).* **247**, 462–464.

Yu, S. P., Yeh, C. H., Sensi, S. L., Gwag, B. J., Canzoniero, L. M. T., Farhangrazi, Z. S., Ying, H. S., Tian, M., Dugan, L. L. and Choi, D. W. (1997). Mediation of neuronal apoptosis by enhancement of outward potassium current. *Science (80-.).* **278**, 114–117.

Yuan, G., Peng, Y.-J., Reddy, V. D., Makarenko, V. V, Nanduri, J., Khan, S. A., Garcia, J. A., Kumar, G. K., Semenza, G. L. and Prabhakar, N. R. (2013). Mutual antagonism between hypoxia-inducible factors 1α and 2α regulates oxygen sensing and cardio-respiratory homeostasis. *Proc. Natl. Acad. Sci. U. S. A.* **110**, E1788-96.

Zhang, X., Zhou, K., Wang, R., Cui, J., Lipton, S. a, Liao, F.-F., Xu, H. and Zhang, Y. (2007a). Hypoxia-inducible factor 1alpha (HIF-1alpha)-mediated hypoxia increases BACE1 expression and beta-amyloid generation. *J. Biol. Chem.* **282**, 10873–10880.

Zhang, H., Gao, P., Fukuda, R., Kumar, G., Krishnamachary, B., Zeller, K. I., Dang, C. V. V. and Semenza, G. L. (2007b). HIF-1 Inhibits Mitochondrial Biogenesis and Cellular Respiration in VHL-Deficient Renal Cell Carcinoma by Repression of C-MYC Activity.

Cancer Cell **11**, 407–420.

Zhang, N., Fu, Z., Linke, S., Chicher, J., Gorman, J. J., Visk, D., Haddad, G. G., Poellinger, L., Peet, D. J., Powell, F., et al. (2010). The asparaginyl hydroxylase factor inhibiting HIF-1α is an essential regulator of metabolism. *Cell Metab.* **11**, 364–378.